공학박사학위논문

자율 주행 차량을 위한 확률 예측 제어 기법 기반 차선 변경 판단 알고리즘 개발

Design and Evaluation of Lane Change Decision for Automated Driving Vehicle Using Stochastic Predictive Control

2016년 8월

서울대학교 대학원

기계항공공학부

서 종 상

Abstract

Design and Evaluation of Lane Change Decision for Automated Driving Vehicle Using Stochastic Predictive Control

Jongsang Suh

School of Mechanical and Aerospace Engineering

The Graduate School

Seoul National University

The traffic accidents caused by human error, such as distraction, drowsiness, or mistakes, account for 94 percent of all traffic accidents over last decades. Since safe driving is a goal of road-traffic-vehicle environments, major automakers develop driver assistance and active safety system as key technologies since the early 1990s. For instance, parking assistance system (PAS), lane keeping assistance system (LKAS), smart cruise control (SCC), and automated emergency braking (AEB) already have been developed and commercialized by major automakers. Moreover, in recent years, an interest of automotive industry is changed from the development of active safety to that of automated driving system capable of sensing surrounding environments and driving itself. Google starts to operate an automated driving vehicle on real roads using a pre-measured precise map and environmental information from a laser scanner. The electric vehicle mass production company, Tesla, has applied the 'autopilot' mode to Model S vehicle. BMW has succeeded driving a vehicle autonomously in real traffic from Munich to Ingolstadt in German with robustness, and safety. Mercedes-Benz developed 'Intelligent Drive' system and followed the route with fully autonomous

driving from Mannheim to Pforzheim in German. These trends of automated driving vehicle development promote not only safety of passengers but also convenience. However, the current state-of-the-art in automated driving technology demands sophisticated decision to manage various and complex traffic circumstances.

This dissertation focused on the development of an automated driving control algorithm which can determine appropriate vehicle motion to deal with complex situations such as merging roads in the highway. In order to enhance decision to drive a vehicle safely, the potential behaviors of surrounding vehicles, the current and predicted states with sensor uncertainties of surrounding vehicles should be considered. Based on the prediction of surrounding vehicles, the lane change or keeping mode is determined by risk monitoring. A safe driving envelope which indicates the safe drivable area is also defined in consideration of prediction states of other traffics. The subject vehicle plans lane change or keeping motion such as accelerating, overtaking, and braking. To obtain desired control inputs which have been planned in advance, the predictive control problem is formulated. However, for automated driving vehicles in dynamic road environments, the uncertainty has to be considered from states of vehicle dynamic model and actual sensing values. For this reason, Stochastic Model Predictive Control with adaptive uncertainty propagation is developed to improve performance.

The performance of the proposed algorithm is validated via computer simulations and vehicle tests. Automated driving with the proposed algorithm shows smooth and safe driving behavior in various road traffic situations, such as lane keeping with preceding vehicle following, lane change in a multi-vehicle environment. The effectiveness of the proposed automated driving algorithm is evaluated via vehicle tests. Test results show the robust performance on a motorway scenario.

Keywords: Automated driving vehicle, Stochastic model predictive control, Collision probability, Safe driving envelope decision, Lane change decision, Adaptive uncertainty propagation.

Student Number: 2012-20672

Contents

List of Figures

List of Figures

Chapter 1

Introduction

1.1. Background and Motivation

According to the accident report from Volvo, human error is a major reason for nearly 90% of accidents [Volvo13]. A lane change maneuver is a cause for various severe highway accidents due to an inaccurate estimation of surrounding traffic or illegal maneuver. For instance, according to the previous research [Pohl06], unintended lane departure accounted for 15 percent of all traffic accidents occurred over the last ten years in German roadways, and 35 percent of those have been fatal. Furthermore, traffic accidents during a lane change maneuver accounted for about 12 percent of all traffic accidents. Moreover, during many types of collision accidents, almost drivers do not attempt to avoid crashes due to unawareness of collision risks [Tideman07].

For this reason, the advanced driver assistant system (ADAS) is regarded as a solution to reduce human errors. Various researches have been conducted to develop active safety systems which assist drivers to manage hazardous situations or mitigate collision such as lane keeping assistance system (LKAS), lane change assistance system (LCA), smart cruise control system (SCC), advanced emergency braking system (AEBS), traffic jam assistance (TJA), parking assistance system (PAS) and blind spot intervention (BSI). These systems have been commercialized by major automakers due to significant improvements in sensor and actuator technologies.

Currently, automated driving has been widely considered as a mainstream of the automakers since it offers increased safety and comfortability. Many vehicle manufacturers aim to commercialize self-driving cars by 2020 and spur research of the intelligent vehicle for its realization. Many kinds of research have been attempted to integrate individual active safety systems for improvement of the automated driving system [Bishop00, Eskandarian12]. Many laboratories of academia and industry continuously research in the field of the automated driving. 'Super Cruise' system which can drive on the highway without human driver's intervention has been developed and introduced by GM. Toyota has researched to develop 'Automatic Highway Driving Assist' technology. BMW managed to drive 100% automated in real traffic on the freeway from Munich to Ingolstadt, showing a robust, comfortable, and safe driving behavior, even during multiple automated lane change maneuvers. The objectives of driver

assistance and automated driving system are to maintain safety of the subject vehicle and reduce fatigue on driving.

Especially, Google develops technology actively for automated driving vehicle. The automated driving system is required capabilities, detecting road environment, recognizing traffic situation to determine vehicle behaviors, and traveling autonomously without any support of human drivers.

From a considerable amount of literature, automated driving technology has the potentiality to decrease severe accidents, reduce traffic congestion, and increase safety of driving. However, the cutting-edge technologies in automated vehicle area require a sophisticated decision to manage various and complex traffic circumstances.

This dissertation describes an automated driving control algorithm which can enhance the safety of the subject vehicle with possible behaviors of surrounding traffics in near future while planning motion of the subject vehicle with consideration of sensor and prediction uncertainties.

1.2. Previous Researches

Some studies have been introduced for the development of an automated driving control algorithm. Regarding vehicle control, environmental information including information about other vehicles is necessary for driving vehicles safely. For this reason, some previous studies have identified surrounding information using exterior sensors [Chellappa04, Chang10]. Utilizing this information, a large variety of threat assessment and decision-making algorithms have been proposed [Jansson02, Falcone11]. Of these, time to collision (TTC) and time to line crossing (TLC) are two of the simplest [Fancher01, Mammar06]. In several researches that attempt to use advanced methods instead of simple ones, the motion of the vehicle is planned and controlled using its trajectory [Falcone07, Jansson08].

The development of the intelligent vehicle constitutes a previous step of the automated driving vehicle. In longitudinal control, California Partners for Advanced Transit and Highways (PATH) developed a control system in which vehicles moved along the highway in a platoon driving formation. Moreover, Adaptive Cruise Control (ACC) is already produced in commercial vehicles [Moon09]. A Lane Keeping Assistance System (LKAS), representative of lateral vehicle control technology, generates assistant steering torque to prevent unintended lane change [Enache09]. Recently, traffic jam assist, which controls the speed of a car and distance from the preceding vehicle in dense traffic on motorways and takes over steering is

about to be commercialized.

Previous researches for a lane change in the automated driving systems shows cost function based approaches [Wei10]. L. Wan et al. analyzed a pattern of a lane change of human driver data to determine lane change timing [Wan11]. An object-oriented Bayesian network approach is introduced for the detection of lane change maneuvers [Kasper12]. The learning based approach using a neural network for prediction the maneuver trajectory [Tomar10] and fuzzy logic for solving the lane change decision-making problems [Naranjo08].

The lane change trajectory is generated according to the vehicle states, surrounding vehicles, and road information. Some researchers suggest that a guidance trajectory planning algorithm needs to be designed to plan and follow the appropriate path according to the vehicle states [Usman09]. Different models are compared for generating ideal lane change trajectories. For vehicle maneuver on roadways using steering input, sinusoidal, polynomial clothoid, trapezoidal acceleration profile (TAP), and sigmoid functions are considered for lane change path planning [Chee94].

In general driving situations, lane change should be decided within a certain time frame to ensure a safe automated driving control. In particular, since lane change control requires both longitudinal and lateral control, it is difficult to implement. Some studies exist about not only a time necessary to change lanes but also a distance and speed of the subject vehicle, to be determined in advance [Vanholme13].

Since lane change for automated driving system is required to predict not

only other traffic but also the subject vehicle, an MPC approach has been implemented widely due to its capability to handle several constraints actively [Anderson10, Gray13a]. The MPC method utilizes a dynamic model to predict the future states of the system and calculates an optimal control sequence for every step to minimize a cost function under the constraints [Mayne00]. In [Falcone07], Falcone et al. present an MPC based active steering controller for tracking the desired trajectory as closely as possible while satisfying various constraints. In order to compensate for the effect of the control performance by model uncertainties and exogenous disturbances, a robust MPC approach which adds a linear feedback control input to the nominal control inputs based on the analysis of robust invariant sets, has been introduced and used to design an autonomous control algorithm [Mayne05]. However, robust MPC approaches that deal with worst-case disturbances may be too conservative and computationally expensive [Gray13b]. A chance-constrained optimization in [Vitus13] shows the tactical planning problem for automated driving vehicles in uncertain environments.

In most of these researches mentioned above, the desired trajectory over a finite horizon is predefined regardless of other traffics. However, in order to design an automated driving system, we should decide a drivable area or desired path in real time using the information of surrounding environment. Erlien et al. use a safe driving envelope which means a safe region of states in which the system should be constrained. In this research, the safe driving envelope consists of a stable handling envelope to ensure vehicle stability

and an environmental envelope to constrain the position states for the collision avoidance. The environmental envelope is defined based on the current states of surrounding environment of the subject vehicle. Carvalho et al. presented a control algorithm for an autonomous ground vehicle to follow the centerline while avoiding collisions with an obstacle and evaluate this approach via experiment test. In experiment test, it is assumed that an obstacle is moving at a constant speed [Carvalho13, Erline14].

According to the patent of Google, an automated driving vehicle should be controlled based on the current state of the subject vehicle, the current and predicted states of surrounding vehicles [Ferguson13]. In addition, vehicle motion planning uses an information of probabilistic prediction behaviors of surrounding vehicles for collision-free automated driving [Suh16].

1.3. Thesis Objectives

This dissertation focuses on designing an automated control algorithm that handles potentially dangerous lane change situations while satisfying control performance with respect to model parameter uncertainties and exogenous disturbances. In order to enhance safety with respect to the potential behaviors of surrounding vehicles, the vehicle motion for lane change or keeping is defined in consideration of probabilistic prediction of future states of the surrounding environment. The safe driving envelope is defined to guarantee safe driving for automated driving vehicle. A target state decision can manage lane change motion of automated driving to change lane in complex surrounding traffic situations. Then, the SMPC problem is formulated to determine the desired control input while maintaining the subject vehicle within the safe driving envelope. In order to guarantee the robust performance under the model and exogenous uncertainties, the adaptive uncertainty propagation is developed.

Mainly three research issues are considered: a traffic environmental perception, a motion planning, and a vehicle control. In the remainder of this thesis, an overview of the overall architecture of the proposed automated driving control algorithm and simulation and test results will be provided. Simulation and test results show the effective performance on a complex motorway scenario.

1.4. Thesis Outline

This dissertation is structured as follows: the overall architecture of the proposed automated driving control algorithm is described in Section 2. In Section 3, the environment represent model which consists of object tracking and prediction, and collision probability is derived. In Section 4, vehicle model is defined. The motion planning is designed to determine driving mode with the safe driving envelope in Section 5. Section 6 presents SMPC based lower level controller to obtain desired control input with consideration of uncertainties. Section 7 presents the simulation and test results for the evaluation of the performance of the proposed algorithm. The contribution of this research and introduction of future works are summarized in Section 8.

Chapter 2

Overall Architecture of an Automated Driving System based on Stochastic Model Predictive Control

The proposed automated driving system architecture is shown in Figure 2.1. The proposed automated driving control algorithm consists of three layers. The *Environment Representation* block calculates probabilistic predictions of the states of surrounding vehicles and collision probability. All system modules make use of information from equipped various sensors. The main sensing components are a vision, lidar, radars and vehicle sensors. The probable behaviors of surrounding vehicles are predicted over a finite prediction horizon using the sensing information. The *Motion Planning* block uses the sensor information along with the predicted information of environment to determine the lane change or keeping mode decision to plan a behavior of the subject vehicle. The *Motion Planning* algorithm determines

the driving mode and safe driving envelope while considering the current states and predictable dangerous situations among the potential changes of surrounding traffic. Target states are determined to change or keep a lane for safety. The *Vehicle Control* block uses environment, planned vehicle motion, and safe envelope information to formulate an SMPC to optimize the steering angle and longitudinal acceleration inputs to the subject vehicle. Due to uncertainties of vehicle dynamics model, the disturbance analysis and the adaptive uncertainty propagation are conducted.

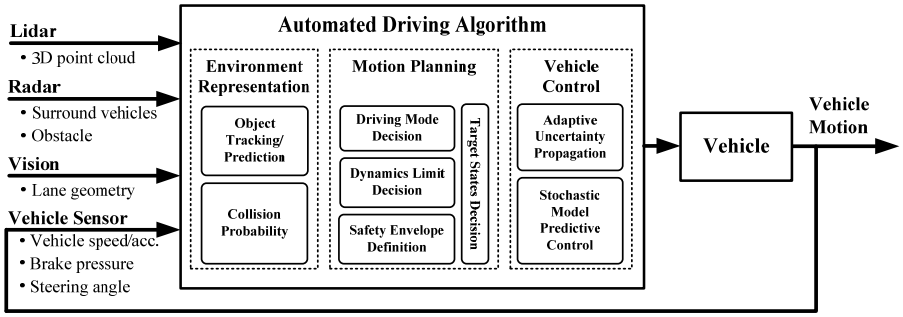

Figure 2.1 Overall Architecture of the proposed automated driving system. The proposed algorithm consists of the following three steps: an environment representation, a motion planning, and a vehicle control.

Chapter 3

Environment Representation

Precise and comprehensive environment perception is a basis for safe and comfortable autonomous driving in complex traffic situations [Vanholme13]. We modified the serial-production sensor setup already available in our test vehicles as follows: A multilayer laser scanner was added for monitoring static obstacles with increased precision. For lane detection, an additional monocular vision system was mounted on the windshield. The complete sensor setup is shown in Figure 3.1.

The environment representation has two main modules: an object tracking/prediction and a collision probability. The object tracking/prediction module computes the reachable sets for traffic participants. The Markov chain is used to approximate the stochastic processes of each traffic participants. It is assumed that a driver may maintain the current vehicle behavior and keep the relevant lane in the finite prediction horizon. A simple path following model and a vehicle state predictor interact with each other during one cycle

of the prediction process.

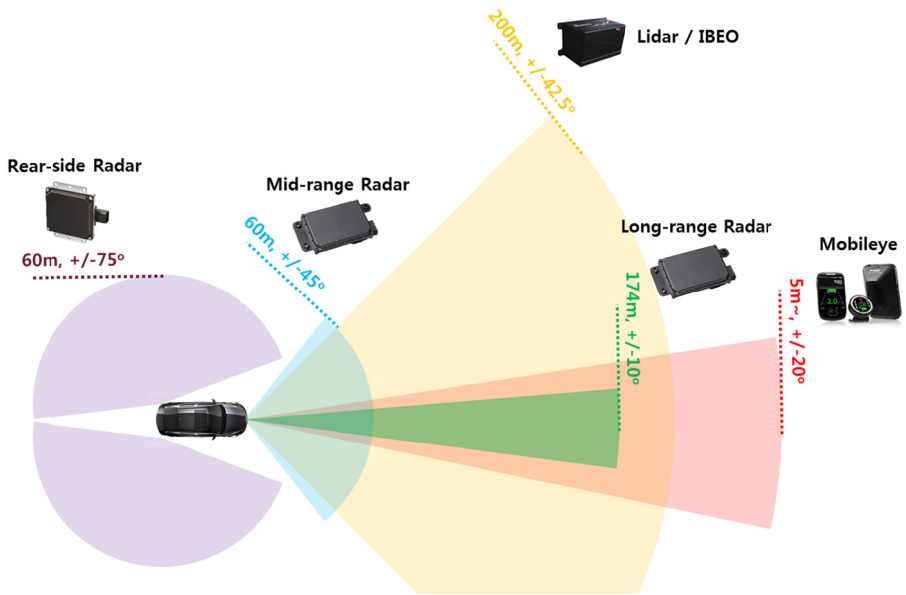

Figure 3.1 Experimental vehicle configurations

3.1. Probabilistic Prediction of Surrounding Vehicle's Behavior

One of a common approach to predict the future states of traffic situation surrounding the subject vehicles is a deterministic prediction which assumes that other vehicles surrounding the subject vehicle maintain its current movement during a finite time-horizon. However, since this approach ignores the probability of all possible movements of surrounding vehicles, it could not recognize unexpected driving situations properly. Then this could cause incorrect interpretation of the current driving situation.

In order to compensate the shortcomings of a deterministic prediction of the behaviors of surrounding vehicles, the possible behaviors of surrounding vehicles are predicted, and the risky behaviors among the possible behaviors of other vehicles surrounding the subject vehicle are considered in determining the safe driving envelope.

For the prediction of the reasonable and realistic behaviors of surrounding vehicles, the interaction between vehicles and the restriction on surrounding vehicles' maneuvers due to the road geometry should be considered [Althoff09]. Therefore, in predicting the possible behaviors of surrounding vehicles, it is assumed that surrounding vehicles are driven with the consideration of the presence of other vehicles and interactive motions with other vehicles respectively. It means that the minimum safe distance between surrounding vehicles should be maintained for collision avoidance.

In addition, it is assumed that drivers of the surrounding vehicles maneuver the vehicle with the consideration of the road geometry. It means that the speed of the surrounding vehicle should be adapted to the road geometry and road condition.

Moreover, it is assumed that drivers of the surrounding vehicles obey general traffic rules [Vanholme13]. It means that the surrounding vehicle's behavior is assumed to keep the lane or change one lane at a time, not two or more lanes at a time. If one of surrounding vehicles changes the lane, then that vehicle is assumed to keep the relevant lane in the far-off future. Furthermore, the violation of the centerline of surrounding vehicles is prohibited as shown in Figure 3.2.

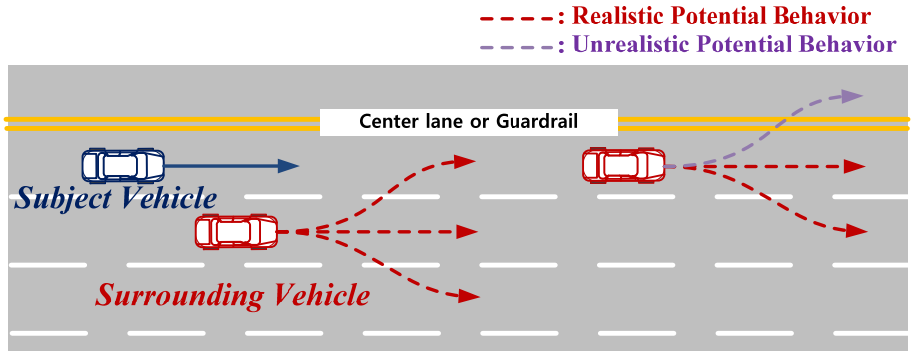

Figure 3.2 Possible behaviors of surrounding vehicles with the consideration of general traffic rules

In predicting reasonable ranges of the future states of surrounding vehicles, driving data is collected on the test track and real road to analyze the probabilistic movement characteristics of other vehicles. For implementation of these assumptions, a path-following model is designed while interacting

with a vehicle state predictor during one cycle of the prediction process. In the vehicle state predictor, the vehicle's probable position and its error covariance over a finite time horizon are predicted by Extended Kalman Filter using the desired yaw rate obtained by the path-following model as virtual measurements.

Figure 3.3 depicts the overall architecture of probabilistic prediction of surrounding vehicles. Using measurements from the various sensors, such as vehicle sensors, radars and a vision sensor, the range of the predicted states with corresponding uncertainty is determined as shown in Figure 3.3. p_x is the longitudinal position of the vehicle, p_y is the lateral position of the vehicle, N_p denotes the length of the prediction horizon, and subscript 'j' means the j-th objects. In predicting the position of the surrounding vehicles, it is assumed that the size of the object is equivalent to the subject vehicle.

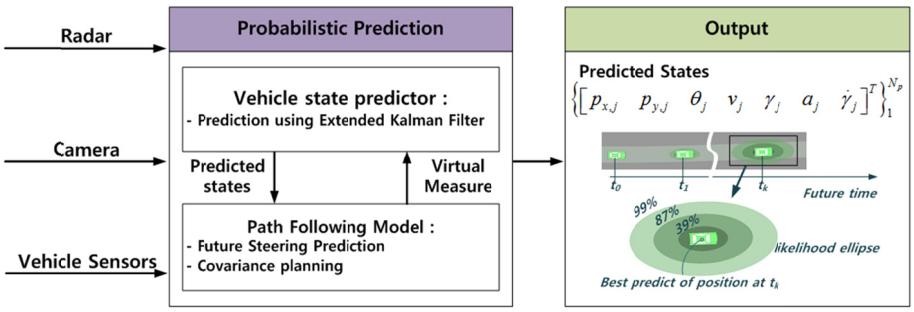

Figure 3.3 Overall architecture of probabilistic prediction of surrounding vehicle's behavior

The overall procedure of probabilistic prediction is depicted in Figure 3.4. In brief, the prediction of the surrounding vehicle's future states and the correction of the predicted future states by a path-following model are conducted successively during one cycle of the prediction process. The ellipse in Figure 3.4 indicates the predicted probable range of the center gravity of the vehicle at the prediction time. As shown in Figure 3.4, the size of the ellipse increases as the prediction time is going to be far. A detailed description of the computational procedures to predict the probabilistic range of future states during a finite prediction horizon is described concretely in [Kim14].

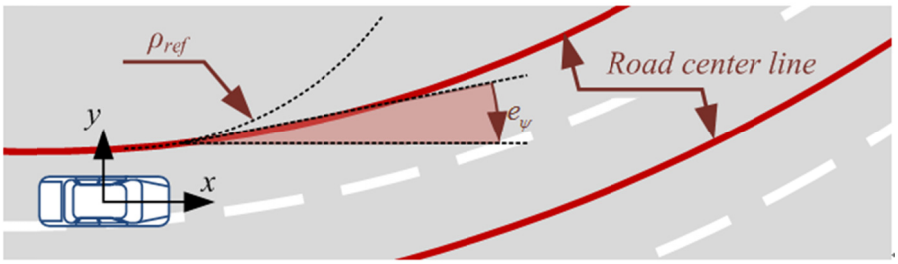

(a) The relationship between the subject vehicle and the road center line of each lane

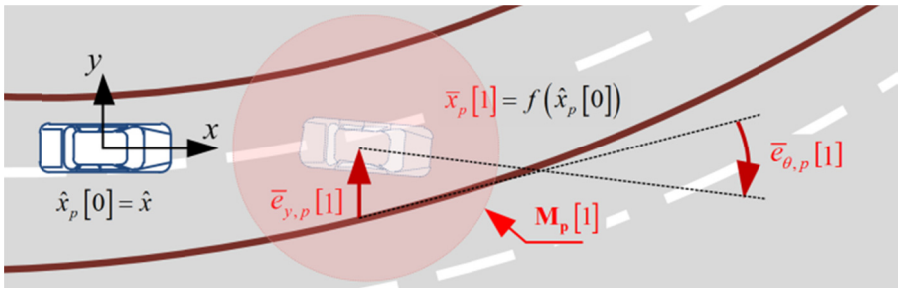

(b) The time-update-predicted subject vehicle states and the relative error

states with respect to road geometry defined on current body coordinate

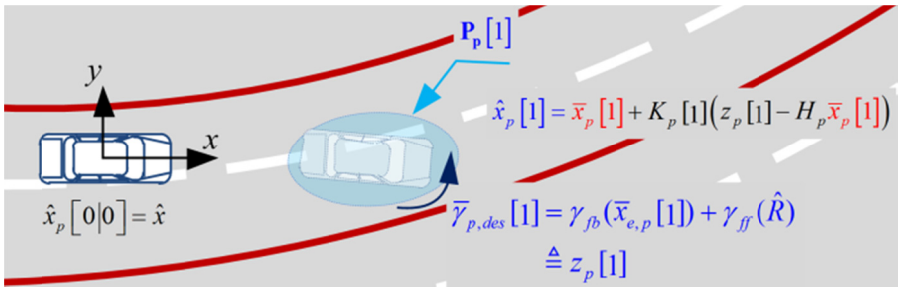

(c) The measurement-update-predicted subject vehicle states where the predicted desired yaw rate to keep the lane is defined as virtual measurement

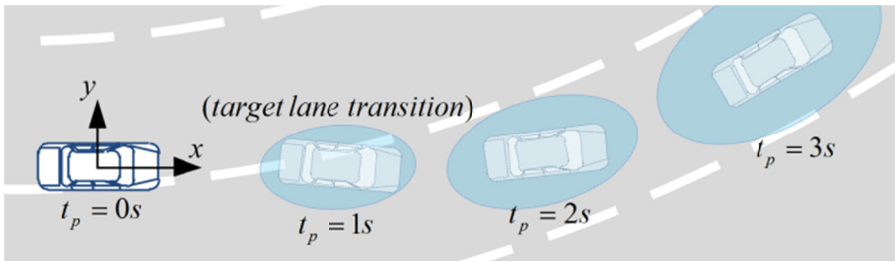

(d) Prediction results for 1s, 2s, and 3s of prediction time, t_p, at a lane-changing instant

Figure 3.4 Overall procedure of probabilistic prediction of surrounding vehicle's behavior

The simulation results for uncertainty propagation of target vehicle as shown in Figure 3.5. The red square describes vehicle shape. When the prediction step grows, the uncertainty gets larger. The uncertainty at current step has 0.68m, after sixth step has 1.22m, and after 12th step has 1.95m.

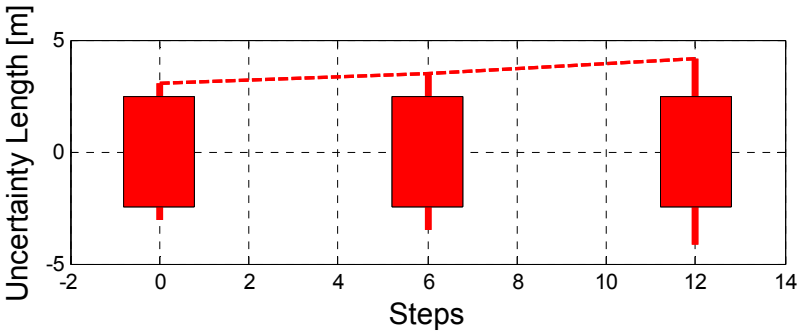

Figure 3.5 Uncertainty propagation of target vehicle

3.2. Collision Probability

The concepts of probabilistic collision risk are summarized and presented in Figure 3.5. As the beginning of the collision probability estimation, we randomly generate a given number N state vectors based on the given initial probability density function from the prediction algorithm. The parameter N could be chosen by a designer as a trade-off between computational effort and collision probability approximation accuracy. The state vectors are called particles and denoted as:

$$\mathbf{x}_{n,p}^{i} = \begin{bmatrix} \hat{\mathbf{x}}_{host,p} \\ \hat{\mathbf{x}}_{n,p} \end{bmatrix} + \left(\sqrt{\begin{bmatrix} \hat{\mathbf{P}}_{host,p} & \\ & \hat{\mathbf{P}}_{n,p} \end{bmatrix}} \right) \cdot \tilde{\mathbf{r}}^{i} \quad \left(i = 1, \cdots, N \right) \tag{3.1}$$

where the subscript p is the predictive time step; $\hat{\mathbf{x}}_{host}$ is the predicted position and orientation state vector of the subject vehicle; $\hat{\mathbf{x}}_{n}$ is the predicted pose state vector of n-th traffic participant; $\hat{\mathbf{P}}$ denotes the appropriate size of the covariance matrix of each predicted state; $\tilde{\mathbf{r}}$ is a white noise random vector of the proper size.

For every possible pair of subject and one of traffic participants, we investigate whether the vehicle bodies of the traffic participant can intersect the subject vehicle at each predicted time step. To determine the body intersection, a body-shaped diagram is introduced. ***Algorithm 1*** shows a pseudo code of the algorithm.

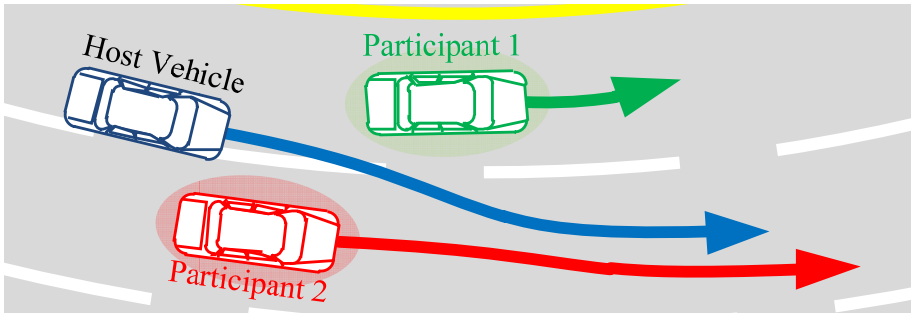

(a) Environment description based on sensor fusion: road geometry, subject vehicle's current motion, and multi-traffic-participant.

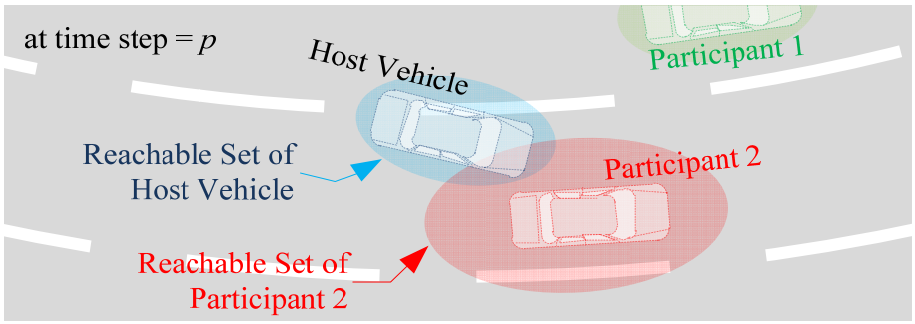

(b) Visualized example of prediction of multi-traffic pose and their covariance at predictive time step. Reachable set of each participant as stochastic distribution.

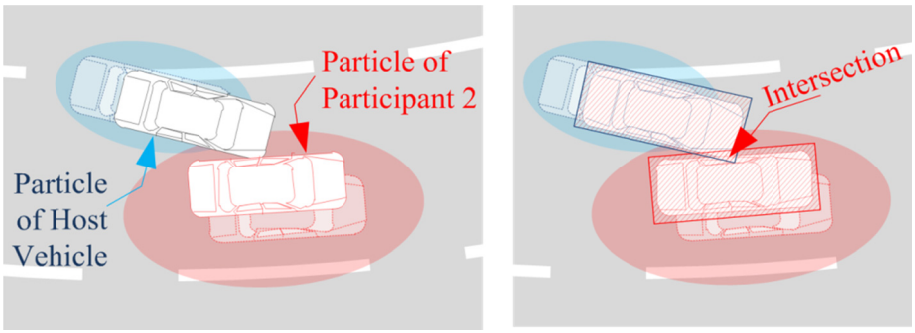

(c) A collision case example of the generated N particles and its two vehicle-body-shaped-polygons. Intersection between two polygons.

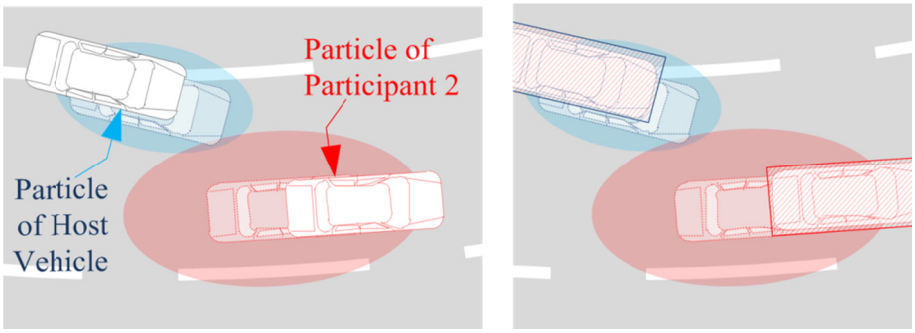

(d) A non-collision case example of the generated N particles and its two vehicle-body-shaped-polygons.

Figure 3.6 Procedure and concept of approximation of collision probability

Algorithm 1

<u>Input</u>

Predicted states and its covariance within a pre-defined prediction horizon for all tracked traffic participants.

<u>For</u> all tracked traffic participants, $n = 1, \cdots, N_{target}$

<u>For</u> every predictive time step, $p = 0, \cdots, N_p$

- Initialize collision count with participant n at predictive time step p, $C.P.cnt_n^i = 0$
- From given predicted state and covariance, randomly generate N particles, $\mathbf{x}_{n,p}^i$

<u>For</u> every particle, $i = 1, \cdots, N$

- Generate two vehicle-body-shaped-polygons.
- Check if the vehicle bodies can be possibly intersected.
- If intersection is detected, $C.P.cnt_n^i = C.P.cnt_n^i + 1$
- Else, $C.P.cnt_n^i = C.P.cnt_n^i$

<u>End</u>

- Approximate collision probability with participant n at predictive time step p
- $C.P._n^i = C.P.cnt_n^i / N$

<u>End</u>

<u>End</u>

Chapter 4

Vehicle Dynamics Model

A vehicle dynamics model should be derived to obtain the desired control inputs with SMPC approach. In this research, we design a linear parameter varying (LPV) model of the vehicle dynamics from nonlinear vehicle model.

The nonlinear differential equations are used to describe the motion of the vehicle in the road-aligned coordinate frame [Gray13b],

$$\dot{v}_x = v_y \gamma + a_x \tag{4.1a}$$

$$\dot{v}_y = -v_x \gamma + \frac{1}{m}\left(2F_{yf} + 2F_{yr}\right) \tag{4.1b}$$

$$\dot{\gamma} = \frac{1}{I_z}\left(2l_f F_{yf} - 2l_r F_{yr}\right) \tag{4.1c}$$

$$\dot{e}_\psi = \gamma - \kappa \dot{s} \tag{4.1d}$$

$$\dot{e}_y = v_x \sin\left(e_\psi\right) + v_y \cos\left(e_\psi\right) \tag{4.1e}$$

$$\dot{s} = \frac{1}{1-\kappa e_y}\left(v_x \cos\left(e_\psi\right) - v_y \sin\left(e_\psi\right)\right) \tag{4.1f}$$

where l_f and l_r denote the distance from the vehicle's center of gravity to the front and the rear axles, respectively; m and I_z denote the vehicle mass and yaw inertia, respectively; e_ψ is the orientation error of the vehicle with respect to the road; e_y denotes the lateral offset with respect to the center line of the lane; κ is curvature of the road from camera sensor; s denotes the longitudinal position of the vehicle along the road; F_{yf} and F_{yr} are lateral force of front and rear in the body frame, respectively. Figure 4.1 depicts a diagram of the vehicle model.

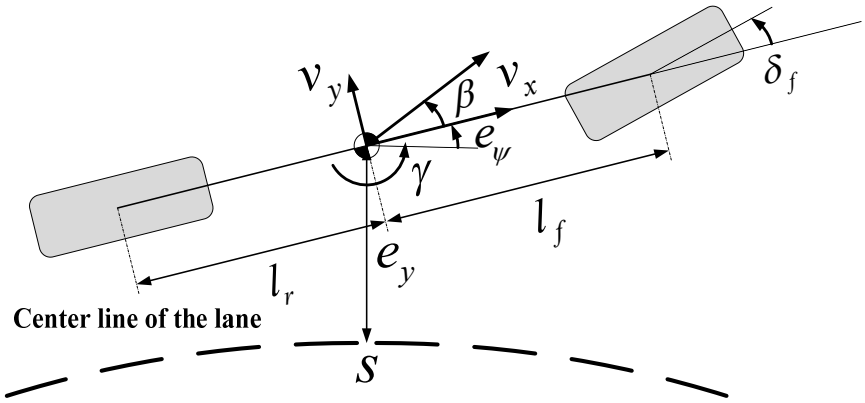

Figure 4.1 Diagram of dynamics model

The lateral force can be rewritten as,

$$F_{y*} = k_* C_* \alpha_*, \quad * \in \{f, r\} \tag{4.2}$$

where k_* is the cornering stiffness adjustment coefficients to reflect a tire saturation characteristic. These adjustment coefficients are assumed to be

estimated in this paper. C_* denotes the lateral tire cornering stiffness, and α_* denotes the lateral tire slip angle. The lateral slip angle can be written as follows:

$$\alpha_f = \delta_f - \frac{v_y + l_f \gamma}{v_x}, \quad \alpha_r = -\frac{v_y - l_r \gamma}{v_x} \tag{4.3}$$

where δ_f is the front steering angle. The nonlinear vehicle model can be compactly defined as follows:

$$\dot{x}(t) = f\left(x(t) \quad u(t) \quad d(t)\right) \tag{4.4}$$

where $x = \begin{bmatrix} v_x & v_y & \gamma & e_\psi & e_y & s \end{bmatrix}^T$, $u = \begin{bmatrix} \delta_f & a_x \end{bmatrix}^T$, and $d = \kappa$ are the states, inputs, and disturbance vectors, respectively.

However, the computational load to solve the nonlinear predictive problem constitutes the critical barrier to implementation in real-time. To deal with this issue, we apply a linearized tire model to obtain an LPV model of the vehicle dynamics. There is an assumption to linearize the vehicle dynamics model.

Assumption 1. The angular error e_ψ, lateral velocity v_y and yaw rate γ are small enough. $\sin(e_\psi) \approx e_\psi$, $\cos(e_\psi) \approx 1$, $v_y \gamma \approx 0$, and $v_y e_\psi \approx 0$.

From the *Assumption 1*, the system dynamics (4.4) can be rewritten as,

$$\dot{x}(t) = \mathbf{A}_l\left(\rho(t)\right)x(t) + \mathbf{B}_l u(t) \tag{4.5}$$

where $\rho = \begin{bmatrix} v_x & \kappa \end{bmatrix}^T$ is the parameter vector.

$$\mathbf{A}_l = \begin{bmatrix} 0 & 0 & 0 & 0 & 0 & 0 \\ 0 & \dfrac{-2\left(k_f C_f + k_r C_r\right)}{m v_x} & -1 + \dfrac{-2\left(l_f^2 k_f C_f - l_r^2 k_r C_r\right)}{m v_x} & 0 & 0 & 0 \\ 0 & \dfrac{-2\left(k_f C_f l_f - k_r C_r l_r\right)}{I_z v_x} & \dfrac{-2\left(l_f^2 k_f C_f + l_r^2 k_r C_r\right)}{I_z v_x} & 0 & 0 & 0 \\ -\kappa & 0 & 1 & 0 & 0 & 0 \\ 0 & 1 & 0 & v_x & 0 & 0 \\ 1 & 0 & 0 & 0 & 0 & 0 \end{bmatrix} \quad (4.6a)$$

$$\mathbf{B}_l = \begin{bmatrix} 0 & 1 \\ \dfrac{2k_f C_f}{m} & 0 \\ \dfrac{2k_f C_f l_f}{I_z} & 0 \\ 0 & 0 \\ 0 & 0 \\ 0 & 0 \end{bmatrix} \quad (4.6b)$$

For visual clarity, we express the system matrix $\mathbf{A}_l(\rho)$ as $\mathbf{A}_l$.

To account for uncertainties due to disturbances and uncertainties, an additive stochastic disturbance w is applied in (4.5). The modified LPV model is discretized as,

$$x_{k+1} = \mathbf{A}_{l,k} x_k + \mathbf{B}_{l,k} u_k + \mathbf{D}_{l,k} w_k \quad (4.7)$$

where $w_k \sim N(0, \Sigma_w)$. The disturbance covariance, Σ_w, is estimated in chapter 6. Table 4.1 lists the numerical values of the nominal parameters of the vehicle.

Table 4.1 Nominal parameters of the vehicle

Symbol	**Value**	**Symbol**	**Value**
C_f	65602 *N/rad*	m	1653 *kg*
C_r	101868 *N/rad*	I_z	2765 kgm^2
l_f	1.402 *m*	l_r	1.646 *m*

Chapter 5

Motion Planning for Lane Change and Keeping Decision

When driving on the road, an appropriate lane change is necessary for various reasons, such as a slow preceding vehicle or a plan to go out to upcoming exit way. That is, the automated driving vehicle determines its vehicle motion to adjust for following the traffic situations. After the lane change or keeping mode is determined by the proposed decision algorithm, the dynamics limit decision module calculates using the information of other traffic. Furthermore, assuring the safe driving area is important to avoid a collision with other vehicles or obstacles. As human drivers consider surrounding environment and predict short period of future states of the subject and other vehicles, the object prediction information, in chapter 3, is used to plan the subject vehicle's motion. In order to develop the highly automated driving system, the desired driving mode and safe driving envelope should be determined with the current and near future states of the traffic situations, simultaneously. The target states decision calculates target states as

using references for the safe lane change in complex lane change situations. The *TTC* and collision probability are adopted for the safe guarantee in probabilistic prediction.

5.1. Classification of Lane Change Situation

In real driving, there are many lane change necessity situations such as interchange section, a destination for some reasons, construction site ahead, or slow preceding vehicle as shown in Figure 5.1.

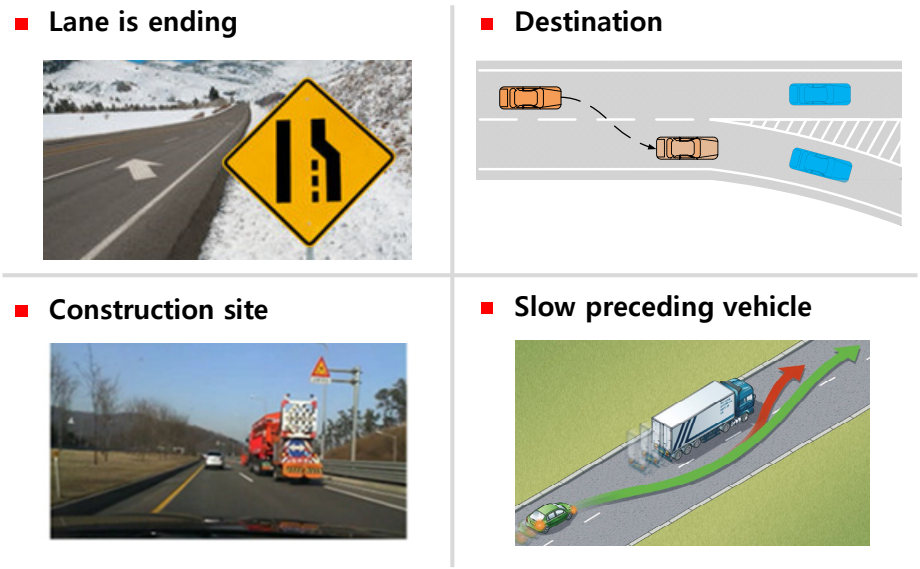

Figure 5.1 When should we change lanes?

The subject vehicle cannot maintain its desired speed or even driving if the driver tries to stay its lane. These various reasons for changing lane can be summarized as 2 cases. Firstly the subject vehicle is hard to keep its originating lane with desired speed. However, the subject vehicle does not need to change the lane in this situation taking a risk. Secondly, there is a

destination where the subject vehicle has to change lane such as highway exit or merging section.

For this reason, lane change or keeping mode is determined basically in real time. However if the subject vehicle needs to change its lane, the subject vehicle sets lane change mode.

Figure 5.2 shows the flow chart of motion planning algorithm for lane keeping and change decision. On a motorway, lane keeping is the maneuver performed by a driver most of the time. The subject vehicle keeps its lane to follow preceding vehicle or desired speed in lane keeping mode. However, the subject vehicle judges that lane change is needed or not. There are two reasons for changing lane, necessary lane change, and conditional lane change. The necessary lane change procedure has to change its lane for several reasons, so it does not need to determine lane change mode or direction which is already decided. If there is a risk to change lane, the decision algorithm classifies that the road has the time and space constraints or not. If the subject vehicle should change lane on the constrained road such as merge and split, it changes lane using reference acceleration calculation. If not, the decision algorithm calculates reference position calculation. The conditional lane change procedure decides lane change mode and direction decision. Since the conditional lane change does not need to accept the risk for changing lane. If the risk does not exist, the subject vehicle changes its lane.

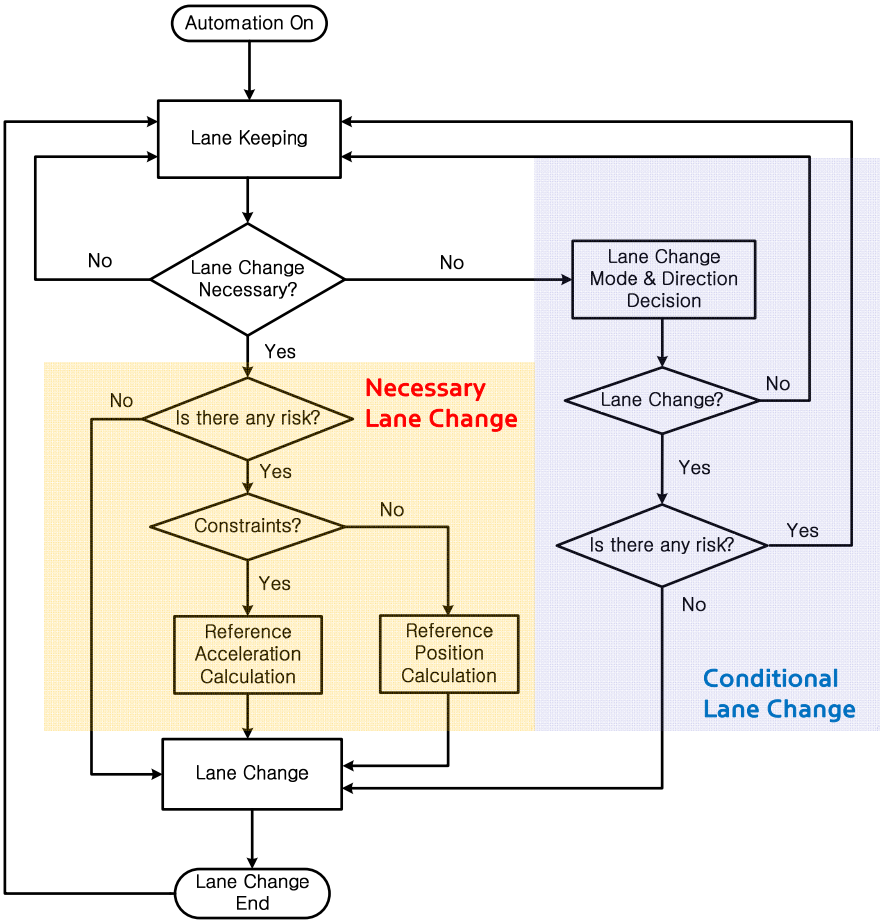

Figure 5.2 Flow chart of lane change motion planning

5.2. Lane Change and Keeping Mode Decision

Vehicle behavior can be divided two parts mainly, lane keeping and lane change motion. Since the control strategy of lane keeping and change for the automated driving vehicle is different, it is critical to determine vehicle motion.

The driving mode decision algorithm presents the vehicle modes of the subject vehicle to change or stay in the lane depending on the traffic circumstances. The fundamental task of the driving mode decision algorithm is to decide a desired mode of lane change or keeping.

Determining the driving mode from environmental information needs to consider lane change timing, lane change direction, and lane change risk. The lane change timing is determined by a cost function based decision method for necessity and point of time of lane change. The lane change direction indicates that which direction is safe to change the lane. If the subject vehicle cannot change a lane for various reasons, especially safety, then the lane change risk module prevents to start lane change.

5.2.1. Lane Change Timing and Direction

The lane change timing is considered by the cost function with the magnitude of acceleration, the minimum distance and the difference between desired and traffic flow of in-lane or side-lane.

In order to obtain the process time of lane change, the motion of vehicle should be previous research suggested the pattern of vehicle behavior when

human drivers drive vehicles [Wan11]. From this research, the lateral acceleration for lane change maneuver and the longitudinal acceleration for following preceding vehicle can be standardized as sinusoidal and trapezoidal shape. However, regarding ride quality, the sinusoidal shape has excessive acceleration jerk value. In this dissertation, the hyperbolic tangent path is suggested for low acceleration jerk. Figure 5.3 shows the general hyperbolic tangent and lateral acceleration which can be derived with second derivatives.

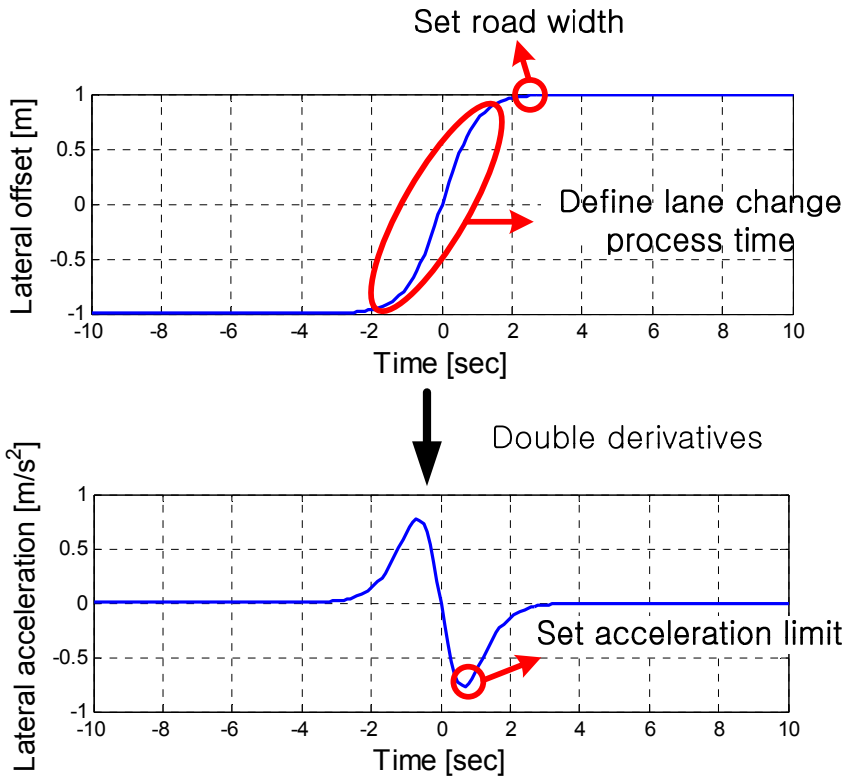

Figure 5.3 Hyperbolic tangent based lateral offset and acceleration

There are three issues to get the proper lateral acceleration: road width, lane

change process time, and acceleration limit. Fortunately, road width can be measured using information of vision sensor. The acceleration limit can be analyzed based on human driver data. Figure 5.4 shows the human driver data based acceleration analysis results.

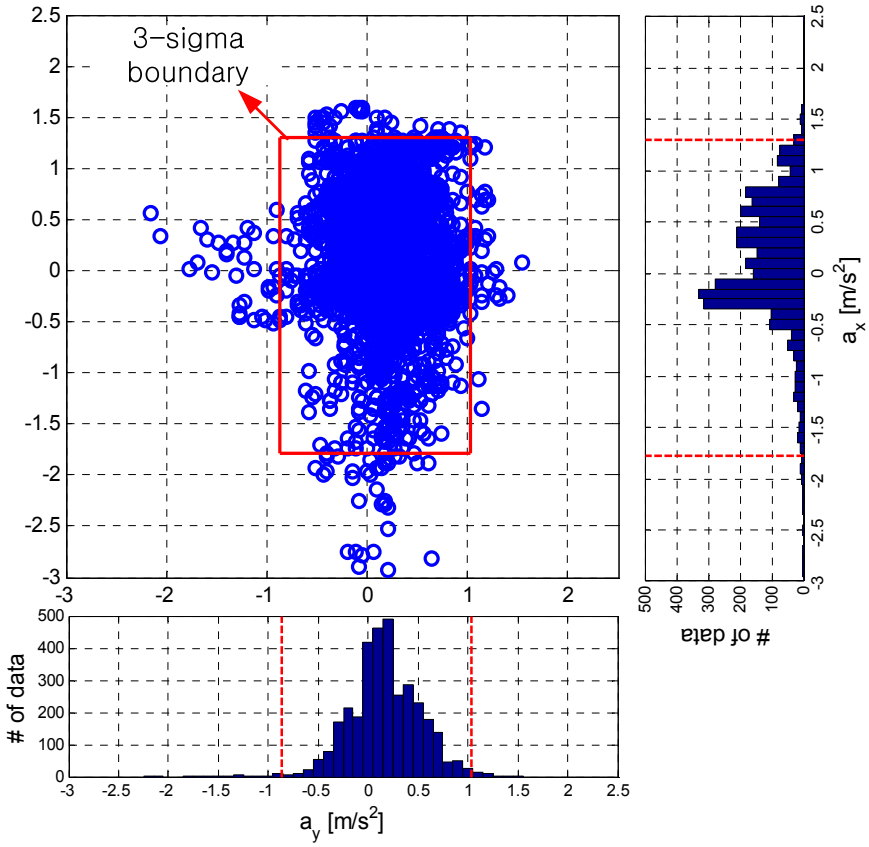

Figure 5.4 Human driver data based acceleration analysis (20 drivers)

From Figure 5.4, human drivers use lateral acceleration less than 1m/s^2 in almost situations. It is reasonable to set the maximum lateral acceleration,

1m/s^2.

Then, define the hyperbolic tangent path as follows:

$$e_y(t) = C_1 \cdot \tanh(C_2 \cdot t + C_3) + C_4 + v_{y,0} \cdot t + e_{y,0} + L_p \tag{5.1}$$

where C_* is a constant value from 1 to 4; subscript 0 denotes current information; L_p denotes preview distance; t denotes time parameter. There are two assumptions to derive the hyperbolic tangent based lateral acceleration; $v_{y,0}$ and $e_{y,0}$ denote the lateral velocity and the lateral offset when the subject vehicle starts to change lane. The positive and negative signs of $v_{y,0}$ and $e_{y,0}$ are the left and right motion of the subject vehicle.

Assumption 2. Lateral velocity, $v_{y,0}$, is zero.

Assumption 3. The lateral motion does not rely on the longitudinal velocity as shown in Figure 5.5. Thus, preview distance for lateral motion is always the same value.

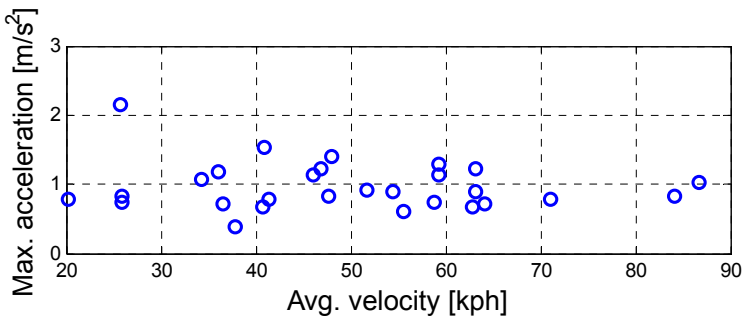

Figure 5.5 Human driver data based maximum acceleration for average velocity

When the subject vehicle crosses from the originating lane to next lane, it travels the distance between current lateral position and center of next lane. Then the constant C_1 and C_4 can be derived intuitively as,

$$C_1 = \frac{\pm W_{road} - e_{y,0}}{2} \tag{5.2a}$$

$$C_4 = \frac{\pm W_{road} - e_{y,0}}{2} \tag{5.2b}$$

where W_{road} denotes road width.

Let differentiate Eq. (5.1), lateral acceleration can be obtained as follows:

$$a_y(t) = -2 \cdot C_1 \cdot C_2^2 \tanh(C_2 \cdot t + C_3) \cdot \operatorname{sech}^2(C_2 \cdot t + C_3) \tag{5.3}$$

Using the lateral acceleration limit, $a_{y,\lim}$,

$$\begin{aligned} C_1 \cdot C_2^2 &= \frac{a_{y,\lim}}{a_{y,0}} \\ \Leftrightarrow C_2 &= \sqrt{\frac{\pm a_{y,\lim}}{a_{y,0}} \cdot \frac{1}{C_1}} \end{aligned} \tag{5.4}$$

where $a_{y,0}$ is the original maximum value of lateral acceleration as shown in Figure 5.1. From (5.2) to (5.4), positive values are left lane change motion, and negative values are right lane change motion.

As shown in Figure 5.1, since the hyperbolic tangent is origin symmetry, lane change start time should have displacement to the right. Let define the lane change process time, t_{LC}. The hyperbolic tangent based acceleration has to move to the right up to half of lane change process time. The interaction formula between the parameter C_2 and C_3 can be expressed as,

$$\frac{C_3}{C_2} = -\frac{t_{LC}}{2} \tag{5.5}$$

Consider lateral offset after lane change process time which is center position of next lane. Then an equality constraint can be obtained from Eq. (5.6).

$$e_y\left(t_{LC}\right) = W_{road} \tag{5.6}$$

From Eq. (5.1) to (5.6), the lane change process time can be written as,

$$t_{LC} = \frac{2}{C_2}\tanh^{-1}\left\{\frac{W_{road} - C_4 - e_{y,0}}{C_1}\right\} \tag{5.7}$$

Figure 5.6 shows the hyperbolic tangent based path and acceleration which reflects the parameters.

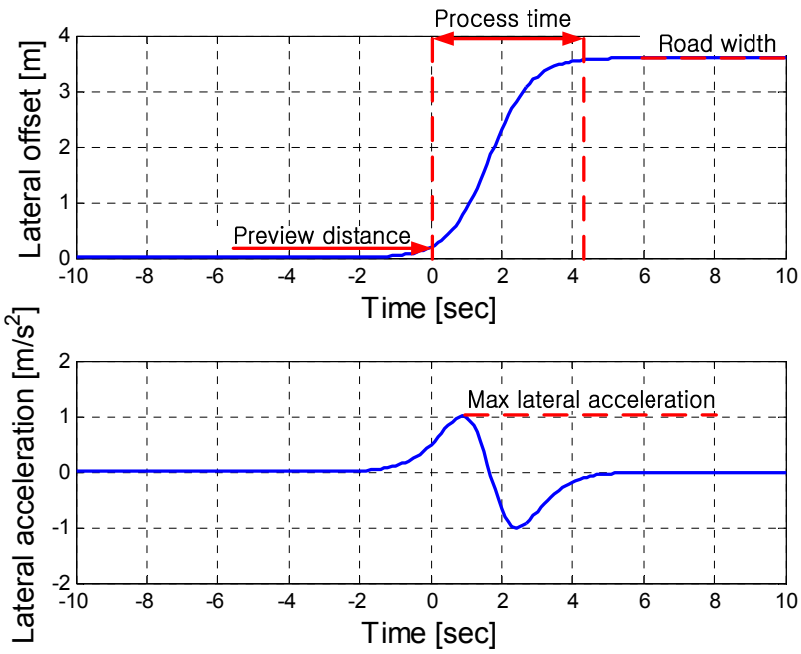

Figure 5.6 Hyperbolic tangent based lateral offset and lateral acceleration

In the case of the lane keeping, the subject vehicle only considers the preceding vehicle or the cut-in vehicle which is slower than its speed. As mentioned above, since the longitudinal acceleration is trapezoidal shape, it is allowable in terms of acceleration jerk. Figure 5.7 shows the trapezoidal shape longitudinal acceleration.

The delay between desired longitudinal acceleration and actual longitudinal acceleration is considered as a t_{ax}. t_{LK} denotes the lane keeping process time, and the longitudinal limitation value is $a_{x,\lim}$.

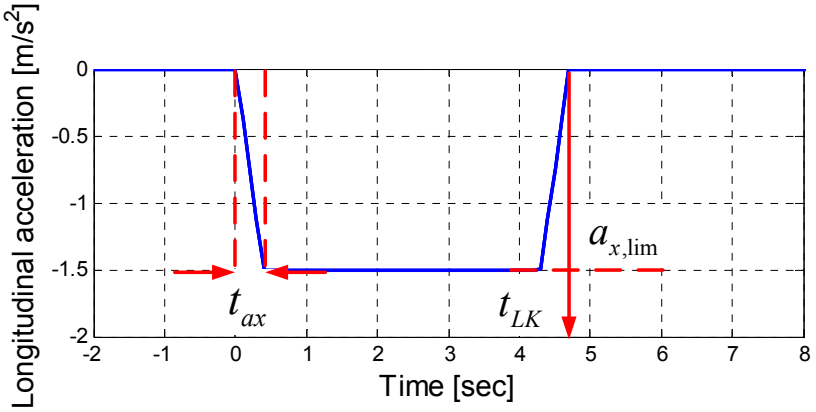

Figure 5.7 Trapezoidal shape based longitudinal acceleration

Let assume that t_{LK} and t_{LC} are same value. In that case, $a_{x,\lim}$ is depends on the desired clearance that the subject vehicle maintains. For instance, there are two vehicles, the subject, and the preceding vehicle. If the preceding vehicle is slower than the subject vehicle, the subject vehicle slows down

speed when it determines to keep its originating lane. Then $a_{x,\lim}$ can be defined as follows:

$$a_{x,\lim} = \frac{v_{f,N_P} - v_x}{t_{LK} - t_{ax}} \tag{5.8}$$

where subscript N_P and f denotes the final step of prediction horizon and the preceding vehicle, respectively.

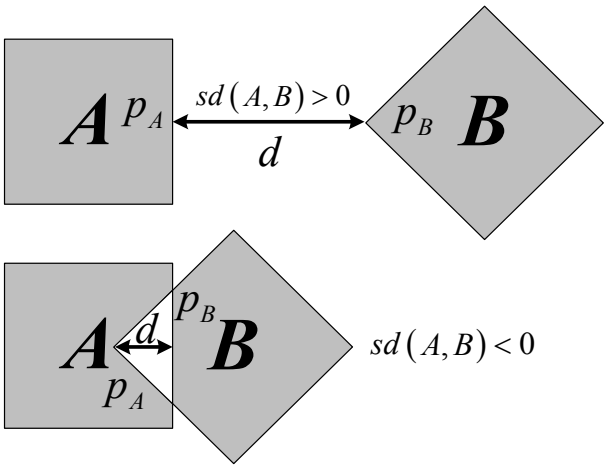

Figure 5.8 Conceptual diagram of signed distance

The definition of minimum distance which is calculated using predicted states of the subject and surround vehicles is the minimum distance between the subject and the preceding vehicle. We employ the minimum distance calculation approach that in [Schulman13]. The signed minimum distance, $sd(A,B)$, between two sets A and B that is nonzero for non-intersecting convex sets, especially the vehicle shape for this thesis, is defined as the

length of the smallest translation. This concept is illustrated in Figure 5.8. The signed minimum distance is presented in detail [Schulman13].

Recall that the predicted position of surround vehicles is provided. At any time instant t, let the predicted position vector of the target vehicle at time $t+k$ be denoted as $\mathbf{x}_{\text{target},t+k|t}$ and that of the subject vehicle be denoted as $\mathbf{x}_{t+k|t}$. The target vehicle is defined as a set of square shape $T_{k+t|t}$, and the subject vehicle is represented by a set of $S_{t+k|t}$. $T_{t+k|t}$ and $S_{t+k|t}$ are a function of the target and subject vehicle's position, respectively. The minimum distance can be expressed as follows:

$$sd\left(T_{t+k|t}, S_{t+k|t}\right) = dist\left(T_{t+k|t}, S_{t+k|t}\right) - penetration\left(T_{t+k|t}, S_{t+k|t}\right) \tag{5.9a}$$

$$dist\left(T_{t+k|t}, S_{t+k|t}\right) = \inf\left\{\|d\| \middle| (d+T) \cap S \neq \varnothing\right\} \tag{5.9b}$$

$$penetration\left(T_{t+k|t}, S_{t+k|t}\right) = \inf\left\{\|d\| \middle| (d+T) \cap S = \varnothing\right\} \tag{5.9c}$$

where d denotes the length of the smallest translation. (5.9) has to be always maintained positive.

The difference between desired vehicle speed and traffic flow speed is also considered. In previous researches, the traffic flow has microscopic and macroscopic point of view [Li04]. This thesis focuses on microscopic point of view for the traffic flow since local sensors of the subject vehicle can measure limited area.

The left, right, and in-lane traffic flows are defined using the recursive least

square method with forgetting factors. The cost function of recursive least square with forgetting factors is as follows:

$$J\left(\hat{v}_{flow}\right)=\frac{1}{2}\sum_{k=1}^{N}\lambda^{t-k}\left\|\overline{v}_k-\hat{v}_{flow}\right\|_2^2 \tag{5.10}$$

where λ denotes forgetting factor; t denotes current time; $\overline{v}$ denotes the average speed of object vehicles during a near future which can be estimated from the object vehicle prediction; $\hat{v}_{flow}$ denotes traffic flow.

A derivative of Eq. (5.10) equals zero which means a minimum cost. From this method, the traffic flow is derived as,

$$\hat{v}_{flow}(t)=\left(\sum_{k=1}^{t}\lambda^{t-k}\right)^{-1}\left(\sum_{k=1}^{t}\lambda^{t-k}\overline{v}_k\right) \tag{5.11}$$

Substitute $P(t)$ for $\left(\sum_{k=1}^{t}\lambda^{t-k}\right)^{-1}$ and simple mathematical techniques, traffic flow can be rewritten as,

$$\hat{v}_{flow}(t)=\hat{v}_{flow}(t-1)+P(t)\left(\overline{v}(t)-\hat{v}_{flow}(t-1)\right) \tag{5.12a}$$

$$P(t)=\frac{1}{\lambda}\left[P(t-1)-P(t-1)\left(\lambda I+P(t-1)\right)^{-1}P(t-1)\right] \tag{5.12b}$$

The traffic flow is defined as speed which makes the subject vehicle maintain safe area after the lane change or lane keeping procedure is finished. The preceding vehicle is much slower than the subject vehicle; a lane change is better than keeping. However, the difference is small enough, keeping the lane is much better than change.

Before the lane change decision, the lane change direction should be judged

by considering the status of an adjacent lane. There are various principles to decide the lane change direction.

- If destination exists for passing intersection or junction section of road, then the destination is a priority of lane change direction.
- If there is no destination to change originating lane of the subject vehicle,

→ The direction that has no adjacent vehicle is a priority to change.

→ If the both lanes to change are occupied, the lane change direction is defined using lane change risk compared between both lanes.

- Considering prohibited lane or area, such as guardrail or construction site.
- It is regarded as no advantages to change the lane if the front-side vehicle is behind the preceding vehicle.

Simple costs to compare left and right lane are expressed as,

$$J_{Left} = \begin{cases} J_{Right} - 1 & if\ LC_{des} = 1 \\ k_1 \cdot TTC_{Left} + k_2 \cdot C.P_{Left} & otherwise \end{cases} \tag{5.13a}$$

$$J_{Right} = \begin{cases} J_{Left} - 1 & if\ LC_{des} = 2 \\ k_1 \cdot TTC_{Right} + k_2 \cdot C.P_{Right} & otherwise \end{cases} \tag{5.13b}$$

where subscript Left and Right denote left lane and right lane; $LC_{des} = \{0 \quad 1 \quad 2\}$ denotes a destination of lane change; {0} for lane keeping, {1} for lane change to the left, and {2} for lane change to the right. The smaller cost value of left or right is selected.

Based on the above consideration, cost function is written as follows:

$$J_{LC} = \begin{cases} k_3 \min_k \left(sd_{LC,k} \right) + k_4 \left| v_{x,des} - \hat{v}_{flow,l} \right| + k_5 \max_k \left(a_{y,k} \right) & J_{Left} < J_{Right} \\ k_3 \min_k \left(sd_{LC,k} \right) + k_4 \left| v_{x,des} - \hat{v}_{flow,r} \right| + k_5 \max_k \left(a_{y,k} \right) & Otherwise \end{cases} \quad (5.14a)$$

$$J_{LK} = k_3 \min_k \left(sd_{LK,k} \right) + k_4 \left| v_{x,des} - \hat{v}_{flow,in} \right| + k_5 \max_k \left(a_{x,k} \right) \quad (5.14b)$$

$$k = 1, \ldots, N_p$$

where subscript *LC* and *LK* denote lane change and lane keeping; k_i is i-th weighting factors; subscript *in*, *l* and *r* are in-lane, left and right, respectively.

From the results of (5.14), the lane change or keeping mode is determined by small cost value compared to lane change and keeping cost. Compare the costs of the lane change and keeping and choose the smaller one to do chosen process.

Table 5.1 Weighting parameters

Symbol	**Value**	**Symbol**	**Value**	**Symbol**	**Value**
k_1	1	k_2	3		
k_3	10	k_4	1	k_5	10

5.2.2. Lane Change Risk Monitoring

The lane change risk constraints should be calculated to determine the lane change direction. For example, if a fast rear-side vehicle comes after to the subject vehicle crossing the lane, the hazardous situation would occur. The

lane change and keeping mode decision algorithm estimates risk situation using uncertainties of other vehicles. The lane change risk monitoring investigates a safety of the subject vehicle to judge risk during the lane change process. The lane change risk is monitored that process time is larger than *TTC*, or distance between the subject and other vehicle is less than a safe distance. If one or more of these conditions is violated, the lane change risk generates on flag signal to prevent the lane change. Also, the probabilistically predicted information of the subject and other vehicles can be obtained in Chapter 3. Therefore, even if risk constraint uses deterministic indices, *TTC,* and safe distance, but these indices are calculated in every predicted step. It means that the lane change risk monitoring uses probabilistic information for judging risk situation.

The lane change risk constraints can be written as,

$$\begin{aligned} &|c_k| > c_{safe} \\ &c_{safe} = c_{th} + \max_k(\sigma_{n,k}) \end{aligned} \tag{5.15a}$$

$$TTC_{n,k} \geq (t_{LC} - k \cdot t_{samp}),\ k = 1,\ldots,N_p \tag{5.15b}$$

where c denotes clearance; c_{safe} denotes minimum safety distance; c_{th} denotes acceptable minimum distance to avoid a collision; σ denotes uncertainties of the position of other vehicles; n denotes the target vehicle number; t_{samp} denotes the sampling time.

The lane change risk constraints are illustrated in Figure 5.9. s_0 is the longitudinal position of the subject vehicle and v_{rel} denotes relative velocity.

From Eq. (5.15), there are two constraints for monitoring lane change risk. The blue and red area as shown in Figure 5.9 is described by Eq. (5.15a) and (5.15b), respectively. Especially the constraints for (5.15b) have several areas which indicate to consider prediction steps of the constraints. It is evident that the red constraint decreases its area as prediction step goes.

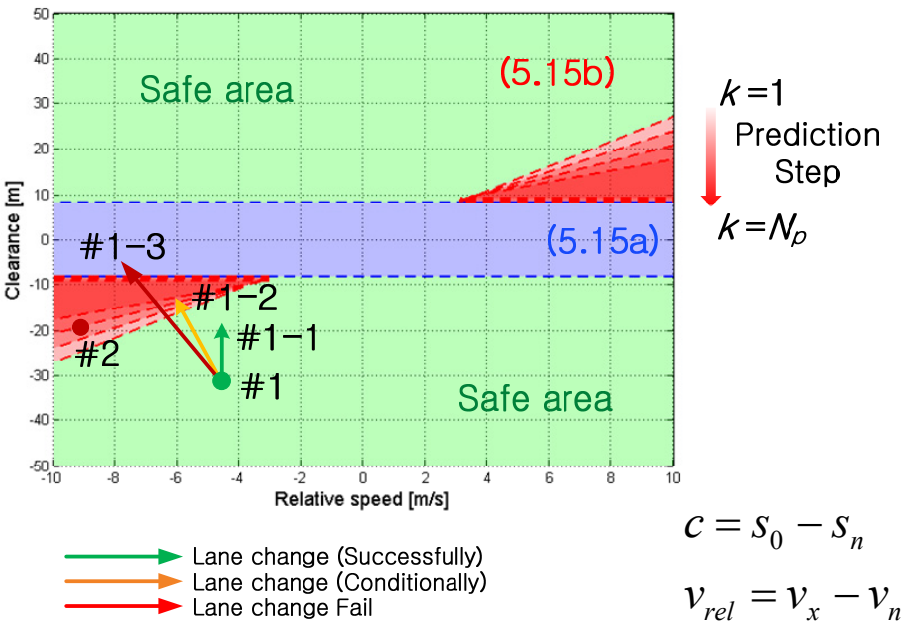

Figure 5.9 Risk monitoring for lane change procedure

Let assume that the subject vehicle wants to change its lane. However, there is a side-rear vehicle which is faster than the subject vehicle. The subject vehicle could be in danger in this situation. From this assumption, three detailed scenarios can be deduced.

First, #1 is in the lane change safe area. It can be predicted the subject vehicle can change lane successfully. If there are enough space and similar

relative speed, the subject vehicle can change its lane as #1-1. As the subject vehicle moves to next lane, required lane change time goes smaller. Accordingly, the lane change process can be still in progress whether the distance is larger than constraint for Eq. (5.15b). However, let assume that the side-rear vehicle has been accelerated more but not much. Then the #1 draws a trajectory like #1-2. In this case, the risk monitoring algorithm invests that whether the vehicle behavior will violate the *TTC* constraints considering prediction time. If the side-rear vehicle accelerates much more, then the #1 is expected to go #1-3. It means that clearance between the subject vehicle and side-rear vehicle is less than the constraint (5.15a). Therefore, the lane change risk algorithm prevents the subject vehicle from changing lane. If the subject vehicle tries to change lane in #2, the lane change risk also keeps off lane change.

5.3. Dynamics Limit Decision

If the lane change mode is activated, the subject vehicle starts to change the lane. However, the adjacent vehicle accelerates unexpectedly when the subject vehicle on its way to next lane. The subject vehicle can predict that a collision probability between subject vehicle and side-rear vehicle is increased. In this situation, the dynamics limit decision algorithm loosens lateral acceleration limit how much it needs using *TTC* information. The loosened lateral acceleration limit is defined as follows:

$$a_{y,\lim} = C_1 \cdot a_{y,0} \left\{ \frac{2}{TTC} \tanh^{-1} \left(\frac{W_{road} - C_4 - e_{y,0}}{C_1} \right) \right\}^2 \tag{5.16}$$

Eq. (5.16) can be calculated by Eq. (5.1) through (5.7).

Figure 5.10 describes the conceptual diagram of dynamics limit decision algorithm.

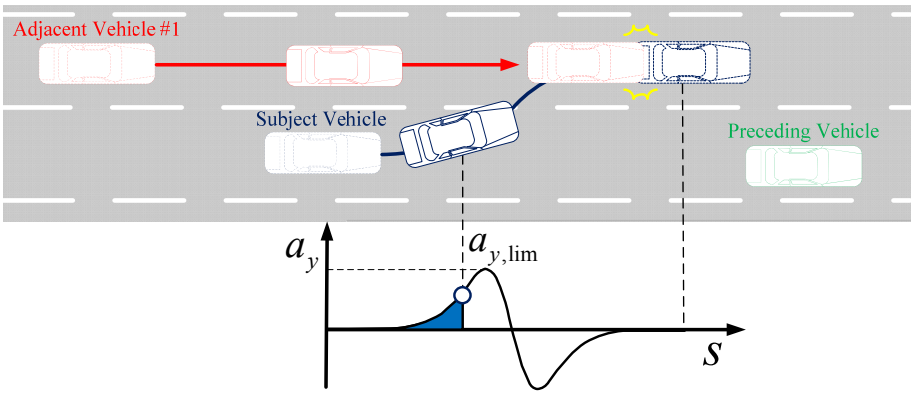

(a) Collision probability increased

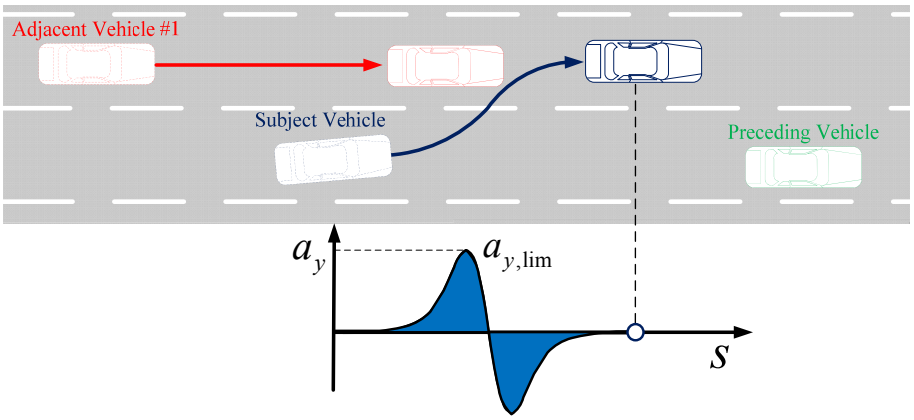

(b) Loosen maximum lateral acceleration

Figure 5.10 Dynamics limit decision example

5.4. Safe Driving Envelope Definition

After the lane change or keeping mode is determined, the subject vehicle needs constraints to guarantee safety in various situations, such as remaining in its lane, maintaining distance from other vehicles, or changing the lane. In lane keeping, human drivers maintain the safe distance from their vehicle to the preceding vehicle and are aware of potential cut-in vehicles. Otherwise, in the lane change situation, they confirm that there is enough space for the subject vehicle to change lanes, and also maintain the safe distance.

For the decision of the safe driving envelope to improve safety, a potentially hazardous situation should be considered. Various dangerous situations among the future behaviors of the surrounding vehicles could be classified roughly into three types. Firstly, if the preceding vehicle in the originating lane of the subject vehicle decelerates unexpectedly, then the collision probability between the preceding vehicle and the subject vehicle would be increased. Secondly, if the approaching vehicle in the adjacent lane accelerates during a lane change maneuver of the subject vehicle, then the collision between the approaching vehicle and the subject vehicle could be expected. Thirdly, there could be a potential risk of collision due to a sudden cut-in vehicle from the adjacent lane. Therefore, determining the safe driving envelope considers not only current states of the surrounding environment of the subject vehicle but also these potentially dangerous behaviors of the surrounding vehicles over a finite prediction horizon to improve safety.

As already mentioned above, there are two driving modes: lane keeping and lane change. For the lane keeping mode, the driving envelope is determined to keep the originating lane and maintain safety. Let us assume that the longitudinal or lateral clearances expected at the prediction time step k between the subject vehicle and surrounding vehicle are larger than the predefined threshold value. Then, the collision risk decreases, and the environmental envelope for e_y is determined to prevent a lane change. On the other hand, if the longitudinal or lateral clearances at the prediction time step k are expected to be smaller than the thresholds, this means that the collision risk is high. Therefore the environmental envelope for e_y is determined to remain in the originating lane while evading the approaching adjacent vehicle. Figure 5.11 describes the definition of the safe driving envelope to remain in the originating lane while maintaining safety with respect to the surrounding vehicles. In Figure 5.11, the pink ellipse indicates the area of the potential behavior of other vehicles with consideration of sensor uncertainty.

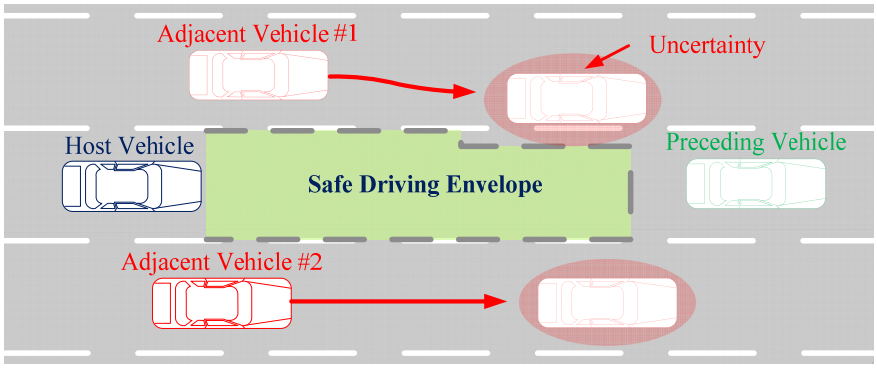

Figure 5.11 Environmental envelope to remain in the originating lane

For the lane change mode, the safe driving envelope is determined to change lane to the proper direction. Similar to the safe driving envelope for lane keeping mode, the current and predicted states of surrounding vehicles are considered. However, since the drivable area should be secured to next lane for the safety lane change, the safe driving envelope for lateral expands its area to next lane. The safe driving envelope for longitudinal considers a nearer vehicle between the preceding or the side-front vehicle to determine a drivable area. The preceding vehicle and the side-front vehicle should be regarded as one vehicle, since when the subject vehicle changes the lane the subject vehicle is located on both lanes, simultaneously. As the side-rear vehicles are already considered for driving mode decision to guarantee safety, the safe driving envelope is defined using current and predicted states of surround vehicles. The safe driving envelope for lane change mode is illustrated in Figure 5.12.

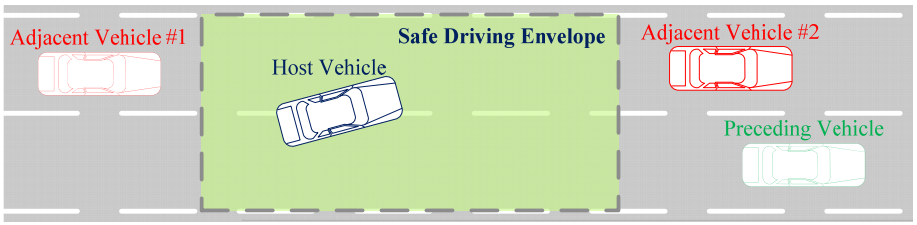

Figure 5.12 Environmental envelope in lane change mode

Before the determination of the environmental envelope to guarantee longitudinal safety, it is necessary to define the state of the target vehicle for the control of longitudinal acceleration. In the lane keeping mode, if the width of the safe driving envelope for e_y over a finite prediction horizon is large enough, then possible behaviors of adjacent vehicles are predicted to remain in their lanes. Then, the preceding vehicle is chosen as the target vehicle for the control of longitudinal acceleration. If there is no preceding vehicle in the originating lane or the clearance between the subject vehicle and the preceding vehicle is too long to consider, the desired velocity is set to follow, similar to the function of cruise control.

On the other hand, one of the neighboring vehicles in the adjacent lane could be expected to approach the originating lane of the subject vehicle or cut into the originating lane of the subject vehicle when the subject vehicle keeps its lane. The width of the environmental envelope for e_y could be smaller than the predefined minimum safety width. This means that the subject vehicle cannot avoid collision if it remains its originating lane. When human drivers recognize that the adjacent vehicle is entering the originating

lane of the subject vehicle, they tend to decelerate the subject vehicle [Moon10]. Therefore, the information of the target vehicle should be determined to improve safety and the acceptance of passengers simultaneously. According to previous research [Moon10], longitudinal states are generated by coupling the preceding vehicle in the originating lane and the potential target vehicle in the adjacent lane. The potential target vehicle means threatening or affecting the subject vehicle. The clearance and relative speed information of the potential target vehicle in the adjacent lane and the preceding vehicle from the subject vehicle are integrated for generating the longitudinal states to control. Figure 5.13 shows that the width of the safe driving envelope for e_y at the prediction time step *j* is expected to be smaller than the minimum safety width threshold. Then a weighting factor, ω_{LK}, is calculated to determine the longitudinal states of the target vehicle for longitudinal control as shown in Eq. (5.17).

$$\begin{aligned}\omega_{LK} &= f(k, \mathbf{Risk}), \qquad \left(0 < \omega_{LK} \le 1\right) \\ &= \max\left(\max\left(\frac{\min\left(TTC^{-1}{}_{k}, TTC^{-1}{}_{th}\right)}{TTC^{-1}{}_{th}}, 1 - \frac{\min\left(\mathbf{q}_k, \mathbf{q}_{th}\right)}{\mathbf{q}_{th}}\right)\right)\end{aligned} \tag{5.17}$$

where *k* in (13) denotes the prediction time step at which the width of the environmental envelope is smaller than the minimum safety width; and $\mathbf{q}$ indicates the non-dimensional warning index [Moon08]. The non-dimensional warning index uses braking and warning critical distances, which are functions of vehicle velocity, relative velocity, tire-road friction, the system delay, and a minimum headway time.

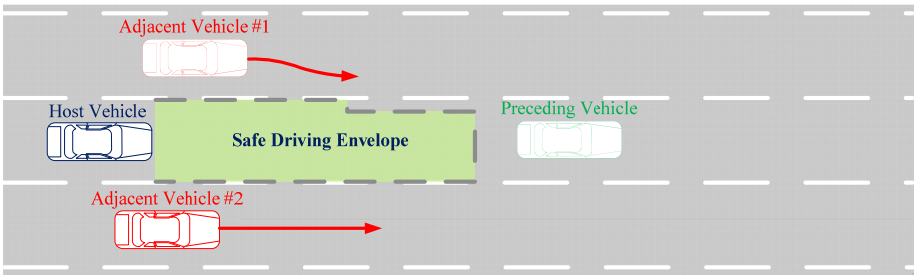

(a) Environmental envelope at the prediction time at $k = 0$

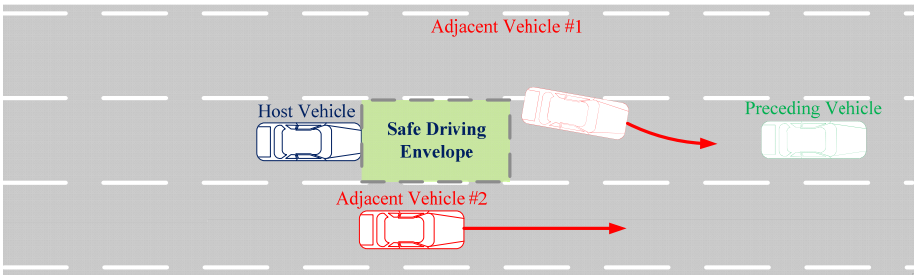

(b) Environmental envelope at the prediction time at $k = j$

Figure 5.13 Determination of the target vehicle for longitudinal acceleration control in a lane keeping mode

The collision risk between the subject vehicle and the potential target vehicle in the adjacent lane is assessed by using *TTC* and $\mathbf{q}$ at the prediction time step at which the width of the environmental envelope for e_y is smaller than minimum safety width. The thresholds for the warning index and inverse of the *TTC* are chosen as 1.19 and 0.21s^{-1}, respectively, based on the previous research [Moon08].

Consequently, the integration between the preceding vehicle in the originating lane and the potential target vehicle in the adjacent lane is defined as shown in Eq. (5.18).

$$s_{env,k} = \omega_{LK} \cdot s_{k,side} + \left(1 - \omega_{LK}\right) \cdot s_{k,in}, \qquad k = 1,\ldots,N_P \tag{5.18}$$

where s denotes longitudinal position; subscript *in* and *side* denotes in-lane vehicle and side-lane vehicle, respectively.

In the case of the lane change mode, the longitudinal states of the target vehicle are determined by the integration between the preceding vehicle and the surrounding vehicle in the adjacent lane of the lane change direction. For instance, if the subject vehicle changes its lane in a particular direction, then the longitudinal states of the target vehicle are determined by integration between the preceding vehicle and the adjacent vehicle in that direction.

Consequently, the condition for the safe driving envelope on lateral and longitudinal can be written as follows:

$$\mathbf{G}_k^T \cdot x_k \le h_k, \quad k = 1,\ldots,N_p \tag{5.19}$$

$$\mathbf{G}_k = \begin{bmatrix} 0 & 0 & 0 & 0 & 1 & 0 \\ 0 & 0 & 0 & 0 & 0 & 1 \\ 0 & 0 & 0 & 0 & -1 & 0 \\ 0 & 0 & 0 & 0 & 0 & -1 \end{bmatrix}^T \in \mathbf{R}^m$$

$$h_k = \begin{cases} \left[\frac{3}{2}W_{road}, \min\left(s_{lf}, s_{in}\right) - \tau_h \cdot v_x, \frac{1}{2}W_{road}, -s_{lr} - \tau_h \cdot v_x\right]^T & \textit{if} \text{ left} \\ \left[\frac{1}{2}W_{road}, \min\left(s_{rf}, s_{in}\right) - \tau_h \cdot v_x, \frac{3}{2}W_{road}, -s_{rr} - \tau_h \cdot v_x\right]^T & \textit{elseif} \text{ right} \\ \left[\frac{1}{2}W_{road}, s_{env} - \tau_h \cdot v_x, \frac{1}{2}W_{road}, -\tau_h \cdot v_x\right]^T & \textit{otherwise} \end{cases}$$

where the subscript *lf*, *rf*, *lr*, *rr* denote right-front, left-front, right-rear, and left-rear, respectively. If there is no side-front or preceding vehicle to consider, the predefined threshold value is replaced. As similar way, if there is no side-

rear vehicle, the predefined threshold value is replaced to define the safe driving envelope for longitudinal. τ_h is headway time which is the mean value of the time gap for collected driving data in the steady-state following situation.

5.5. Target States Decision

As mentioned above, after the lane change and keeping mode is determined, the appropriate velocity and lateral motion is necessary. However, it may occur that the subject vehicle has to conduct lane change in some situations such as merge, split or intersection. Then the automated driving vehicle needs to adjust its longitudinal position and velocity to change the lane for matching the traffic flow to next lane.

In order to change lane smoothly, the desired lateral position is needed. According to ***Assumption 3***, the lateral lane change motion does not depend on vehicle acceleration or velocity. It means that general lateral motion for lane change is similar in various situations.

For the lane keeping mode, since the subject vehicle needs to exist in the safe driving envelope regardless of preceding vehicle, the lateral position is determined the center of the originating lane. The longitudinal position and velocity are defined to follow the desired speed generally. However, if the preceding vehicle which is slower than the subject vehicle exists, the desired speed is set as velocity of preceding vehicle.

For the lane change mode, as far as safety is guaranteed, the velocity maintains the desired speed. However, the risk is predicted in near future, the longitudinal position and velocity of the subject vehicle are determined to follow the traffic flow of the target lane, the destination of the subject vehicle. In addition, we define the lateral position to change the lane like human driver.

It is assumed that the lateral acceleration is represented by a hyperbolic tangent shape when the subject vehicle changes lanes and the initial lateral velocity is zero as in ***Assumption 2***. Recall the Eq. (5.1), the lateral position for reference trajectory can be rewritten as follows:

$$e_{y,ref,t+k|t} = \begin{cases} C_1 \cdot \tanh\left(C_2 \cdot \left(t_{samp}k + t\right) + C_3\right) + C_4 + e_{y,0} + L_p & \left|e_{y,t+k|t}\right| < W_{road} \\ W_{road} & e_{y,t+k|t} \geq W_{road} \\ -W_{road} & e_{y,t+k|t} \leq -W_{road} \end{cases} \tag{5.20}$$

The lateral position has to change with time since the prediction horizon is not long enough to cover the entire lane change procedure. In addition, intuitively, the maximum reference lateral position of lane change is the center point of the adjacent lane. Thus, the maximum reference lateral position is the road width.

When the subject vehicle keeps its lane, it needs to maintain sufficient clearance between the subject vehicle and the preceding vehicle. For this reason, the desired clearance should be defined. The desired clearance is regarded as boundary problem because if the clearance from the subject vehicle to preceding vehicle is too far to consider, the subject vehicle does not need to accelerate to adjust this clearance. However, if the clearance is too close to be danger the subject vehicle should slow down its speed to be safe. The desired clearance is defined as follows:

$$c_{des} = \tau_h \cdot v_x + c_{safe} \tag{5.21}$$

where τ_h is a headway time gap.

In order to obtain the proper value of the time gap, human driver's manual

driving data had been collected and analyzed using the recursive least-squares method [Yi04]. Collected driving data in steady-state following situation is shown in Figure 5.14. According to the previous research [Moon08], the driving characteristics vary with age and sex. The mean value of time gap increases as the driver's age increases. Furthermore, the mean value of time gap of female drivers is larger than that of male drivers. Meanwhile, the mean value of the clearance at the zero speed for all of the drivers is almost 2 meters.

In this dissertation, in order to embrace driving characteristics of all of the drivers, the time gap, τ_h, is chosen as 1.36 sec which is the mean value of time gap for collected driving data in steady-state following situation. In addition, the minimum safety longitudinal clearance, C_{safe}, is chosen as 2 meters which is equal to the mean value of the clearance at the zero speed for all of the drivers.

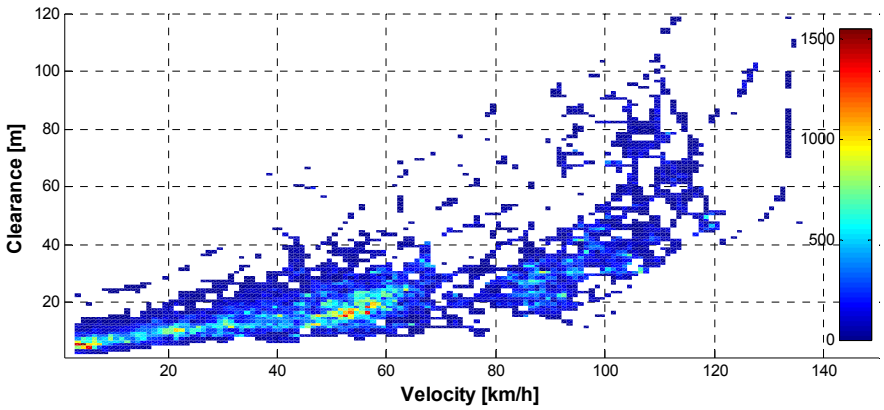

Figure 5.14 Driving characteristics of drivers in steady-state following situation

Let assume that the subject vehicle needs to change the lane but it is hard to change the lane for various reasons. Then the appropriate position and velocity are determined for the subject vehicle to change the lane safely using acceleration. In general, difficulties in lane change situation for human drivers are when traffic flow varies between the originating lane of the subject vehicle and adjacent lane. In this case, the drivers accelerate the subject vehicle to change a lane or to adjust speed of adjacent vehicle, and determine longitudinal position guaranteed safety. Similarly, the decision algorithm sets the speed of target vehicle which has the highest C.P as desired speed to follow. And an optimization problem is formulated to determine longitudinal position as follows:

$$\min_{s_{LC,k}} J_{pos,k} = l_1\left(s_{LC,k} - s_{TTC,k}\right)^2 + l_2\left|s_{LC,k} - s_{dist,k}\right| + l_3\left(s_{LC,k} - s_{CP,k}\right)^2 \quad (5.22a)$$

$$s.t.\ \ s_k < s_{\max,k} \quad (5.22b)$$

$$s_k > s_{\min,k} \quad (5.22c)$$

$$k = 1,\ldots,N_p$$

where s_{TTC}, s_{dist}, and s_{CP} denote positions which are calculated by *TTC*, distance from the subject vehicle, and C.P of surround vehicles. l_i is *i*-th weighting factor. $s_{\max}$ and $s_{\min}$ are maximum and minimum boundaries of longitudinal position defined by safe driving envelope for longitudinal. The reference s_{LC} is calculated at every step which makes minimize this cost function. Figure 5.15 shows that the cost based desired longitudinal position is calculated.

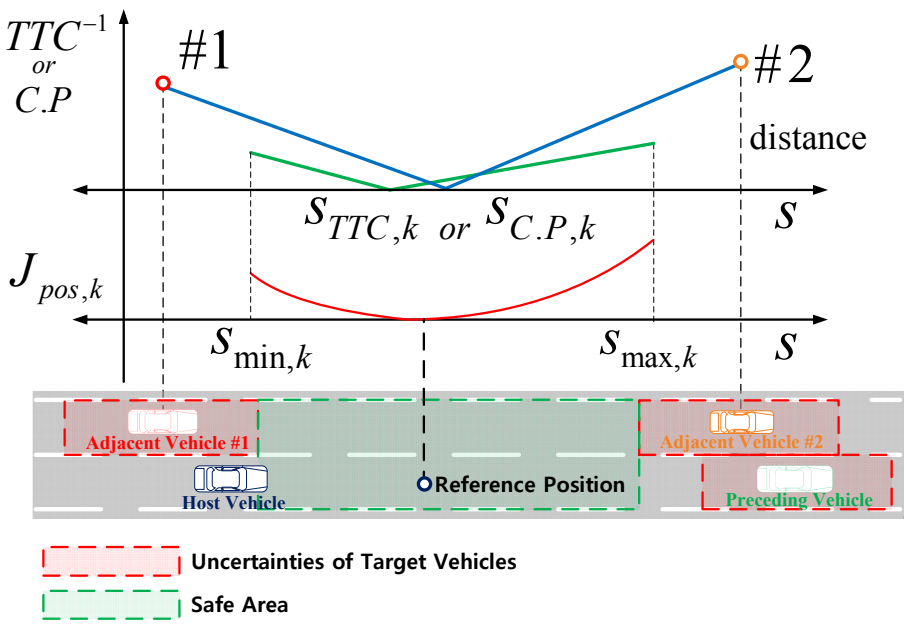

Figure 5.15 Desired longitudinal position calculation at *k* step

Figure 5.15 shows that the desired longitudinal reference position is calculated from the linear proportion of surrounding vehicles' inverse *TTC* and C.P as the blue line. The distance from the subject vehicle to desired longitudinal position is penalized for preventing the excessive acceleration. The longitudinal target position is determined by these considerations inside of minimum and the maximum area which is defined as the safe driving envelope. After the subject vehicle reaches the safe area, the driving mode decision module determines the lane change mode with information of surrounding vehicles.

However, if there are constraints of time or distance such as the merging section or slow preceding vehicle, the subject vehicle needs to change lane in

limited time. Furthermore, if the adjacent vehicles exist in side-lane, safe area is defined as constraints. Figure 5.16 shows an example for constrained situations.

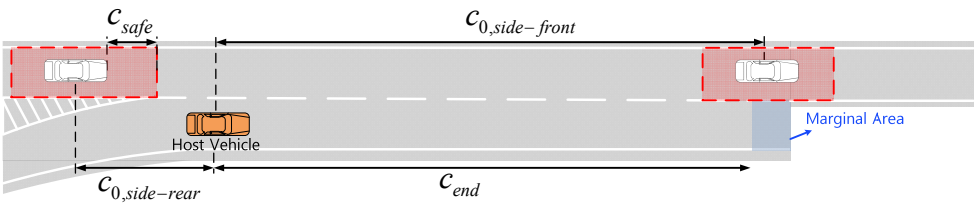

Figure 5.16 Lane change in limited situation

where c_0 denotes the initial clearance; c_{end} denotes the distance from the subject vehicle to road end considering marginal area; c_{safe} denotes the minimum safety distance as mentioned before as Eq. (5.15).

For simple and fast planning for lane change, there is an assumption as follows:

Assumption 4. The vehicle accelerates with constant acceleration when the vehicle changes the lane.

Using this assumption, the velocity profile is derived as shown in Figure 5.17.

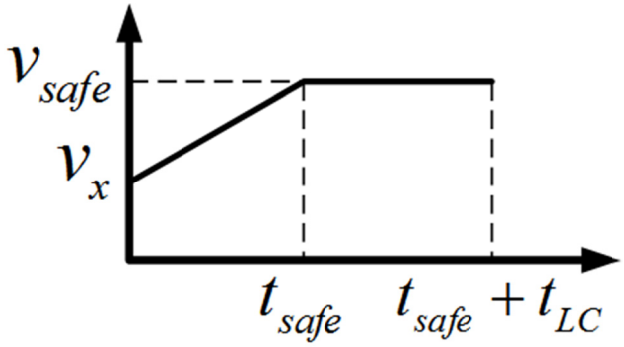

Figure 5.17 Velocity profile for constrained lane change

In order to solve this problem, three constraints are defined as follows:

side-rear constraint: $$\frac{v_x + v_{safe}}{2} t_{safe} - v_{side-rear} t_{safe} \geq c_{safe} + c_{0,side-rear} \tag{5.23a}$$

road constraint: $$\frac{v_x + v_{safe}}{2} t_{safe} + v_{safe} t_{LC} \leq c_{end} \tag{5.23b}$$

side-front constraint: $$\frac{v_x + v_{safe}}{2} t_{safe} + v_{safe} t_{LC} - v_{side-front}\left(t_{safe} + t_{LC}\right) \leq -c_{safe} + c_{0,side-front} \tag{5.23c}$$

where t_{safe} denotes the acceleration completion time.

If there is no side-rear vehicle, (5.23a) is always satisfied. Not only end road situation like merging section but also slow preceding vehicle does not exist, (5.23b) is also satisfied. Similarly, (5.23c) does not need to consider when the side-front does not exist.

The simulation results are presented in Figure 5.18. There are the side-front and side-rear vehicle which are faster than the subject vehicle. The initial speed of side-front and the side-rear vehicle is 80kph, and initial speed of the subject vehicle is 60kph. Distance to the end of the road is 150m.

The black area is side-front vehicle constraint, the red area is side-rear vehicle constraint, and the blue area is road constraint. An area which is overlapped all three of constraint is expressed as green. A cyan line means constant acceleration candidate which has bounds -3m/s^2 through 3m/s^2.

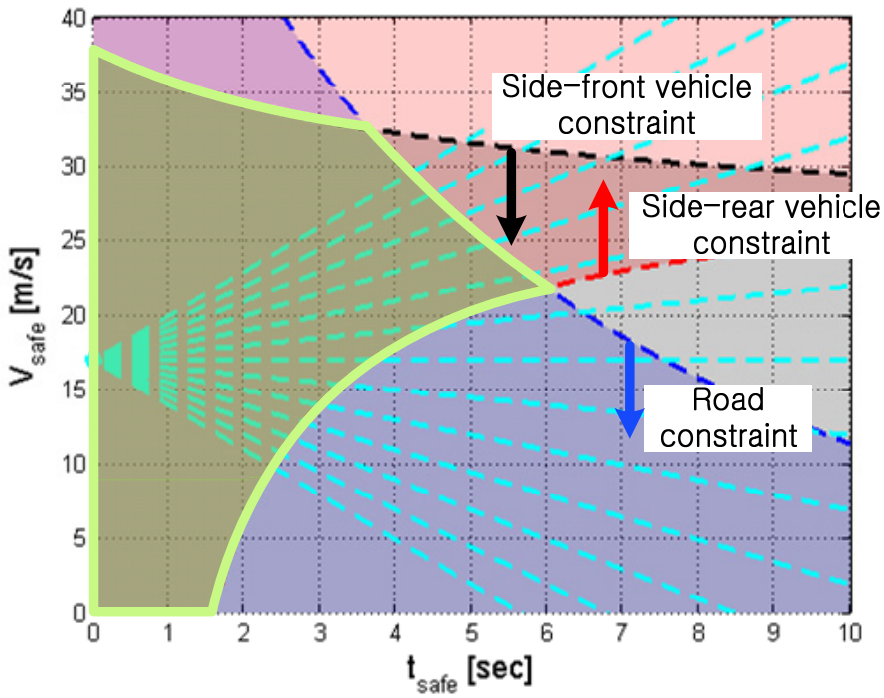

Figure 5.18 Constraints of limited situation

When the subject vehicle enters the road, acceleration, larger than zero, is considered primarily. If solutions which can be one or more are obtained by constraints, the proposed algorithm chooses minimum acceleration among possible candidates. However, if there is no solution in positive acceleration

proposed algorithm calculates the solution using negative acceleration candidate.

For changing lane in various situations, references to lateral and longitudinal states are calculated over the finite prediction horizon to keep or change the lane. The lateral and longitudinal references are operated in SMPC over the finite prediction horizon. The references can be rewritten as follows:

$$v_{x,ref} = \begin{cases} v_{flow} & \textit{if} \ \text{nonconstrained LC} \\ a_{x,ref} \cdot t_{safe} + v_x & \textit{otherwise} \end{cases} \tag{5.24a}$$

$$s_{ref,k} = \begin{cases} s_{LC,k} & \textit{if} \ \text{nonconstrained LC} \\ \frac{1}{2} a_{x,ref}{}^2 \cdot t_{samp} + v_x \cdot t_{samp} + s_{ref,k-1} & \textit{otherwise} \end{cases} \tag{5.24b}$$

$$x_{ref,k} = \begin{bmatrix} v_{x,ref} & 0 & 0 & 0 & e_{y,ref} & s_{ref} \end{bmatrix}^T \tag{5.24c}$$

Chapter 6

Stochastic Model Predictive Control based Vehicle Control

The disturbance analysis and formulation of the predictive control problem are presented. The model utilized for control is introduced and uncertainties are considered. The uncertainties include measurement errors, friction coefficient estimation, and model mismatch to define disturbance covariance. We employ the tightened constraints with uncertainties to formulate SMPC with chance-constraints. This optimization problem is solved at each step and the first terms of the optimal control sequences are applied to the system. To solve the MPC problem in MATLAB, FORCES which is designed to be utilizable in MATLAB is used as the solver [Alexander14]. The sampling time, t_{samp}, is chosen as 0.1 second and the length of the prediction horizon, N_P, is chosen as 20 steps.

6.1. Disturbance Analysis

In order to design the SMPC, the additive stochastic disturbance of the linear dynamic model should be defined. The stochastic disturbance w is identified using experimental data. The one-step state prediction of system model is compared with the measured data. The system model is discretized with a sampling time of 100ms.

$$e_k = x_{k+1} - \mathbf{A}_{l,k} x_k - \mathbf{B}_{l,k} u_k \tag{6.1}$$

Figure 6.1 shows error, e_k, for various circumstances such as acceleration, deceleration, lane change and lane keeping. An error is calculated by Eq. (6.1) to estimate the disturbance covariance as shown in Figure 6.1.

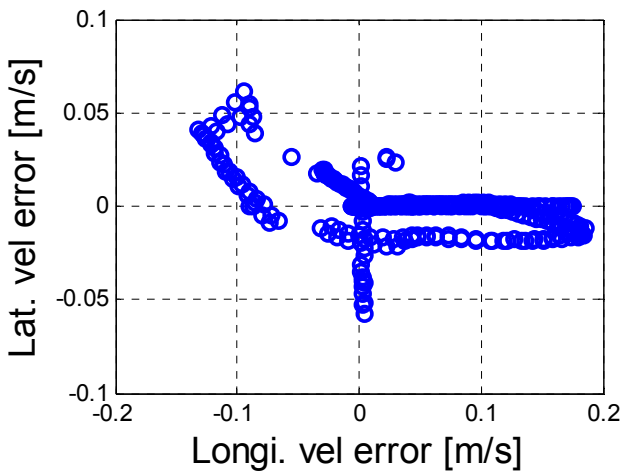

(a) Longitudinal and lateral velocity error

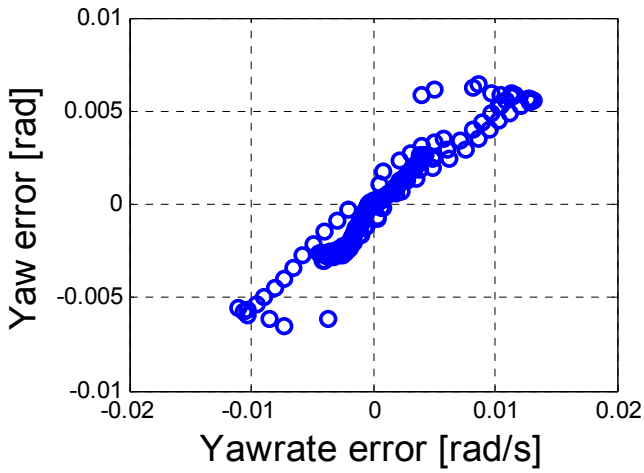

(b) Yaw rate and Yaw error

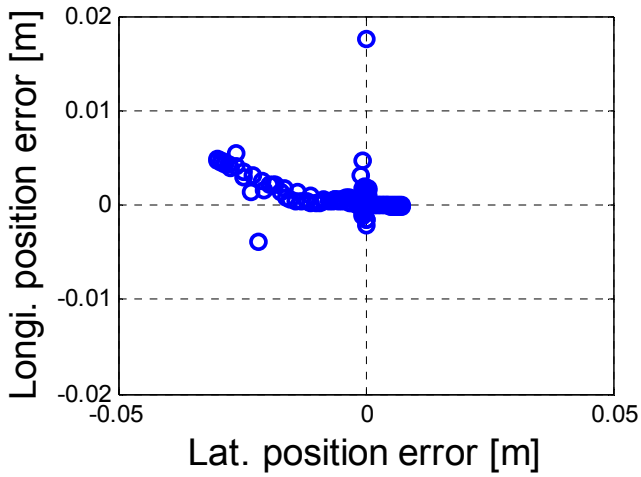

(c) Longitudinal and lateral position error

Figure 6.1 Disturbance analysis

Using the results of disturbances, the disturbance covariance is derived as,

$$\Sigma_w = diag\begin{pmatrix}0.120 & 0.043 & 0.009 & 0.003 & 0.018 & 0.002\end{pmatrix} \tag{6.2}$$

6.2. Stochastic MPC Problem Formulation

The proposed vehicle dynamics model and safe driving envelope described above are used to formulate a chance constrained receding horizon control problem. A chance constrained optimal control problem is solved to determine a sequence of control inputs which minimizes a given cost function. An SMPC is solved to determine a sequence of control inputs which are applied to the system. The solving process of the optimization problem which is repeated at each time step is formulated as follows:

$$\min_{u_k} \sum_{k=0}^{N_p-1} \mathbb{E}\left(\left\|x_{k+1|t} - x_{ref,k+1}\right\|_{\mathbf{Q}}^2 + \left\|u_{k|t}\right\|_{\mathbf{R}}^2 + \lambda\left\|\rho\right\|^2\right) \tag{6.3a}$$

$$s.t.\ \ x_{k+1|t} = \mathbf{A}_{l,k}x_{k|t} + \mathbf{B}_{l,k}u_{k|t} + \mathbf{D}_k w_k \tag{6.3b}$$

$$\Pr\left(\mathbf{G}_{k+1}^T x_{k+1} \le h_{k+1} + \rho\right) \ge p \tag{6.3c}$$

$$u_{k|t} \le u_{\max} \tag{6.3d}$$

$$u_{k|t} \ge u_{\min} \tag{6.3e}$$

$$x_{t|t} = x(t) \tag{6.3f}$$

$$k = 0,\ldots,N_{p-1}$$

where t denotes the current time instant; **Q** and **R** are the weighting matrices; λ denotes the weighting value; ρ denotes the slack variable; $x_{t+k,t}$ denotes the predicted subject vehicle state at time $t+k$ obtained by applying

the control sequence u_t to the vehicle model (6.3b) with initial condition (6.3f); (6.3c) is the chance-constraint to be satisfied with a specified probability; p denotes the tunable risk parameter; (6.3d) and (6.3e) are maximum and minimum constraints, $u_{\max} = \begin{bmatrix} \delta_{f,\lim} & a_{x,\max} \end{bmatrix}^T$ and $u_{\min} = \begin{bmatrix} -\delta_{f,\lim} & a_{x,\min} \end{bmatrix}^T$ for control inputs, respectively. In this paper, $\delta_{f,\lim}$ is 30deg, $a_{x,\min}$ is -5m/s^2, and $a_{x,\max}$ is 3m/s^2.

Since the chance constraints are one of the most important properties, the definition of chance constraint should be necessary. The predicted positions of target vehicles from the environment model are used to generate linear state constraints as Eq. (5.19).

$$\mathbf{G}_k^T x_k \le h_k \tag{6.4}$$

In general, collision avoidance constraints are non-convex such as Eq. (5.9), linear constraints of the form (6.4) can be obtained by using the collision checking approach [Schulman13]. For this reason, the safe driving envelope constraints are modified as convex. To account for the uncertainty in the target vehicles' predicted position, the vector h_k is assumed to be normally distributed as $N(h_k, \Sigma_k)$. Σ_k denotes the covariance of the vector h_k, and it is assumed $\Sigma_0 = 0$. Since x_k and h_k are stochastic variables, Eq. (6.4) reformulated as the following chance constraint:

$$\Pr\left(\mathbf{G}_k^T x_k \le h_k\right) \ge p \tag{6.5}$$

Dealing with the joint chance constraints, Eq. (6.5) includes calculating

integrals over multivariate probability density function, which is computationally formidable. In this dissertation, Boole's inequality is employed to transform the joint constraints (6.5) into univariate constraints. The Boole's inequality and univariate constraints are shown in ***Theorem 1*** [Ashwin15].

Theorem 1. In probability theory, for any finite or countable set of events, the probability that at least one of the events happens is no greater than the sum of the probabilities of the individual events. Formally, for a countable set of events A_1, A_2, A_3, …, we have

$$\Pr\left(\bigcup_i A_i\right) \le \sum_i \Pr\left(A_i\right) \tag{6.6}$$

$$\Pr\left(g_{k,i}^T x_k \le h_{k,i}\right) \ge p_i \quad i = 1,\ldots,m \tag{6.7}$$

where $g_{k,i}$ and $h_{k,i}$ are the i-th rows of matrix $\mathbf{G}_k$ and vector h_k, respectively; m is the number of rows in the matrix $\mathbf{G}_k$. From the Boole's inequality, $\{p_i\}_{i=1}^m$ which denotes tunable risk parameter should satisfies

$$\sum_{i=1}^m p_i \ge p \tag{6.8}$$

p_i represents the safe associated with the i-th constraint, and Eq. (6.8) constrains the total risk to be higher than the desired value p.

However, the optimization problem Eq. (6.3) cannot be solved directly due to the presence of the stochastic disturbance w in Eq. (6.3b) and the chance constraints in Eq. (6.3c). The constraints should be tightened to account for the state uncertainty.

Table 6.1 lists the weighting matrices of the SMPC problem in Eq. (6.3).

Table 6.1 Weighting matrices of SMPC formulation

Symbol	**Value**	**Symbol**	**Value**
Q	diag(15,0.05,4.5,10,0.5,,1.5)	**R**	diag(200,200)
λ	10000		

6.3. Closed-loop Paradigm Approach

The system as Eq. (6.3b) is assumed to be subject to the soft constraint as Eq. (6.3c). The case of several soft constraints, each of which is to be satisfied with a given probability, can be treated similarly by generating the necessary online conditions for each of the constraints. This framework also includes hard constraints, which are obtained if p is 1. Note that Eq. (6.3c) only includes x_k, the predicted future states are function of both the current and predicted inputs. Therefore, the approach applies to general linear input and state constraints.

Using the closed-loop paradigm introduced in [Kouvaritakis00], the state and input trajectories predicted at time k are decomposed for i = 0,1,… as follows:

$$x_k = z_k + e_k \tag{6.9a}$$

$$u_k = K_k x_k + b_k \tag{6.9b}$$

where $b_k \in \mathbf{R}^2$ denotes optimization variables, $b_{k+i} = 0$ for $i \geq N_P$, for finite prediction horizon N_P. $K_k \in \mathbf{R}^{2\times 6}$ is a stabilizing feedback gain for the vehicle system. e_k denotes k-th error which is propagated by stochastic error as Eq. (6.2).

By substituting (6.9a) and (6.9b) into (6.3b) we obtain,

$$z_{k+1} = \mathbf{\Phi}_k z_k + \mathbf{B}_{l,k} b_k \tag{6.10a}$$

$$e_{k+1} = \mathbf{\Phi}_k e_k + \mathbf{D}_k w_k \tag{6.10b}$$

where $\mathbf{\Phi}_k = \mathbf{A}_k + \mathbf{B}_k K_k$; w_k denotes an additive stochastic disturbance which is normally distributed with covariance Σ_w in Eq. (4.7). The following assumption is applied.

Assumption 5. $\mathbf{\Phi}_k$ is Hurwitz. It means that the system is controllable.

Assumption 6. The system has perfect state feedback, i.e., $x_0 = z_0$. This implies $e_0 = 0$ with probability 1.

The distributions of e_k is determined using the distribution of e_0 and w_k for the uncertainty propagation over the prediction horizon because of the separation of the deterministic and probabilistic components of x_k with tunable parameter *p*. The e_k is distributed as $N(0,\Sigma_k)$. Σ_k is covariance which is defined same of the covariance of h_k. The predicted covariance can be written as follows:

$$\Sigma_{k+1} = \mathbf{\Phi}_k \Sigma_k \mathbf{\Phi}_k^T + \mathbf{D}_k \Sigma_w \mathbf{D}_k^T \tag{6.11}$$

The benefit of using the closed-loop formulation (6.9) is emphasized by (6.11). If the feedback gain is chosen to stabilize the system, the predicted covariance is smaller than that in the case of the open-loop formulation. A common choice of the sequence of feedback gains K_k is the solution of the finite horizon LQR problem for the time-varying system.

According to Kouvaritakis et al., a first step towards guaranteeing that the constraint (6.5) is met in closed-loop is to ensure that the constraint is satisfied by the predicted dynamics at all time instants *k*. Necessary and sufficient conditions for this are given as ***Theorem 2*** [Kouvaritakis10]**.**

Theorem 2. At time k, and for a given prediction horizon N_P and vector of optimization variables $b_k^T = \begin{bmatrix} b_k^T & b_{k+1}^T & \dots & b_{k+N_P-1}^T \end{bmatrix}$, the prediction of the LPV system (4.7) satisfy the probabilistic constraint of (6.5) if and only if:

$$\mathbf{G}_k^T \mathbf{H}_{k,i} b_k + \mathbf{G}_k^T \mathbf{\Phi}_{k,i} z_k \le h_k - \gamma_i \tag{6.12}$$

where $\mathbf{H}_{k,i} = \begin{bmatrix} \mathbf{\Phi}_{k,i-1}\mathbf{B}_{l,k} & \dots & \mathbf{B}_k & 0 & \dots & 0 \end{bmatrix}$ and γ_i for each $i = 1,2,\dots,m$ is defined as the minimum value such that

$$\Pr\left\{ \mathbf{G}_k^T \left(\mathbf{\Phi}_{i-1}\mathbf{D}_k w_k + \dots + \mathbf{D}_k w_{k+i-1} \right) \le \gamma_i \right\} = p \tag{6.13}$$

From the ***Theorem 2***, the probabilistic constraint can be tightened to solve the optimization problem. Therefore, (6.5) can be rewritten as,

$$\mathbf{G}_k^T z_k \le h_k - \gamma_k \tag{6.14a}$$

$$\Pr\left(\mathbf{G}_k^T e_k \le \gamma_k \right) = p \tag{6.14b}$$

where $\gamma_k \in \mathbf{R}^m$ is tightened parameter; m is row number of matrix $\mathbf{G}_k$.

Let think about meaning of (6.12b). It is probability that k-th error, $\mathbf{G}_k^T e_k$, is not larger than γ_k. As Σ_k is propagated with an increasing k, e_k and γ_k are also propagated. It is very important to decide γ_k for considering the error in predictive control.

However, it is difficult to calculate γ_k at once because γ_k is a vector. Recall that Eq. (6.8) shows sum of individual tunable risk parameter is greater

than total risk tunable value p. For this reason, the tightened parameter can be calculated individually. Eq. (6.12a) can be rewritten as,

$$g_{k,i}^{T} z_{k,i} \le h_{k,i} - \gamma_{k,i}, \quad i = 1,...,m \tag{6.15}$$

Intuitively, $\gamma_{k,i}$ is function of p computed from the quantile function of a univariate normal distribution which means inverse function of cumulative normal distribution with $g_{k,i}^{T} e_{k,i} \sim N\left(0, g_{k,i}^{T} \Sigma_k g_{k,i}\right)$.

$$\gamma_{k,i} = \sqrt{2 g_{k,i}^{T} \Sigma_k g_{k,i}}\, erf^{-1}\left(2 p_i - 1\right) \tag{6.16}$$

where erf^{-1} is the inverse error function; p_i denotes i-th risk tunable parameter which has range, $0.5 < p_i < 1$.

The simulation results of uncertainty propagation are presented in Figure 6.2. It is shown that the length and width of vehicle (red) is 4.8m and 1.85m, respectively.

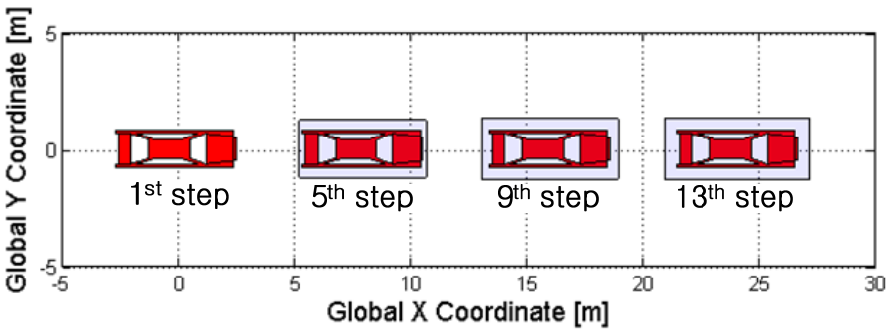

(a) Uncertainty propagation at p = 0.99

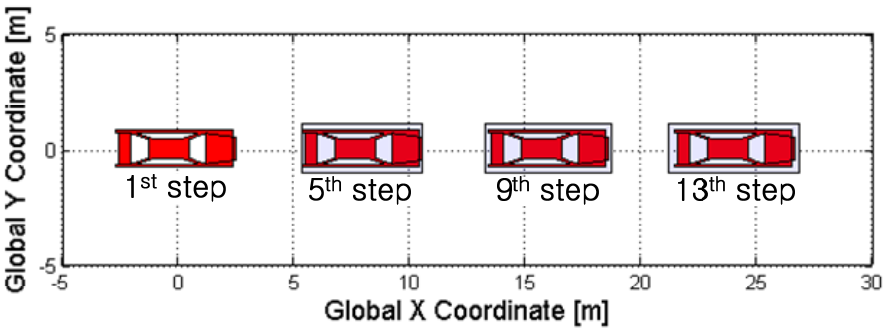

(b) Uncertainty propagation at p = 0.90

Tunable risk parameter	Longitudinal max. error	Lateral max. error
0.99	0.64 *m*	0.49 *m*
0.90	0.35 *m*	0.28 *m*

(c) Uncertainty maximum propagation results

Figure 6.2 Uncertainty propagation simulation results

Obviously, the large tunable risk parameter p means nearly hard constraints. Otherwise, if the tunable risk is small the uncertainty propagation is also small.

Therefore, by replacing (6.3c) with the tightened of constraints (6.14a) and using the feedback law (6.9), the following optimization problem is obtained to be solved at each time step,

$$\min_{b} \sum_{k=0}^{N_p-1} \mathbb{E}\left(\left\| z_{k+1} - x_{ref,k+1} \right\|_{\mathbf{Q}}^2 + \left\| K_k z_k + b_k \right\|_{\mathbf{R}}^2 + \lambda \left\| \rho \right\|^2 \right) \tag{6.17a}$$

$$s.t.\ \ z_{k+1} = \mathbf{\Phi}_k z_k + \mathbf{B}_{l,k} b_k \tag{6.17b}$$

$$u_k = K_k z_k + b_k \tag{6.17c}$$

$$\mathbf{G}_{k+1}^{T} z_{k+1} \leq h_{k+1} + \rho - \gamma_{k+1} \tag{6.17d}$$

$$u_{k|t} \leq u_{\max} \tag{6.17e}$$

$$u_{k|t} \geq u_{\min} \tag{6.17f}$$

$$z_0 = x(t) \tag{6.17g}$$

$$k = 0, \ldots, N_{p-1}$$

6.4. Adaptive Uncertainty Propagation

According to the previous section, the tunable risk parameter p is a dominant term of uncertainty propagation. In addition, the error between states of the vehicle dynamics model and states of the vehicle sensors depends on the motion of the subject vehicle. Considering the error using disturbance analysis including excessive motion is not good in aspect of performance. As mentioned in section 6.1, e_k is propagated based on Σ_k. Σ_k is effected by Σ_w which is derived from disturbance analysis with various situations, so the error using Σ_k cannot reflect the present status of the subject vehicle. In Eq. (6.16), since γ_k is calculated using large error and covariance, constraints are more tightened than real constraints reflected present motion and disturbances. For this reason, the tunable risk parameter should be calculated with reflecting vehicle motion which affects model uncertainties.

According to ***Theorem 1***, p_i which is the tunable risk parameter of i-th row of constraints can be calculated individually. Note that p_i is probability of $g_{k,i}^T e_{k,i} \le \gamma_{k,i}$. If $\gamma_{k,i}$, which is function of p_i from Eq. (6.16), is equal to $g_{k,i}^T e_{k,i}$, $g_{k,i}^T e_{k,i} \le \gamma_{k,i}$ is always satisfied. However, the real-time error which is reflected the present vehicle motion cannot be obtained in general k-th step except the first step because the vehicle sensors and exterior sensors have only present information. Therefore, the assumption is necessary to calculate the tunable risk parameter.

Assumption 7. The tunable risk parameter p_i can be defined using only the real-time error.

The real-time error between states which is derived by vehicle model and measured by external and vehicle sensors is necessary to be calculated every step in real-time. Recall the states and inputs of the vehicle dynamics model, $x = \begin{bmatrix} v_x & v_y & \gamma & e_\psi & e_y & s \end{bmatrix}^T$ and $u = \begin{bmatrix} \delta_f & a_x \end{bmatrix}^T$. With previous control inputs, u_{-1}, and previous and current states from sensors, x_{-1} and x_0, the real-time error can be derived as follows:

$$e_{real-time} = x_0 - \mathbf{A}_l x_{-1} - \mathbf{B}_l u_{-1} \tag{6.18}$$

where $e_{real-time} \in \mathbf{R}^6$.

From this purpose, we need to calculate the error for present in real time and define γ_k to deal with this error. This real time error can be derived with (6.1) in every step. From the concept of SMPC, since the all of error and uncertainties are assumed to normally distributed in the previous section, real time error, $e_{real-time}$, is also distributed as $N(0, \Sigma_w)$.

From Eq. (6.3), (6.10), and (6.11), e_1 and Σ_1 should be considered to derive the first step of the constraints for SMPC formulation as,

$$e_1 = \mathbf{D}_0 e_{real-time} \tag{6.19a}$$

$$\Sigma_1 = \mathbf{D}_0^T \Sigma_w \mathbf{D}_0 \tag{6.19b}$$

According to (6.19), the error needs to real-time error to propagate adaptive uncertainty; however, the covariance is same as nominal SMPC because the real-time error is normally distributed by same error derived by disturbance

analysis.

As shown in Figure 6.3, a green section is described as $g_{1,i}^T e_1 \le \gamma_{1,i}$. Since the tunable risk parameter p_i is defined by the area of the green section, cumulative distribution function is considered to compute parameter p_i. Therefore, the probability of real time error to maximum error can be computed from the cumulative normal distribution function, blue section in Figure 6.3.

$$p_i = \frac{1}{2}\left[1 + erf\left(\frac{g_{1,i}^T e_1}{\sqrt{2 g_{1,i}^T \Sigma_1 g_{1,i}}}\right)\right], \quad i = 1,\ldots,m \tag{6.20}$$

where m is row number of constraints.

This probability can be tunable parameter p_i to calculate γ_k considered the real time error.

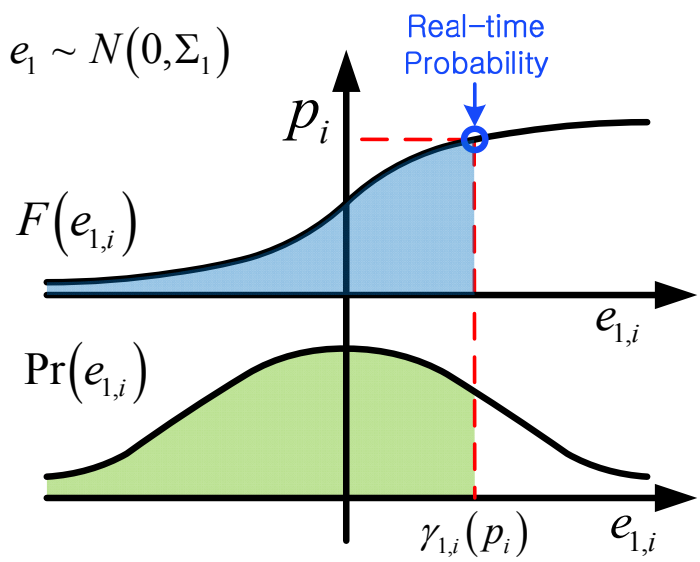

Figure 6.3 Conceptual diagram of adaptive uncertainty propagation

To show the effectiveness of the proposed algorithm, simulation results of the algorithm are compared with constant tuned parameter p. The simulation results indicating the time history of vehicle behavior are depicted in Figure 6.4. The preceding vehicle (green) is driven at 60kph keeping its lane with 70m of initial clearance from the subject vehicle (blue and black) which cruises at 60kph, also. The black and blue vehicles are controlled by the algorithm which has constant and adaptive uncertainty propagation, respectively. The adjacent vehicles (red) move at 80kph. Figure 6.4 (a) shows initial condition of the simulation scenario. The subject vehicle decides to change its lane to the left, but there is risk of collision with adjacent vehicles. The subject vehicle accelerates to change lane. Since the blue vehicle has small uncertainty reachable set to consider, it can change the lane. However, the black one cannot change the lane due to the existence of preceding vehicle, as shown in Figure 6.4 (b). Figure 6.4 (c) shows the blue vehicle changes the lane successfully, and the black one slows down to change lane after the adjacent vehicle passes.

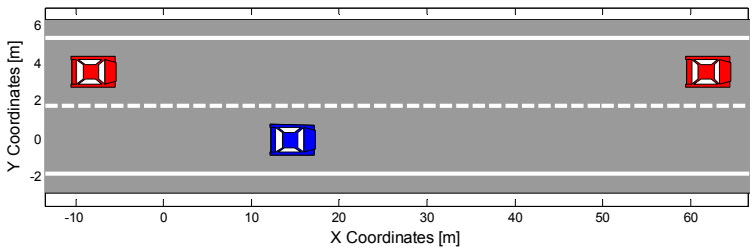

(a) Initial condition of lane change scenario.

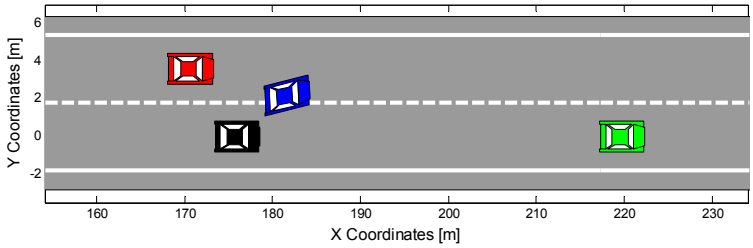

(b) The blue vehicle starts to change lane and the black vehicle maintain its lane.

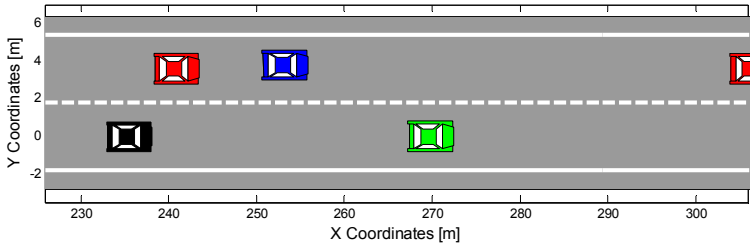

(c) The blue vehicle changes lane successfully and the black vehicle slows down due to preceding vehicle.

Figure 6.4 Trajectory of a lane change scenario

The simulation results via computer simulation are presented in Figure 6.5. Figure 6.5 (a) shows the uncertainty reachable set area for vehicle position. In lane keeping, since the dynamics model has little uncertainties, it can decide change lane with performance and conservative. However, because the algorithm with constant uncertainty propagation has always error reachable set, the black vehicle determines that there is a risk to change lane. Figure 6.5 (b) shows lateral acceleration which exists under the lateral acceleration limitation. The blue vehicle accelerates and keeps its speed about 80kph, but

the black vehicle slows down to keep originating lane as shown in Figure 6.5 (c).

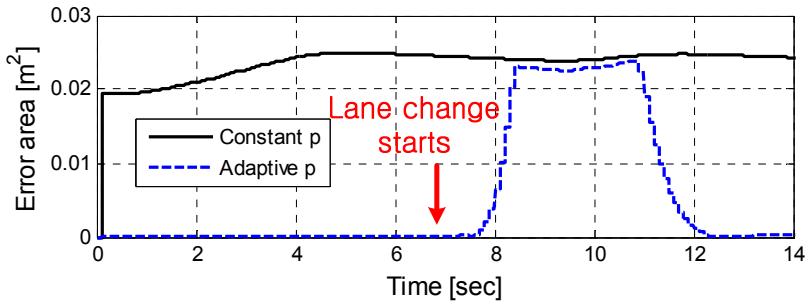

(a) Uncertainty propagated area for vehicle position

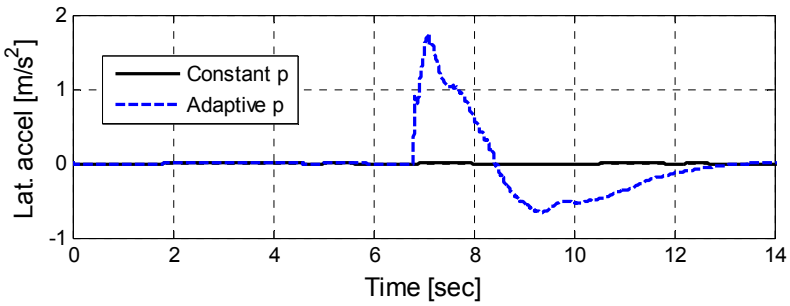

(b) Vehicle acceleration

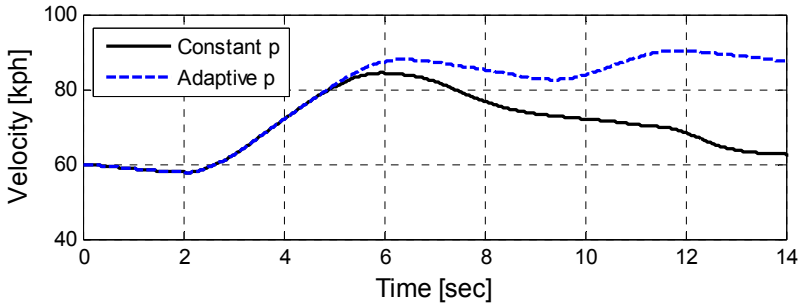

(c) Vehicle velocity

Figure 6.5 Adaptive uncertainty propagation simulation results

Chapter 7

Evaluation

The proposed automated driving control algorithm is evaluated through computer and hardware-in-the-loop (HiL) simulations. The commercial vehicle software, CARSIM and Automotive simulation model (ASM), and MATLAB/Simulink are used for the computer and HiL simulation. In order to show the effectiveness of the proposed algorithm, the simulation scenario is constructed to imitate a driving situation which could commonly happen in a real world. In addition, simulation studies are conducted to verify the appropriate decision for the proposed algorithm under the additional disturbances. HiL tests are conducted on test track to show the similarity between the driving characteristics of human drivers and that of the proposed algorithm. In addition, the vehicle tests are conducted on real road.

7.1. Computer Simulations

7.1.1. Comparison between Probabilistic and Deterministic Prediction

The proposed algorithm has been evaluated through computer simulations using CarSim and MATLAB/Simulink. In order to show the effectiveness of the proposed control algorithm using probabilistic prediction, simulation results of control algorithm based on SMPC using deterministic prediction of surrounding vehicle are compared with those of the proposed algorithm. The primary features of the control algorithm based on SMPC using deterministic prediction can be represented as follows:

Remark 1. The environmental envelope defined using deterministic prediction is defined without respect to the potential behavior of the surrounding vehicle.

Remark 2. The target vehicle for the control of the longitudinal acceleration is generated by integrating the current states of the preceding vehicle in the originating lane and those of the vehicle in the adjacent lane.

Since an automated driving control algorithm should operate in a wide operating region, the performance of the proposed algorithm should be verified in various driving situation. In this dissertation, comparison of probabilistic and deterministic is conducted via computer simulation.

In order to compare the decision performance, simulation scenario is set that the risk prediction is difficult. In other words, after the subject vehicle judges present risk and determines to change lane, the other traffics change their

motion suddenly. Simulation scenario is designed to reproduce the risky highway situation as shown in Figure 7.1.

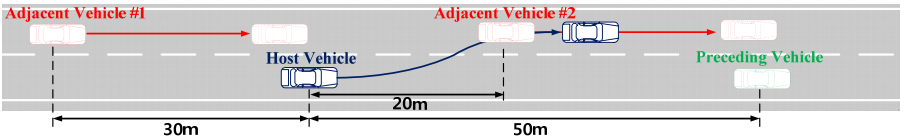

(a) Start to change lane

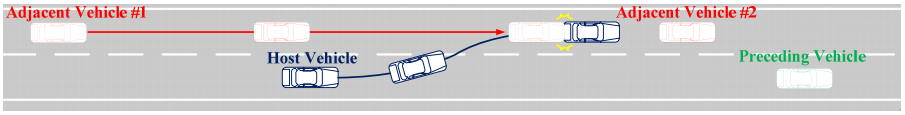

(b) Risk prediction during lane change

Figure 7.1 Simulation scenarios of unexpected traffic

In this situation, initial velocities of adjacent vehicles are set to 80kph and those of subject vehicle and preceding vehicle are set to 60kph. The subject vehicle starts to accelerate until it judges lane change safe. However, the adjacent vehicle #1 accelerates to prevent lane change of the subject vehicle. The initial clearance between the subject vehicle and the adjacent vehicle #1 is 30 meters, and between the subject vehicle and the adjacent vehicle #2 is 20 meters. Also, the initial clearance between the subject vehicle and the preceding vehicle is 50 meters.

Simulation studies have been repeated 11 times for comparing control algorithms which are probabilistic and deterministic prediction. Each simulation has different acceleration magnitude of adjacent vehicle #1 0 to $2m/s^2$ with interval $0.2m/s^2$.

The simulation results are presented in Figure 7.2. Figure 7.2(a) shows the difference between vehicle trajectory using probability prediction and that using deterministic prediction. Depending on the acceleration of the subject vehicle #1, the automated driving algorithm using deterministic prediction cannot change lane successfully. The longitudinal velocity of the subject vehicle is described in Figure 7.2(b). The subject vehicle accelerates similar in both prediction at first, but the automated driving vehicle using probabilistic prediction maintains its speed. Compare the results of Figure 7.2(a) and (b) together, lane change timing using probabilistic method is determined a few seconds later. It means that the subject vehicle using probabilistic prediction secures the distance between the subject vehicle and other vehicles farther than that using deterministic prediction. As shown in Figure 7.2(c), the clearance between the subject vehicle and the adjacent vehicle #1 violates safe distance when the deterministic prediction is used. Especially, the clearance of the subject vehicle using probabilistic prediction has robust performance when the motion of other traffic changes. Figure 7.2(d) shows that clearance between the subject vehicle and adjacent vehicle #1 is kept very similar. It means that the proposed algorithm has robust performance. In other words, algorithm using deterministic prediction does not have reproducibility and robustness. To show the effectiveness of using probability prediction for the safe lane change, risk indices, collision probability and *TTC*, are plotted in Figure 7.2(e) and (f). The average value of collision probability distribution using probabilistic prediction is smaller than that using deterministic prediction. Differently, the average value of *TTC* data using probabilistic

prediction is larger than that using deterministic prediction. It means that the probabilistic prediction is much safer than deterministic prediction.

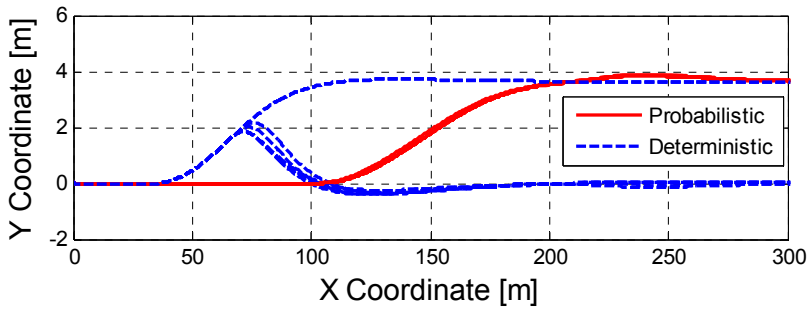

(a) Vehicle trajectory

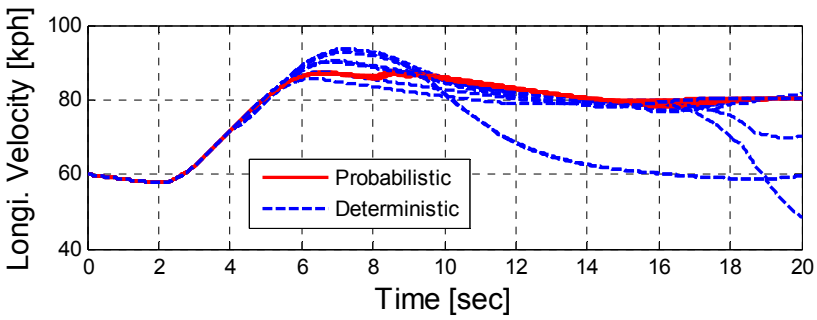

(b) Longitudinal velocity

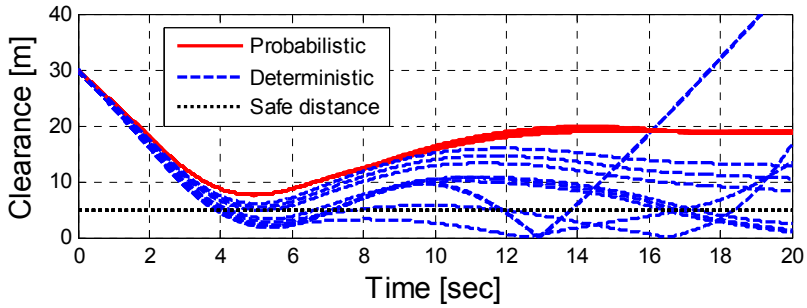

(c) Clearance between the subject vehicle and adjacent vehicle

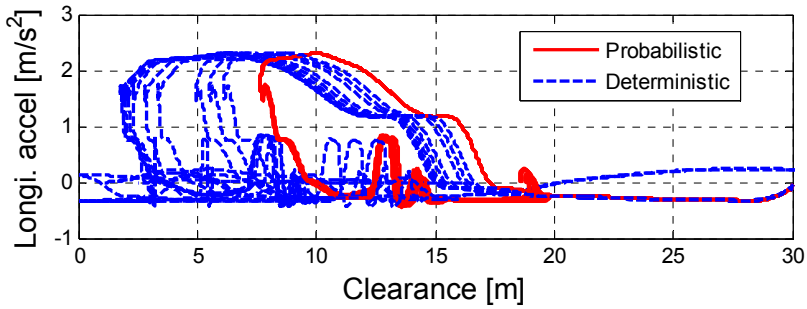

(d) Longitudinal acceleration and clearance

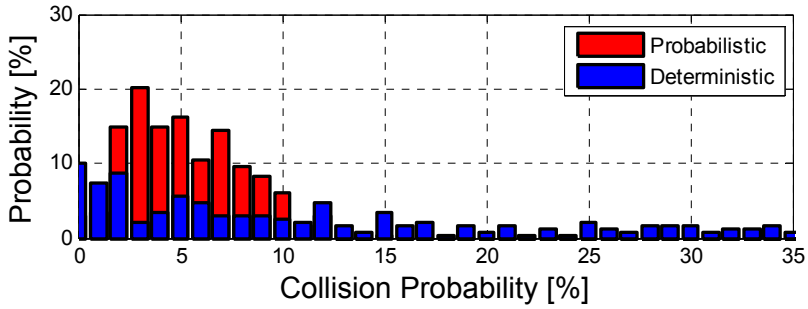

(e) Collision probability

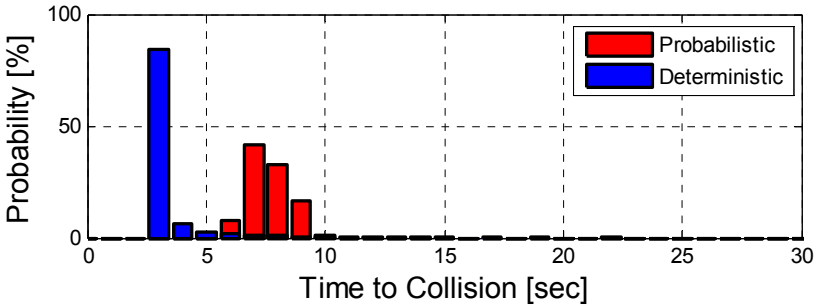

(f) Time to collision

Figure 7.2 Comparison performance results between probabilistic and deterministic prediction

7.1.2. Constrained Scenario Simulation

The simulation scenarios are designed to reproduce the merging motorway situation as shown in Figure 7.3. In this situation, initial velocity of the subject vehicle is 60kph and adjacent vehicles are 80kph. The side-front vehicle exists 40m ahead from the subject vehicle. Since the road is end 150m ahead, the subject vehicle should make a decision how to change lane. The subject vehicle determines its behavior different when the distance between the side-rear vehicle and the subject vehicle is 25m and 35m.

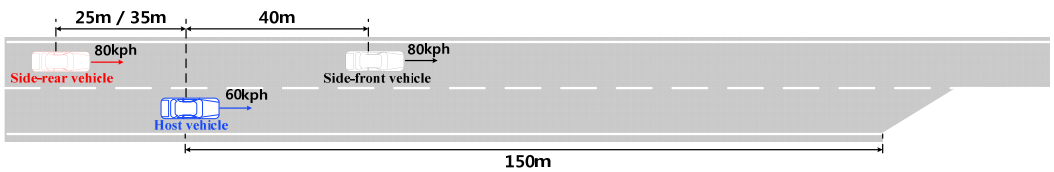

Figure 7.3 Simulation scenarios of merging section

The simulation results when the side-rear vehicle exist rear from the subject vehicle at 25m are presented in Figure 7.4. Figure 7.4(a) shows the difference between the desired and actual vehicle trajectory. As shown in Figure 7.4(b), the risk monitoring calculates that it is risky situation to change lane. Thus, the subject vehicle slows down its speed as shown in Figure 7.4(c). The side-rear vehicle has passed the subject vehicle and after the safety distance between the side-rear and the subject vehicle is secured at 5.2 sec. Figure 7.4(b) shows that the driving mode is activated and lane change direction indicates change the lane to the right. Also, the subject vehicle starts to

accelerate for satisfying traffic flow of the right lane. As shown in Figure 7.4(d), the lateral acceleration has reasonable maximum value and lane change procedure time. Figure 7.4(e) and (f) show the position of the vehicles at certain time. Especially in Figure 7.4(f), it is obvious that the subject vehicle determines to let the side-rear vehicle go to change lane safely. When the subject vehicle enters the merging section, the proposed algorithm calculates longitudinal acceleration to follow. In Figure 7.4(g), the side-front and road constraints can be satisfied in enough time. However, the side-rear constraint will be violated in very near future. So the proposed algorithm selects deceleration among the acceleration candidates.

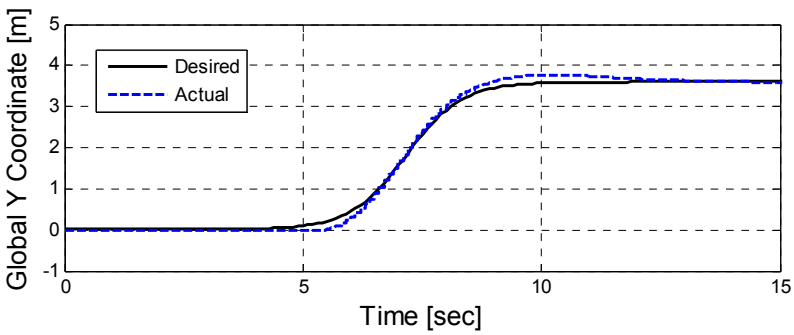

(a) Vehicle trajectory

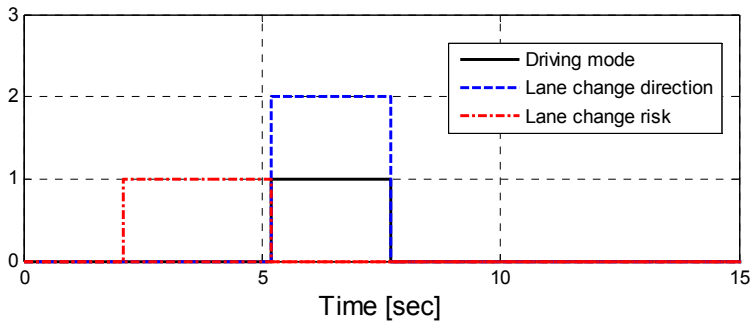

(b) Driving mode, lane change direction, and risk monitoring

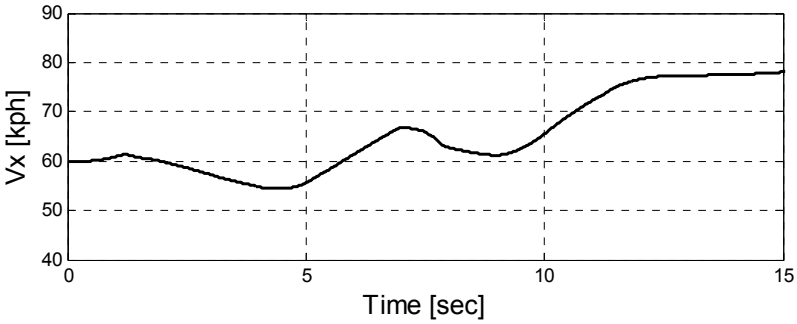

(c) Vehicle velocity

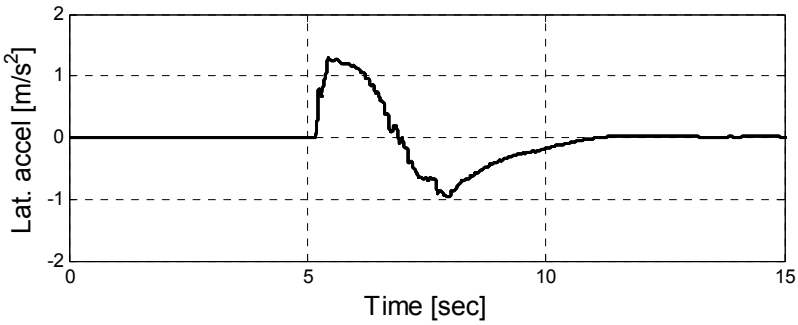

(d) Lateral acceleration

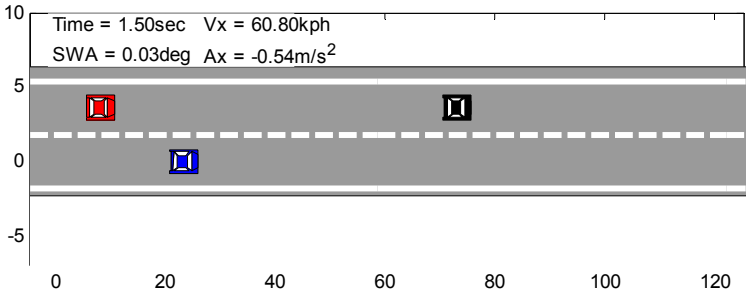

(e) Vehicle position at 1.5 sec

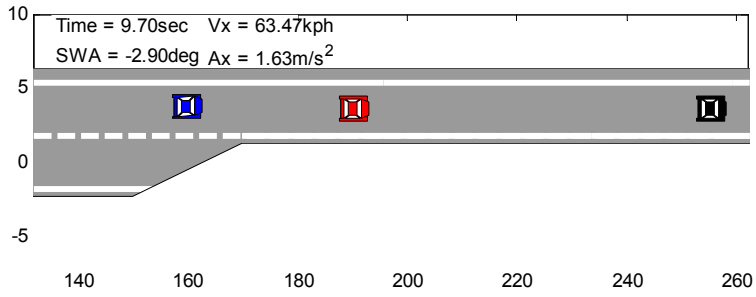

(f) Vehicle position at 9.7 sec when lane change ends successfully

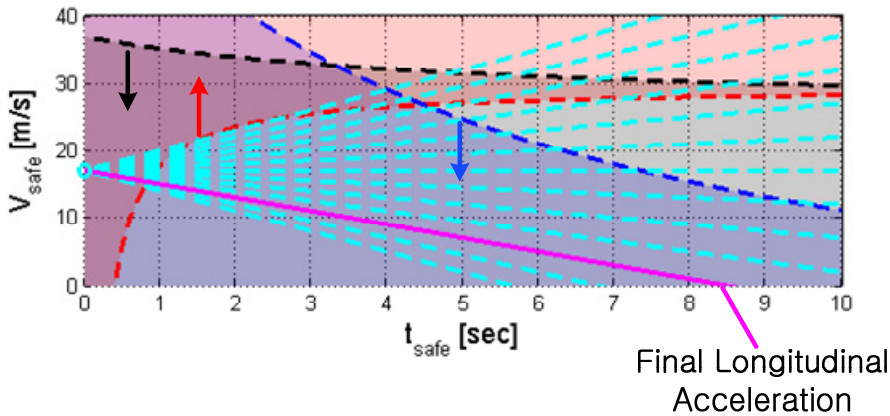

(g) Planning longitudinal acceleration to change lane safely in merging section. Side-front vehicle, side-rear vehicle, and road constraint satisfy lower area of black dashed line, upper area of red dashed line, and lower area of blue dashed line.

Figure 7.4 Simulation results when distance between the side-rear and the subject vehicle is 25m

Consider that the distance between the side-rear and the subject vehicle is

35m. The Figure 7.5 shows the simulation results. Figure 7.5(a) shows the difference between the desired and actual vehicle trajectory. As shown in Figure 7.5(b), the risk monitoring calculates that there is no risk to change lane. From the risk monitoring result, the subject vehicle can change the lane to the right. The driving mode and lane change direction are activated. Thus, the subject vehicle accelerates to adjust traffic flow of the right lane as shown in Figure 7.5(c). As shown in Figure 7.5(d), the lateral acceleration has reasonable maximum value and similar shape between desired and actual values. Figure 7.5(e) and (f) show the position of the vehicles at certain time. In Figure 7.5(f), the subject vehicle passes the side-rear vehicle ahead and changes lane safely. When the subject vehicle enters the merging section, the proposed algorithm calculates longitudinal acceleration to follow. In Figure 7.5(g), all of the constraints can be satisfied in enough time. So the proposed algorithm selects acceleration among the acceleration candidates.

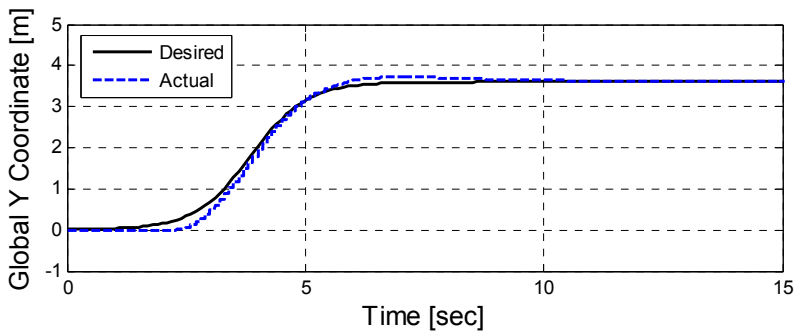

(a) Vehicle trajectory

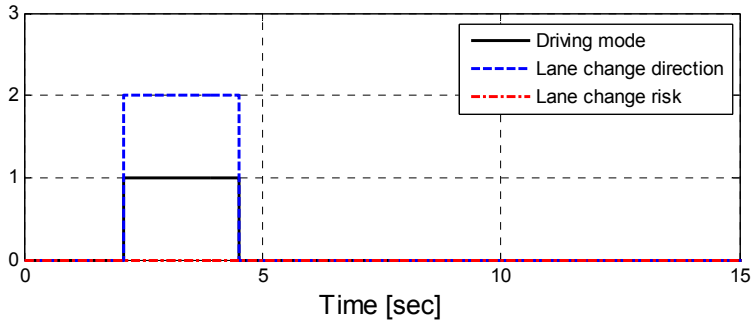

(b) Driving mode, lane change direction, and risk monitoring

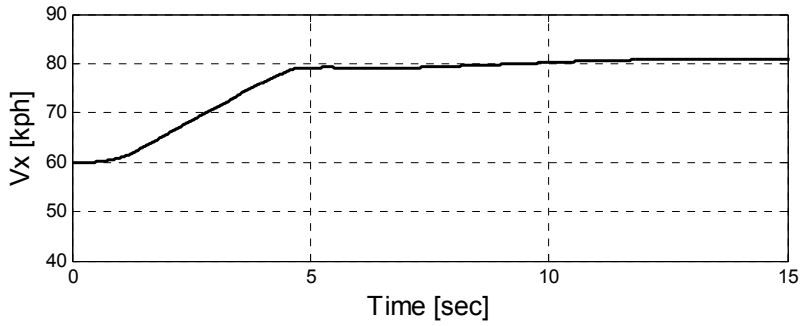

(c) Vehicle velocity

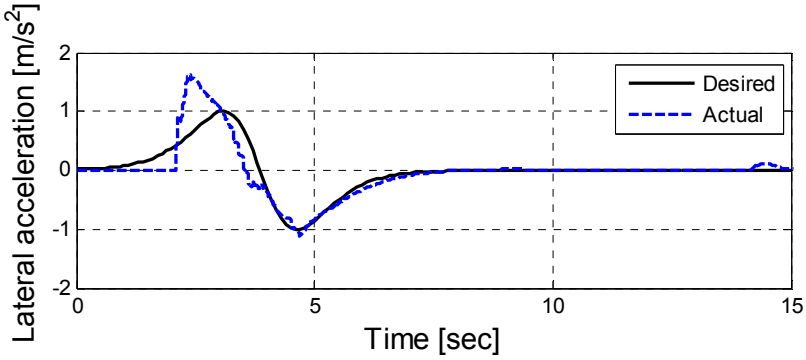

(d) Lateral acceleration

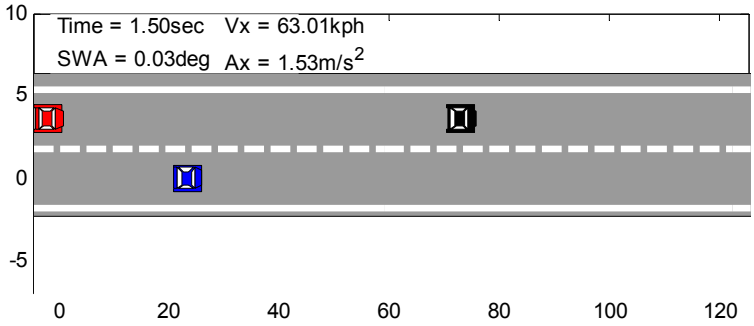

(e) Vehicle position at 1.5 sec

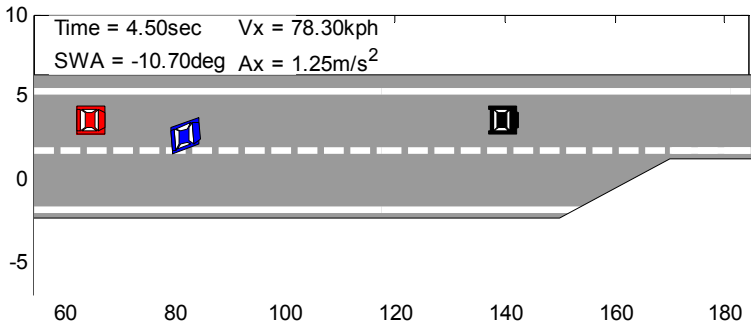

(f) Vehicle position at 4.5 sec when lane change ends successfully

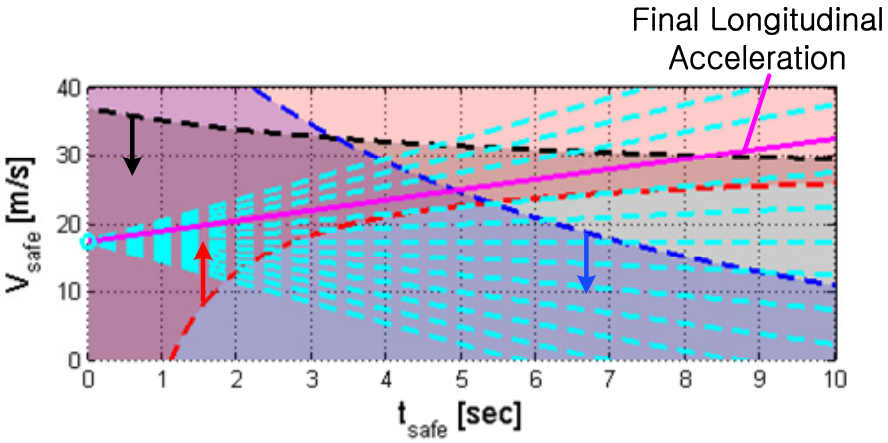

(g) Planning longitudinal acceleration to change lane safely in merging section. Side-front vehicle, side-rear vehicle, and road constraint satisfy lower area of black dashed line, upper area of red dashed line, and lower area of blue dashed line.

Figure 7.5 Simulation results when distance between the side-rear and the subject vehicle is 35m

7.2. ECU-in-the-loop evaluation using a vehicle traffic simulator

To evaluate the proposed SMPC using disturbance rejection based automated driving controller, we consider control performance in real-time. Since control performance is affected by calculation time, depending on the computational load, the evaluation of the controller in real-time is necessary. For this reason, the Vehicle Traffic Simulator has been developed and used for the evaluation of the proposed automated driving controller. As the Vehicle Traffic Simulator can evaluate various scenarios, such as difficult or hazardous situations, it is used actively on ADAS and automated driving control areas. In this chapter, the control performance of the proposed algorithm has been investigated by a real-time test. The calculation time of the perception layer is 100ms, and that of motion planning and the lower-level controller are 50ms.

7.2.1. Configurations of a vehicle traffic simulator

The control performance of the proposed controller has been investigated by the Vehicle Traffic Simulator. As shown in Table 7.1, the Vehicle Traffic Simulator consists of four parts: Driving Simulator Cabin, Real-time Simulator, Visual Graphic Generator, and Motion Platform. The configuration of the Vehicle Traffic Simulator is shown in Figure 7.6.

The driver simulator cabin consists of Grandeur 3.3 parts to compose the

human-vehicle interface. Motor driven power steering (MDPS) and electronic stability control (ESC) hardware modules and mass produced ECUs are included to describe real vehicle signals.

The real-time simulator calculates the behaviors of the vehicle model, which is controlled by the proposed controllers in real time. A dSPACE MicroAutobox II and a dSPACE Simulator are used as the RT test hardware in the Vehicle Traffic Simulator. In the RT test, the ASM from dSPACE is used as the vehicle simulation model.

The visual graphic generator provides a visual representation of the driving situation. Using the vehicle behaviors that are obtained from the real-time simulator, the visual graphic generator projects a visual representation of the driving conditions via three 50-inch monitors. It creates 3-D model of a real-time simulation environment, such as road surface, guardrail, other vehicles, etc.

The driver simulator cabin is mounted on a 3 DOF electric motion platform, which applies the behavior of the vehicle model to the simulator body. The motion platform allows displacements up to a maximum of about ±10 deg (roll and pitch) and ±120 mm (heave).

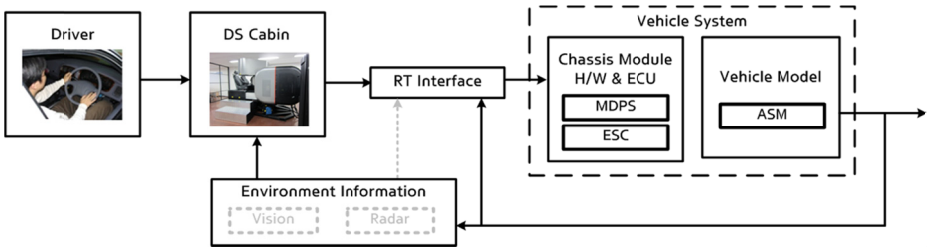

(a) Driver-in-the-loop simulation on a Vehicle Traffic Simulator

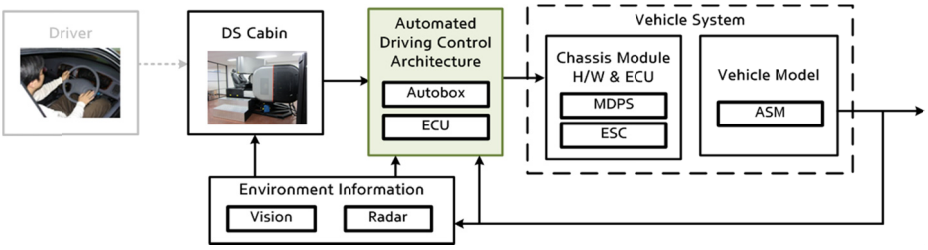

(b) ECU-in-the-loop automated driving real time simulation on a Vehicle Traffic Simulator

Figure 7.6 ECU-in-the-loop and driver-in-the-loop configuration

Table 7.1 Vehicle traffic simulator hardware component

	Driver Simulator Cabin	Visual Graphic Generator	Real-time Simulation Hardware	Motion Platform
Image				
Function	• HG Grandeur • MDPS Rack Force Test Bench • ESC/EPB Test Bench	• SCANeR Software • Real Road Database • DAQ Software	• dSPACE System • ASM Vehicle Dynamics Model	• 3 DOF Motion - Roll, Pitch, Heave

7.2.2. Evaluation of real-time performance

In this section, we show that the proposed algorithm can operate the motion of the subject vehicle using preceding and potential target vehicles in real time. The computer simulation and RT performance are compared for the algorithm to be implemented successfully in real time. The computer simulation is conducted using MATLAB/Simulink and CARSIM software.

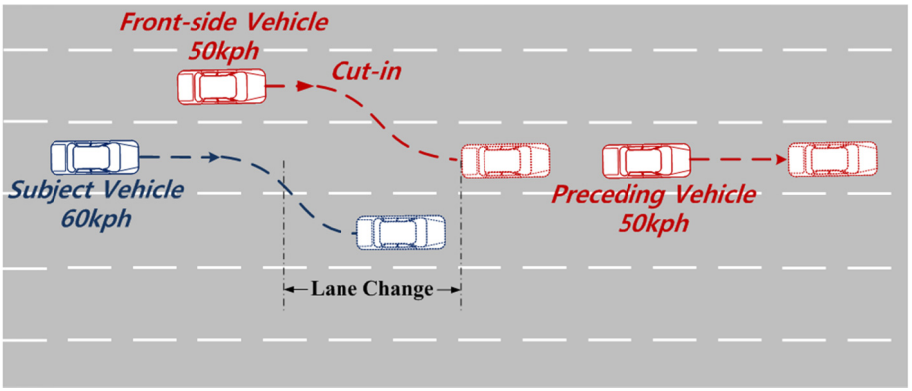

Figure 7.7 Test scenario: Cut-in vehicle

The test scenario is designed to reproduce the cut-in situation as shown in Figure 7.7. In this situation, the initial velocity of the subject vehicle is 60kph, and initial velocities of a front-side and preceding vehicle are 50kph. The front-side vehicle starts to cut in very slowly when the subject vehicle approaches close enough. Then the subject vehicle calculates the longitudinal states using the information of the adjacent vehicle, as the potential target vehicle, and the preceding vehicle. After the proposed controller considers the information of both vehicles, the subject vehicle changes the lane to the adjacent lane to reduce collision risk.

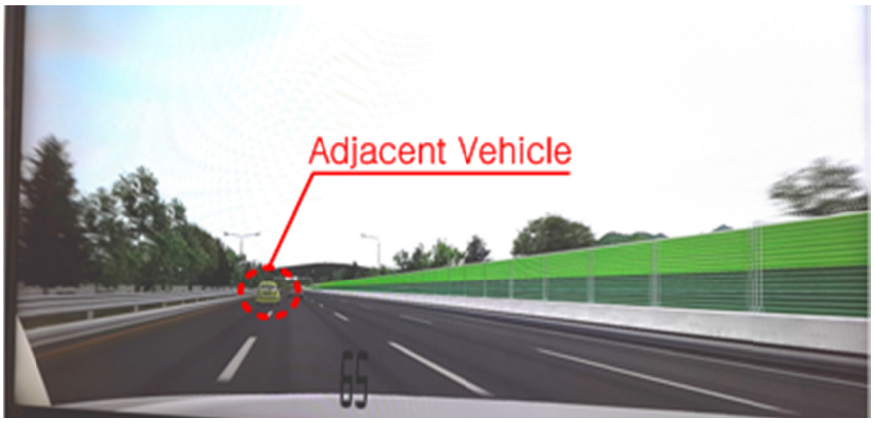

(a) Slow adjacent vehicle (50kph)

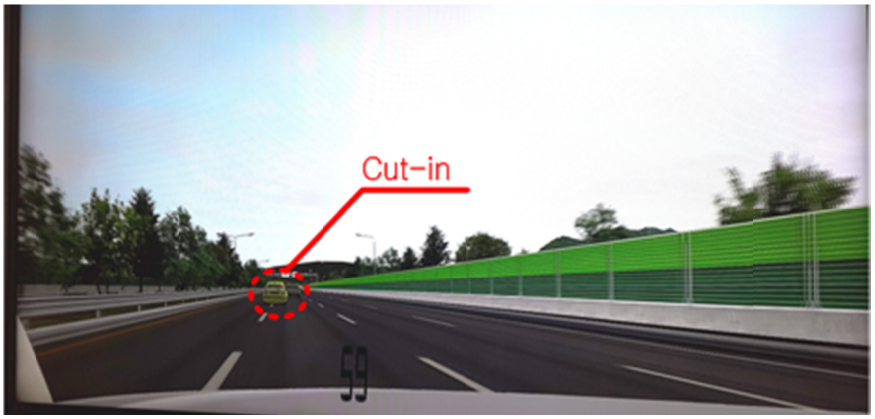

(b) Adjacent vehicle cuts in slowly

Figure 7.8 Test scenario provided visual graphic generator

As in the previous section, the visual graphic generator provides visual circumstances shown in Figure 7.8. Figure 7.8 represents the subject vehicle approaching front vehicles. The adjacent vehicle starts to change its lane to the right lane when the subject vehicle becomes close. The subject vehicle also changes its lane to avoid the potential risk increasing in Figure 7.8.

The test results compared with computer simulation and simulator test in

real time are presented in Figure 7.9. In Figure 7.9(a) and (b), we compare the subject vehicle's control inputs as longitudinal acceleration and steering wheel angle of computer simulation performance and that of real-time(RT) performance. Since the simulation results of longitudinal velocity, as shown in Figure 7.9(c), are different from the results of RT, the simulation and RT results of longitudinal acceleration are also different. From the test, since the longitudinal velocity is difficult to maintain for various reasons, such as actuator and transfer delay, equating the longitudinal speed and longitudinal acceleration between the simulation and RT are also difficult. However, the magnitude and frequency of the steering wheel angle are almost matched. Figure 7.9(d) shows the response of the steering wheel angle as lateral acceleration. The lateral acceleration has a reasonable value, similar to that of a human driver. In Figure 7.9(e), the weighting factor that is used to determine the target vehicle's states by the integration between the preceding vehicle and the potential target vehicle in the adjacent lane is described. Due to this, the proposed algorithm provides the lane change mode before the collision risk increases. The weighting factor has almost the same value between the simulation and RT.

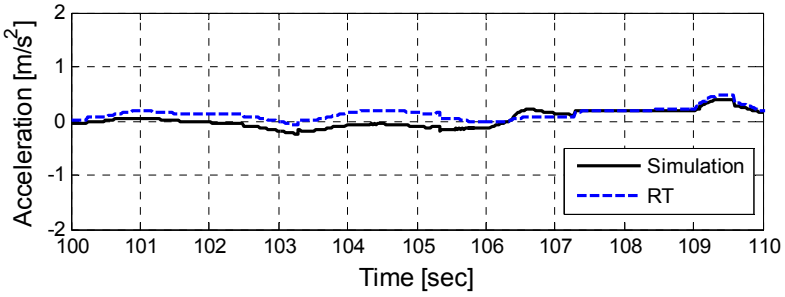

(a) Longitudinal acceleration

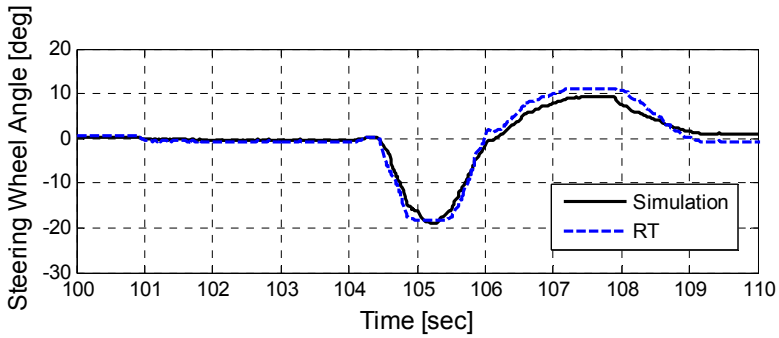

(b) Steering wheel angle

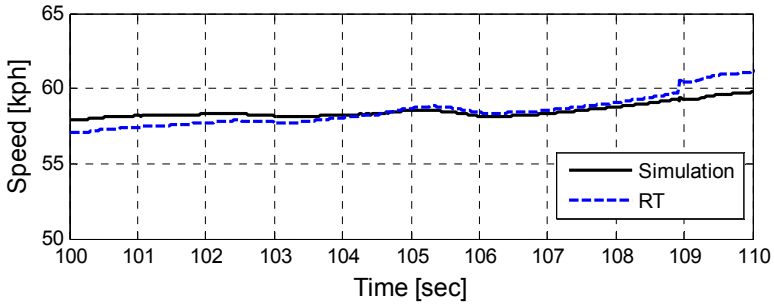

(c) Vehicle speed

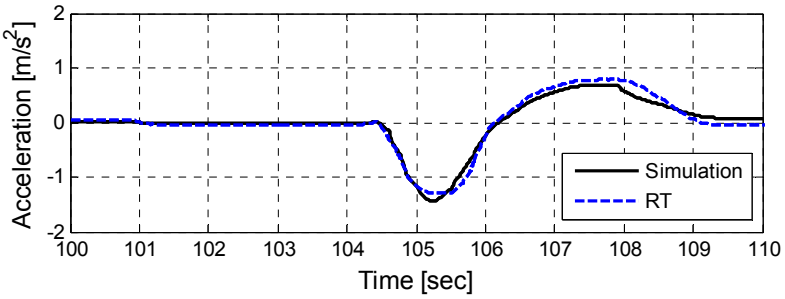

(d) Lateral acceleration

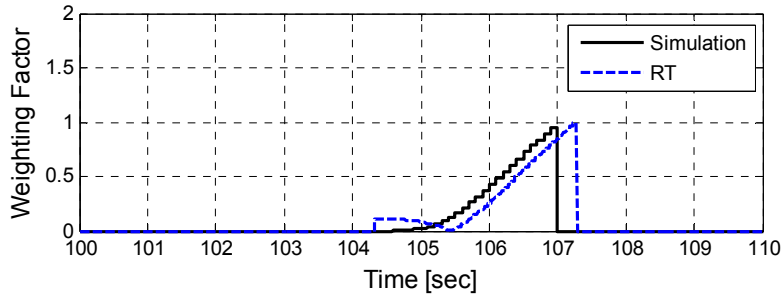

(e) Weighting factor

Figure 7.9 Cut-in scenario Vehicle Traffic Simulator test results

Figure 7.10 shows the sequences of vehicle trajectories with the safe driving envelope. The positions of surrounding vehicles are measured using local radar sensors. As shown in Figure 7.10(a), the subject vehicle remains in its originating lane without detecting the preceding vehicle. The subject vehicle recognizes the behavior of the adjacent vehicle that cuts in the originating lane of the subject vehicle. Then the proposed controller predicts the adjacent vehicle's future behavior and makes the subject vehicle change its lane to decrease the collision risk in advance, as shown in Figure 7.10(b).

After the lane change sequence is completed, then the subject vehicle remains in its lane, as shown in Figure 7.10(c). In the process of lane change or keeping, the magenta circle, the final position, is set as the goal area, and the proposed algorithm calculates the control inputs to reach that position using MPC. The predicted lateral offset is the magenta dashed-line. The safe driving envelope is also updated as a drivable area in every step considering the surrounding environment. The solid yellow line means the upper and lower boundary of the subject vehicle. The light green area shows the drivable area for safe driving.

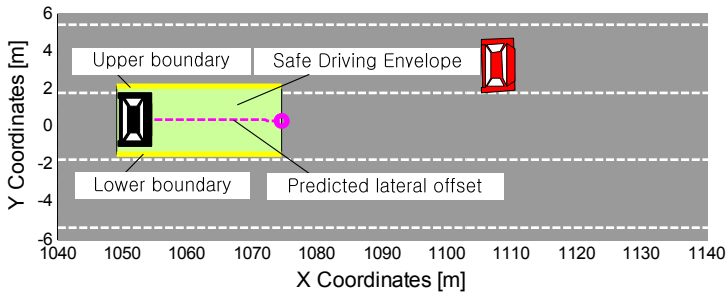

(a) Lane keeping mode, before the preceding vehicle is detected.

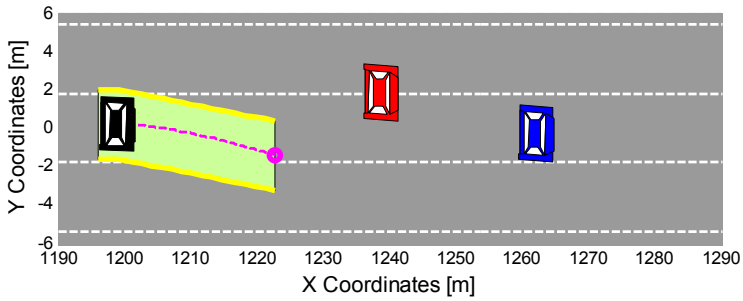

(b) Lane change mode. The adjacent vehicle cuts in to the originating lane of the subject vehicle

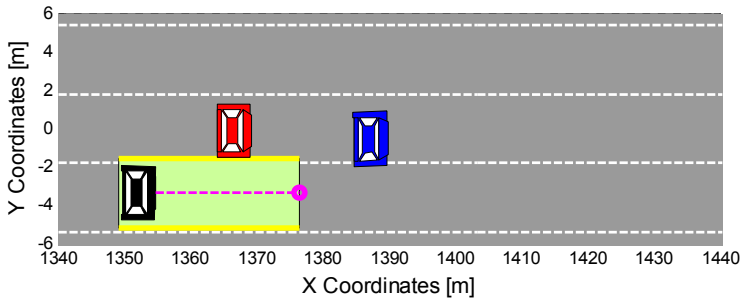

(c) After the lane change sequence, the subject vehicle remains in its originating lane

Figure 7.10 Vehicle trajectory

7.2.3. Comparison between a human driver and automated driving controller

The proposed algorithm used in this paper has been evaluated by comparison between a human driver and controller. The proposed controller has been implemented in real time. The test scenario is set to be the lane change to overtake a slow vehicle and joined the slow flow of other vehicles, as shown in Figure 7.11.

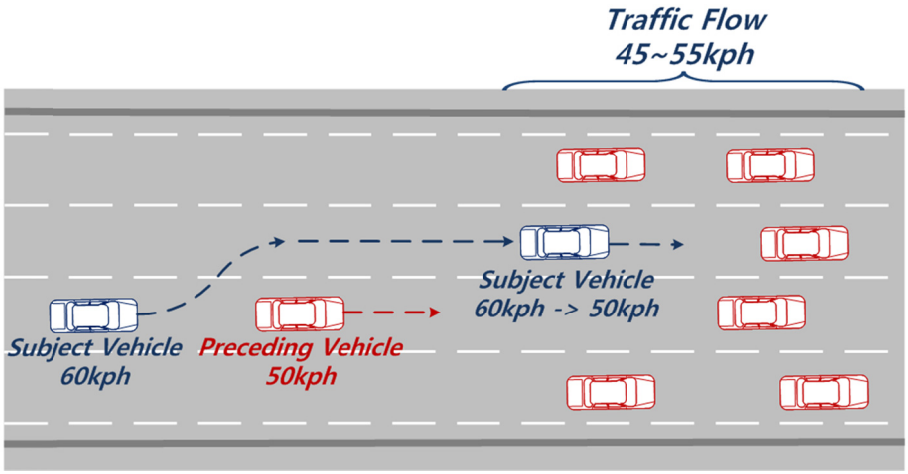

Figure 7.11 Test scenario comparing a human driver and controller

Figure 7.12 presents the visual representation, provided with the visual graphic generator, in the tests with the simulator. The subject vehicle approaches the preceding vehicle, the preceding vehicle moves at a constant speed of about 50kph in a straight lane as shown in Figure 7.12(a). Since the preceding vehicle is slower than the subject vehicle, the collision probability increases. Then, the subject vehicle changes its originating lane to the adjacent lane. Figure 7.12(b) shows the slow traffic flow of other vehicles. The subject vehicle keeps its lane and slows down due to collision risk.

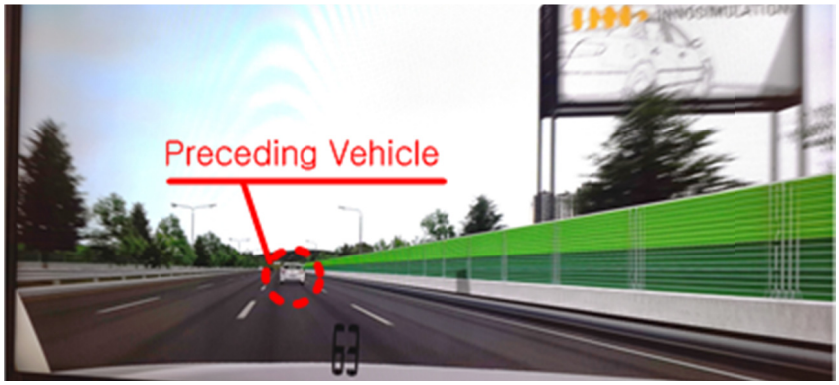

(a) Slow preceding vehicle (50kph)

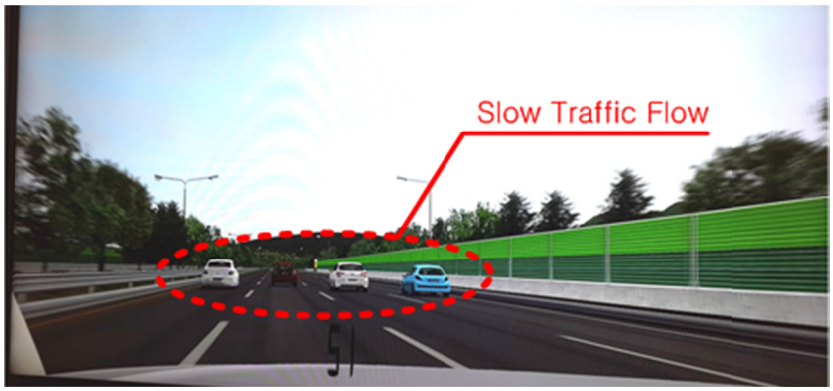

(b) Slow traffic flow of other vehicles (45-55 kph)

Figure 7.12 Test scenario provided visual graphic generator

Tests in the above test scenario have been conducted under the following conditions.

- The preceding vehicle is driven at a constant speed of 50kph.
- The traffic flow speed is 45 ~ 55kph.
- Tire/road friction is set to be 0.85.

In this paper, to show the effectiveness of the proposed automated driving control algorithm, the test results of the control algorithm are compared with

those of a human driver. The test results are divided into two phases: overtaking the preceding vehicle and joining the slow traffic flow. They are presented in Figsure 7.13 and 7.14, respectively.

Figure 7.13 shows overtaking the slow preceding vehicle to compare between a human driver and controller. The magnitude and frequency of the human driver's steering input are quite similar to that of the proposed automated driving controller, as shown in Figure 7.13(a). The vehicle behaviors driven by a human driver and controller, such as vehicle trajectory and lateral acceleration, are also quite similar, as shown in Figure 7.13(b) and (c).

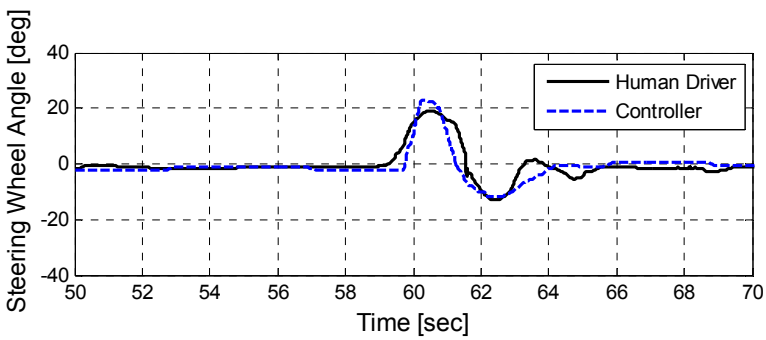

(a) Steering wheel angle

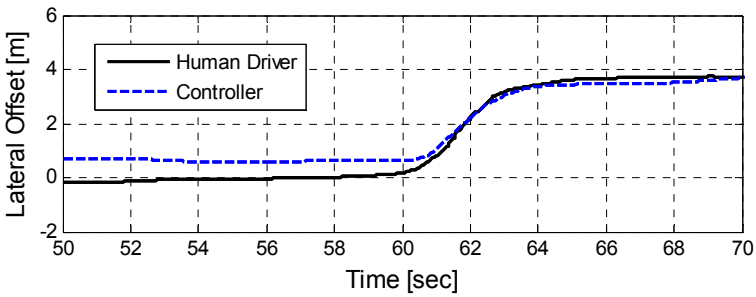

(b) Vehicle trajectory in the lateral direction

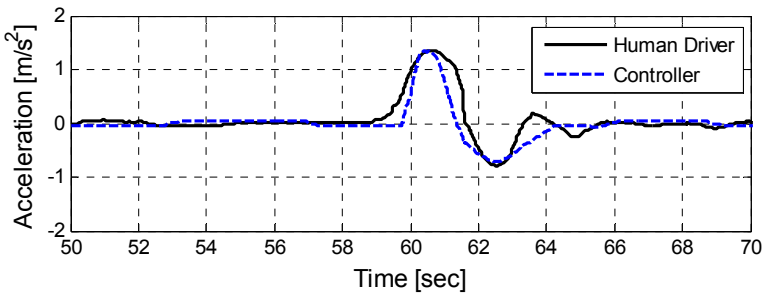

(c) Lateral acceleration

Figure 7.13 Vehicle Traffic Simulator test results for overtaking

Figure 7.14 shows joining the slow traffic flow. It demonstrates that a difference exists between the human driver and controller, but the maximum magnitude of the longitudinal acceleration is almost the same. It can be confirmed by vehicle speed, which is a similar tendency to adjust the traffic flow. The comparison between the human driver and controller shows that the proposed algorithm is very effective for reflecting human driver's driving characteristics.

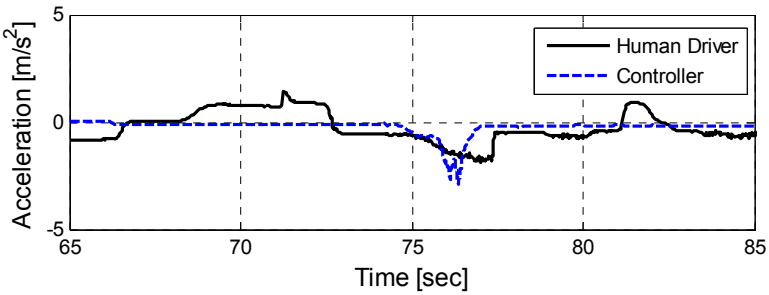

(a) Longitudinal acceleration

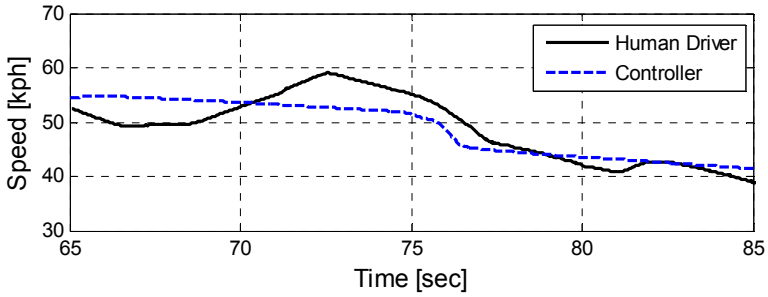

(b) Vehicle longitudinal speed

Figure 7.14 Vehicle Traffic Simulator test results for joining the slow traffic flow

7.3. Vehicle Tests

In order to evaluate the proposed algorithm on a real test vehicle, Hyundai-Kia Motors K7 is used as a test vehicle platform. Figure 7.15 shows the test vehicle configuration. In order to measure lateral offset, heading angle, and road curvature, a Mobileye camera system is equipped on the test vehicle. The proposed algorithm has been implemented on MicroAutobox II, which is used for the real-time application. Delphi radars are equipped on the test vehicle to perceive surrounding environments. IBEO laser scanner is equipped on the test vehicle to detect the static obstacles. The hardware components mentioned above communicate through a CAN bus.

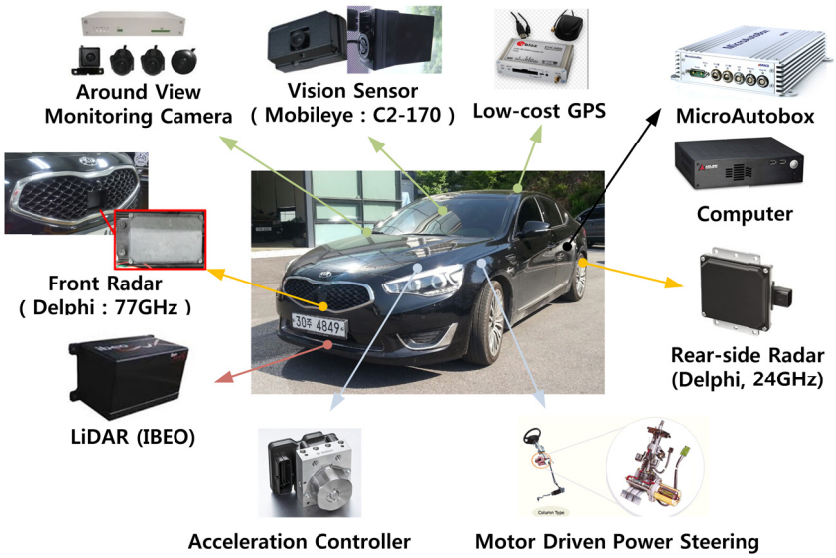

Figure 7.15 Test vehicle configuration

Vehicle tests have been conducted for several times at the enter section of

Yeongdong expressway. The details of test roads are depicted in Figure 7.16. The test vehicle drives the given route fully autonomously without a driver manipulation. The automated driving vehicle needs to consider other traffic participants such as preceding vehicles and adjacent vehicles and detect guardrails while the subject vehicle runs at high speed.

Figure 7.16 Configuration of test route at the enter section of Yeongdong expressway (2km). The route contains a variety of different traffic situations as e.g. straight, curved and merging roads with other traffic participants such as preceding vehicle, adjacent vehicles, and static obstacles like guardrails.

The proposed automated driving algorithm has shown the satisfactory control performance and the test results are given in Figure 7.17. As shown in Figure 7.17, the subject vehicle drives through a junction section with static obstacles, the preceding and adjacent vehicles. Comparisons with center path between raw data (red solid line) and estimated data (blue solid line) of vision are given. Control input sequences from SMPC solver are depicted as blue vehicle shape which follows center path well. The blue and red square shapes mean reachable set using uncertainty propagation. The green area means safe driving envelope.

Figure 7.17(a) shows that the human driver drives at an exit section of junction with other vehicles and both side static obstacles. It is normal driving situation to follow preceding vehicle. In Figure 7.17(b), the proposed algorithm can take over the control authority from human driver when the driver pushes an automation button. Then the subject vehicle accelerates to join the expressway which has faster traffic flow. The subject vehicle maintains its speed after reaching the traffic flow of expressway. As shown in Figure 7.17(c), the proposed algorithm makes the vehicle to change lane when the safety is secured. The vehicle changes lane smoothly and keeps safe driving envelope. After the subject vehicle changes lane successfully, it keeps its lane with following traffic flow of its lane as shown in Figure 7.17(d). To verify a safety performance of the proposed algorithm, collision probabilities and *TTC* have been analyzed. We divide the vehicle status into two, lane keeping and lane change. Figure 7.17(e) shows the histogram of the collision probability. As can be seen in Figure 7.17(e), the proposed control algorithm

determines lane change procedure safely and maintains collision probability which is lower than a certain level. As similar way, Figure 7.17(f) shows time to collision results which are larger than lane change expected time, especially. It means that the subject vehicle keeps its safety clearance from other vehicles.

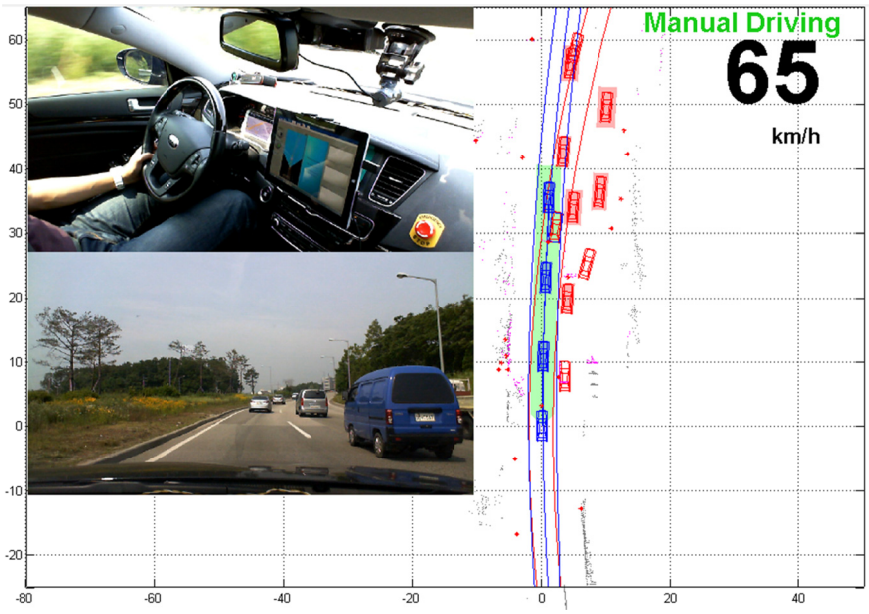

(a) Human driver drives at enter section of expressway

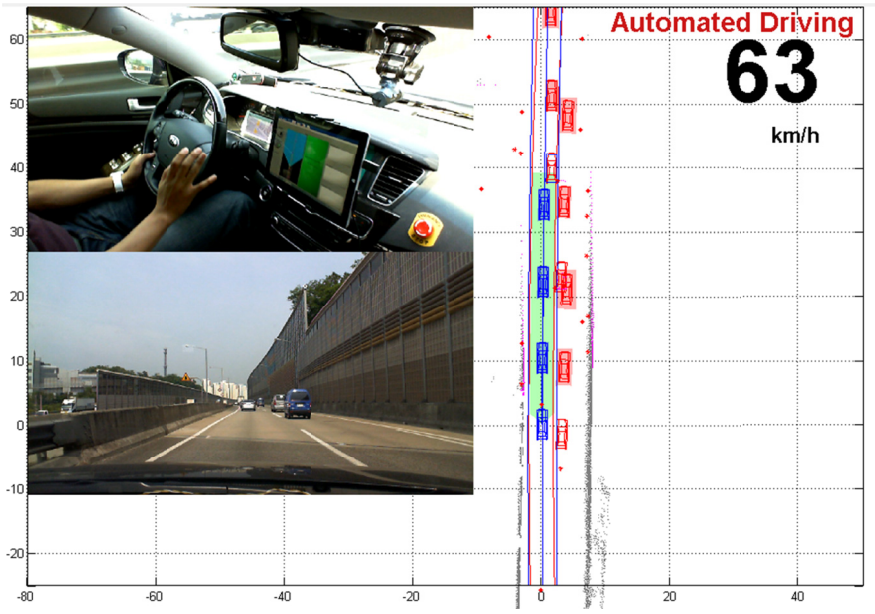

(b) Proposed algorithm takes over the control authority from human driver

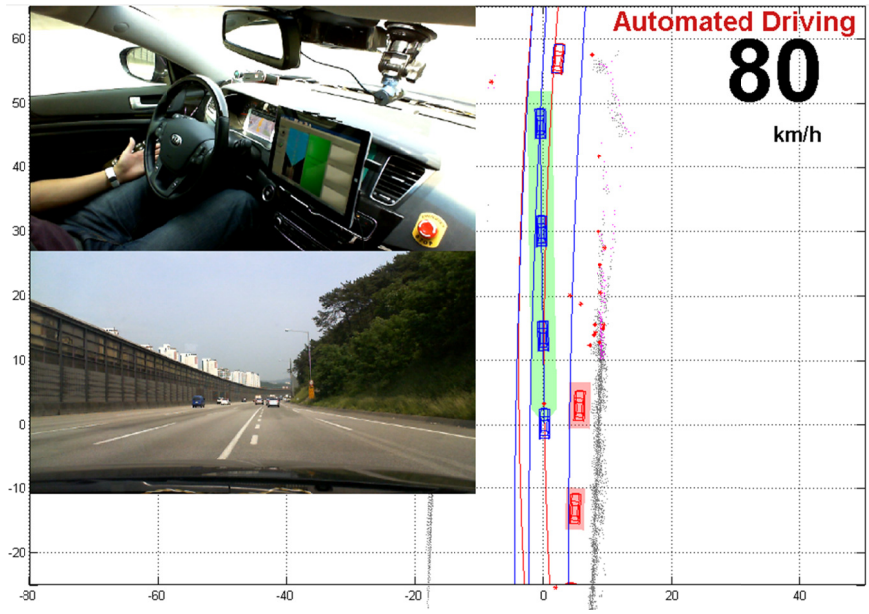

(c) The automated driving vehicle accelerates up to traffic flow of expressway and changes lane.

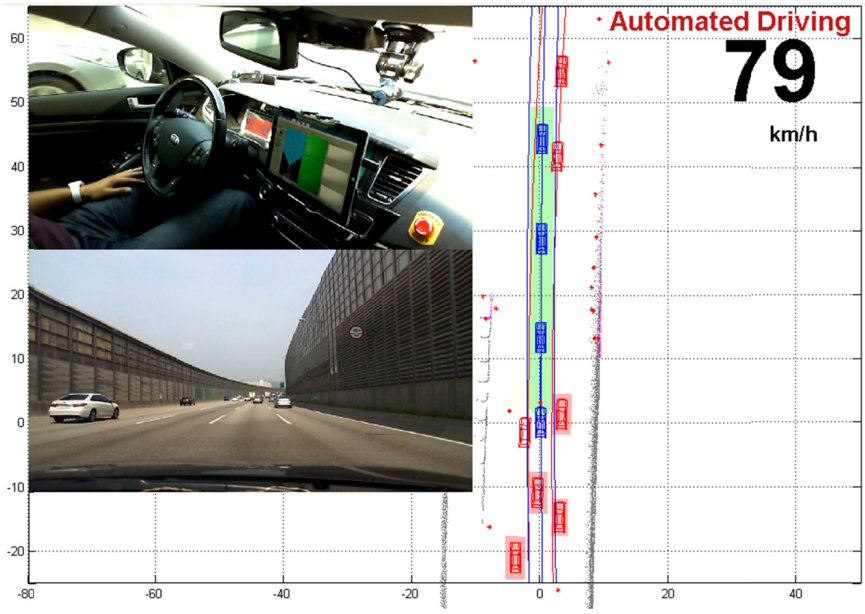

(d) Lane change is completed.

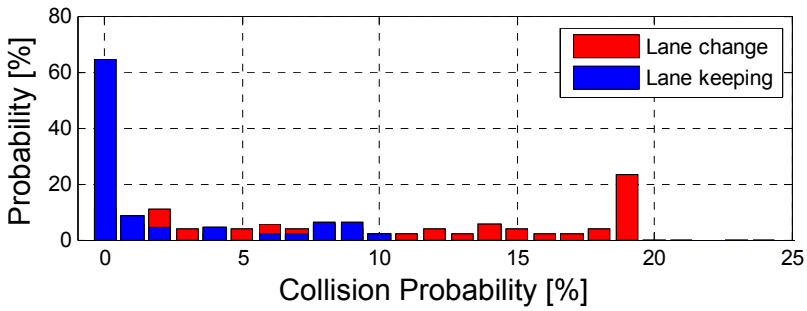

(e) Collision probability

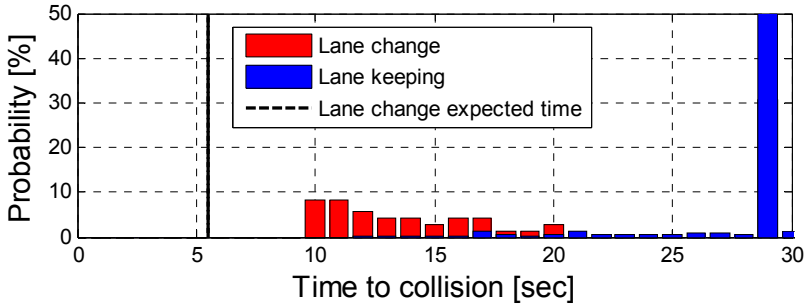

(f) Time to collision

Figure 7.17 Vehicle test results

Chapter 8

Conclusions and Future Works

This dissertation has proposed a fully automated driving algorithm which is capable of automated driving on motorway with guaranteed safety. The proposed algorithm consisted of the following three steps: an environment representation, a motion planning, and a vehicle control. In an environment representation, object tracking and prediction, and collision probability calculation have been developed. And a motion planning algorithm, which includes driving mode decision, dynamics limit decision, safety driving envelope decision and target states decision, has been developed. The developed motion planning algorithm solves a chance-constraint optimization problem.

The effectiveness of the proposed automated driving algorithm has been evaluated via computer simulations, hardware-in-the-loop tests, and vehicle tests. Based on the results, it has been shown that the proposed algorithm enhances safety with respect to the potential change of traffic situation and improves ride comfort. Furthermore, it has been shown that the proposed

algorithm could guarantee the control performance under stochastic disturbances. It has been demonstrated that the proposed algorithm could reflect human driver's driving characteristics.

However, driving mode decision module should reflect the sophisticated behavior of skilled drivers, such as lane change timing, vehicle behavior, safe distance, and so on. In the aspect of ride comfortability, the feel of passenger is analyzed under various criteria. Also, actuator delays are considered to develop the vehicle control performance.

In the future, evaluations in more situations should be conducted for the verification of the reliability of the proposed algorithm. In addition, the human driver data analysis based lane change decision is needed using machine learning such as Gaussian mixture model and Gaussian mixture regression.

Bibliography

[Alexander14] Alexander Domahidi and Juan Jerez, Forces Professional, embotech GmbH (httpembotech.comFORCES-Pro), July 2014

[Althoff09] M. Althoff, O. Stursberg, and M. Buss. “Model-based probabilistic collision detection in autonomous driving”, IEEE Transactions on Intelligent Transportation System, Vol. 10, No. 2, pp. 299-310, June 2009.

[Anderson10] S. J. Anderson, S. C. Perters, T. E. Pilluti, K. Iagnemma, “An optimal control based framework for trajectory planning, threat assessment, and semi-autonomous control of passenger vehicles in hazard avoidance scenarios”, International Journal of Vehicle Autonomous Systems, Vol. 8, No. 2, pp. 190-216, Apr. 2010.

[Ashwin15] C. Ashwin, S. Lefevre, G. Schildbach, J. Kong, and F. Borrelli, “Automated driving: The role of forecasts and uncertainty – A control perspective”, European Journal of Control, Vol. 24, pp. 14-32, 2015

[Bishop00] R. Bishop, “A survey of intelligent vehicle applications worldwide”, IEEE Intelligent Vehicles Symposium, Dearborn Michigan, USA, pp. 25-30, 2000.

[Chang10] B. R. Chang, H. F. Tsai, and C. Young. "Intelligent data fusion system for predicting vehicle collision warning using vision/GPS sensing.", Expert Systems with Applications, Vol. 37, No.3, pp. 2439-2450, 2010.

[Carvalho13] A. Carvalho, Y. Gao, A. Gray, H. E. Tseng, F. Borrelli, “Predictive control of an autonomous ground vehicle using a iterative

linearization approach", Proceedings of the 16th International IEEE Annual Conference on Intelligent Transportation Systems (ITSC2013), Hague, Netherlands, Oct. 6-9, 2013.

[Chee94] W. Chee, and T. Masayoshi, "Vehicle lane change maneuver in automated highway systems", California Partners for Advanced Transit and Highways (PATH), 1994.

[Chellappa04] R. Chellappa, G. Qian, and Q. Zheng, "Vehicle detection and tracking using acoustic and video sensors", Acoustics, Speech, and Signal Processing, Vol. 3, IEEE, 2004.

[Enache09] N. Minoiu, M. Netto, S. Mammar, and B. Lusetti, "Driver steering assistance for lane departure avoidance." Control engineering practice, Vol.17, No.6, pp. 642-651, 2009.

[Erlien14] S. Erlien, J. Funke, and J. C. Gerdes, "Incorporating non-linear tire dynamics into a convex approach to shared steering control", American Control Conference, Portland Oregon, USA, pp. 3468-3473, 2014.

[Eskandarian12] A. Eskandarian, 2012, Handbook of Intelligent Vehicles, London: Springer London

[Falcone07] P. Falcone, F. Borrelli, J. Asagari, H. Tseng, and D. Hrovat, "Predictive active steering control for autonomous vehicle systems." Control Systems Technology, IEEE Transactions on Vol.15, No.3, pp. 566-580, 2007.

[Falcone11] P. Falcone, M. Ali, and J. Sjöberg, "Predictive threat assessment via reachability analysis and set invariance theory", Intelligent Transportation Systems, IEEE Transactions on Vol.12, No.4, pp. 1352-1361, 2011.

[Fancher01] P. Fancher, Z. Bareket, and R. Ervin, "Human-centered design of

an ACC-with-braking and forward-crash-warning system", Vehicle System Dynamics Vol.36, No.2 pp. 203-223, 2001.

[Ferguson13] D. Ferguson, and D. Dolgove, “Modifying behavior of autonomous vehicle based on predicted behavior of other vehicles”, Pat. no. 20130261872A1, United States, 2013.

[Gray13a] A. Gray, Y. Gao, J. Hedrick, and F. Borrelli, “Robust predictive control for semi-autonomous vehicles with an uncertain driver model”, IEEE Intelligent Vehicles Symposium, Gold Coast, Australia, pp. 208-213, 2013.

[Gray13b] A. Gray, Y. Gao, T. Lin, J. Hedrick, and F. Borrelli, "Stochastic predictive control for semi-autonomous vehicles with an uncertain driver model", Intelligent Transportation Systems-(ITSC), 16th International IEEE Conference on. IEEE, 2013.

[Jansson02] J. Jansson, J. Johansson, and F. Gustafsson, "Decision making for collision avoidance systems." Society of Automotive Engineering SAE 1, 0403, 2002.

[Jansson08] J. Jansson, and F. Gustafsson, "A framework and automotive application of collision avoidance decision making." Automatica Vol.44, No.9, pp. 2347-2351, 2008.

[Kasper12] D. Kasper, G. Weidl, T. Dang, G. Breuel, A. Tamke, and A. Wedel, "Object-oriented Bayesian networks for detection of lane change maneuvers." Intelligent Transportation Systems Magazine, IEEE Vol.4, No.3, pp. 19-31, 2012.

[Kim14] B. Kim, and K. Yi. "Probabilistic and Holistic Prediction of Vehicle

States Using Sensor Fusion for Application to Integrated Vehicle Safety Systems." Intelligent Transportation Systems, IEEE Transactions on Vol.15, No.5, pp. 2178-2190, 2014.

[Kouvaritakis00] B. Kouvaritakis, J. Rossiter, and J. Schuurmans, "Efficient robust predictive control", Automatic Control, IEEE Transactions on Vol.45, No.8, pp.1545-1549, 2000.

[Kouvaritakis10] B. Kouvaritakis, M. Cannon, S. Rakovic, and Q. Cheng, "Explicit use of probabilistic distributions in linear predictive control." Automatica Vol.46, No.10, pp. 1719-1724, 2010.

[Li04] K. Li, and P. Ioannou, "Modeling of traffic flow of automated vehicles", Intelligent Transportation Systems, IEEE Transactions on Vol.5, No.2, pp. 99-113, 2004.

[Lyons11] D. Lyons, P. Calliess, and D. Hanebeck, "Chance-constrained model predictive control for multi-agent systems." arXiv preprint arXiv: pp.1104.5384, 2011.

[Mammar06] S. Mammar, S. Glaser, and M. Netto, "Time to line crossing for lane departure avoidance: a theoretical study and an experimental setting", Intelligent Transportation Systems, IEEE Transactions on Vol.7, No.2, pp. 226-241, 2006.

[Mayne00] D. Mayne, J. Rawlings, C. Rao, and P. Scokaert, "Constrained model predictive control: Stability and optimality", Automatica Vol.36, No.6, pp. 789-814, 2000.

[Mayne05] D. Mayne, M. Seron, and S. Raković, "Robust model predictive control of constrained linear systems with bounded disturbances",

Automatica Vol.41, No.2, pp. 219-224, 2005.

[Moon08] S. Moon, and K. Yi, "Human driving data-based design of a vehicle adaptive cruise control algorithm", Vehicle System Dynamics Vol.46, No.8, pp. 661-690, 2008.

[Moon09] S. Moon, I. Moon, and K. Yi, "Design, tuning, and evaluation of a full-range adaptive cruise control system with collision avoidance." Control Engineering Practice Vol.17, No.4, pp. 442-455, 2009.

[Moon10] S. Moon, H. Kang, and K. Yi, "Multi-vehicle target selection for adaptive cruise control", Vehicle System Dynamics Vol.48, No.11, pp. 1325-1343, 2010.

[Naranjo08] J. E. Naranjo, C. Gonzalez, R. Garcia, and T. Pedro, “Lane-change fuzzy control in autonomous vehicles for the overtaking maneuver”, IEEE Transactions on Intelligent Transportation System, Vol. 9, No. 3, pp. 438-450, Sep. 2008.

[Ono15] M. Ono, M. Pavone, Y. Kuwata, and J. Balaram, "Chance-constrained dynamic programming with application to risk-aware robotic space exploration", Autonomous Robots Vol.39, No.4, pp. 555-571, 2015.

[Pohl06] J. Pohl, W. Birk, and L. Westervall, "A driver-distraction-based lane-keeping assistance system." Proceedings of the Institution of Mechanical Engineers, Part I: Journal of Systems and Control Engineering Vol.221, No.4, pp. 541-552, 2006.

[Schulman13] Schulman, J., Ho, J., Lee, A., Awwal, I., Bradlow, H., and Abbeel, P, “Finding locally optimal, collision free trajectories with sequential convex optimization”, Robotics: Science and Systems, 2013.

[Suh16] J. Suh, K. Yi, J. Jung, K. Lee, H. Chong, and B. Ko, "Design and evaluation of a model predictive vehicle control algorithm for automated driving using a vehicle traffic simulator", Control Engineering Practice, Vol.51, pp. 92-107, 2016.

[Tideman07] M. Tideman, M. C. van der Voort, B. van Arem, and F. Tillema, “A review of lateral driver support systems”, Intelligent Transportation Systems Conference, Seattle, USA, Sep. 30-Oct. 3, pp. 992-999, 2007.

[Tomar10] R. Tomar, S. Verma, and G. Tomar, "Prediction of lane change trajectories through neural network", Computational Intelligence and Communication Networks (CICN), International Conference on. IEEE, 2010.

[Usman09] G. Usman, and F. Kunwar, "Autonomous vehicle overtaking-an online solution", Automation and Logistics, ICAL'09. IEEE International Conference on. IEEE, 2009.

[Vanholme13] B. Vanholme, D. Gruyer, B. Lusetti, S. Glaser, and S. Mammar, “Highly automated driving on highways based on legal safety”, IEEE Transactions on Intelligent Transportation System, Vol. 14, No. 1, pp. 333-347, Mar. 2013.

[Vitus11] M. Vitus, and C. Tomlin, "On feedback design and risk allocation in chance constrained control", Decision and Control and European Control Conference (CDC-ECC), 50th IEEE Conference on. IEEE, 2011.

[Vitus13] M. Vitus, and C. Tomlin, "A probabilistic approach to planning and control in autonomous urban driving", Decision and Control (CDC), IEEE 52nd Annual Conference on. IEEE, 2013.

[Volvo13] Volvo Trucks. “European accident research and safety report”,

(http://www.volvotrucks.com/SiteCollectionDocuments/VTC/Corporate/Values/ART%20Report%202013_150dpi.pdf), 2013.

[Wan11] L. Wan, P. Raksincharoensak, K. Maeda, and M. Nagai, "Lane change behavior modeling for autonomous vehicles based on surroundings recognition." International Journal of Automotive Engineering, Vol.2, No.2, pp. 7-12, 2011.

[Wei10] J. Wei, M. Dolan, and B. Litkouhi, "A prediction-and cost function-based algorithm for robust autonomous freeway driving", Intelligent Vehicles Symposium (IV), IEEE, 2010.

[Yi04] K. Yi, and I. Moon. "A driver-adaptive stop-and-go cruise control strategy", Networking, Sensing and Control, IEEE International Conference on. Vol. 1, IEEE, 2004.

초 록

자율 주행 차량을 위한 확률 예측 제어 기법 기반 차선 변경 판단 알고리즘 개발

최근 10 여년 간 교통 사고를 분석해보면, 운전자의 졸음, 주의 산만 및 실수에 의한 사고가 94 퍼센트에 달한다. 사고 없는 안전 운전은 도로-교통-차량 환경의 최종 목표이기 때문에, 대다수의 차량 제조사들은 운전자 지원 시스템 (Driver Assistant System) 및 능동 안전 시스템 (Active Safety System)을 개발하고 있다. 예를 들어 적응형 순항 제어 시스템 (ACC: Adaptive Cruise Control), 차선 유지 보조장치 (LKAS: Lane Keeping Assistance System), 차선 변경 보조장치 (LCAS: Lane Change Assistance System), 자동주차 보조시스템 (APA: automated Parking Assist System) 그리고 사각지대 감지경보 (BSI: Blind Spot Intervention) 등의 다양한 능동안전시스템들이 이미 차량제조사들에 의해 출시되었다. 또한, 최근에는 주변 상황을 인지하고 스스로 판단해서 운행할 수 있는 자율 주행 차량에 관심을 돌리고 있다. Google 은 미리 측정한 정밀 지도 및 laser scanner 를 이용한 주변 환경 인지를 토대로 자율 주행을 성공하였다. 전기 자동차 양산 업체인 테슬라는 autopilot 모드를 자사의 Model S

차량에 장착, 선보이기도 하였다. BMW 는 독일의 뮌헨에서 잉골슈타트까지 강건하고 안전한 자율 주행을 성공하였다. Mercedes-Benz 는 'Intelligent Drive' 시스템을 개발하여 독일의 멘하임에서 포르츠하임까지 자율주행을 성공하였다. 이러한 자율주행 차량 개발의 추세는 안전뿐 아니라 탑승자의 편의를 위해서 많은 각광을 받고 있다. 그러나 자율주행의 최신 기술은 다양하고 복잡한 교통 상황을 다루기 위한 정교한 판단 기술을 요구한다.

그러므로, 본 논문에서는 고속도로 등의 복잡한 교통 상황에서 적절한 차량의 거동을 결정하기 위한 자율주행 기술 개발을 그 목표로 한다. 주변 차량의 잠재적 거동에 대해 안전한 주행을 위해 현재와 가까운 미래의 주변 교통의 움직임을 예측하고 불확실성을 고려하여야 한다. 주변 차량의 움직임을 예측한 후 차선 유지 및 변경 모드를 판단한다. 안전 영역을 정의하여 차량이 안전하게 운행이 가능한 영역을 고려하고, 이에 따라 감속, 가속, 차선 유지, 변경 등의 계획을 한다. 예측 제어를 통해 차량의 하위제어 입력, 즉 종방향 가속도와 조향각을 결정한다. 이 때, 자차량의 불화실성과 주변 환경의 외란 등을 고려하고 위해 이를 확률로 정의하는 확률 예측 제어를 도입하고, 현재 상황에 따라 불확실성의 크기를 조절할 수 있도록 하였다.

제안된 알고리즘의 성능은 컴퓨터 시뮬레이션과 실차를 통하여 검증하였다. 자율주행 차량은 다양한 도로 상황 위에서 안전하고 부드러운 움직임을 보여준다. 실차 실험 결과는 일반 도로 위에서도 강건한 성능을 보인다.

주요어: 자율 주행 자동차, 확률 예측 제어, 충돌 확률, 안전 영역 판단, 차선 변경 판단, 통합 안전 제어, 적응 불확실성 전파

학 번: 2012-20672